Genetic Analysis Of Gremlin Functions During Mouse Organogenesis

Genetische analyse van de functie van Gremlin tijdens de organogenese van de muis

(Met een samenvatting in het Nederlands)

Proefschrift

Ter verkrijging van de graad van doctor aan de Universiteit Utrecht op gezag van de Rector Magnificus, Prof. Dr. W.H. Gispen, ingevolge het besluit van het College voor Promoties in het openbaar te verdedigen op vrijdag 29 oktober 2004 des ochtends 10.30 uur.

Odyssé MICHOS

Geboren op 20 augustus 1977 te Cherbourg, Frankrijk

Promoter: Prof. Dr. R. Zeller
Co-Promoter: Dr. A. Zuniga

The studies described in this thesis were performed in the Department of Developmental Biology, University of Utrecht and in the Group of Developmental Genetic, Institute of Anatomy, University of Basel, Switzerland.

This thesis was sponsored by a grant from the Netherlands Research Organization (NOW) and the Swiss National Science Foundation.

ISBN: 90-393-3813-2

Cover: Scanning electronic microscopy of an E11.5 *Gremlin* deficient mouse embryo.

Contents

Abbreviations

ZPA	zone of polarizing activity
AER	apical ectodermal ridge
UB	ureteric bud
MM	metanephric mesenchyme
TGFß	transforming growth factor beta
BMP	bone morphogenetic protein
GDF	growth and differentiation factor
FGF	fibroblast growth factor
SHH	sonic hedgehog
GDNF	glial-derived neurotrophric factor
Gre	gremlin
Fmn	formin
ld	limb deformity
ALK	activin receptor-like kinase
WT	wild type

CHAPTER 1
Introduction

During organogenesis coordinated proliferation, patterning and differentiation of cells results in formation of organs and tissues. These coordinated events are orchestrated by a small group of cells with organizer properties that instruct the surrounding cells with respect to their fate and differentiation potential. Epithelial-mesenchymal signaling interactions are critical for initiation, maintenance and propagation of the morphogenetic signals that coordinate growth and patterning. A surprisingly small number of different types of signaling molecules control various aspects of organogenesis. Among the most relevant families of signals is the Fibroblast growth factors (FGFs), Hedgehogs (HHs), Bone morphogenetic proteins (BMPs) and WNT signals, which are the ones relevant for the studies described here. Research in the last few years has been focusing on how such molecules pattern the embryo. In particular, their functions during morphogenesis have been analyzed in organs/tissues. For example, the developing mouse limb bud and lung and kidney organogenesis are models of paradigmatic values to analyze epithelial-mesenchymal signaling interactions, both molecularly and genetically. The knowledge gained from analyzing development of a particular organ/tissue often results in a better understanding of the general principles regulating embryogenesis (Hogan, 1999; Metzger and Krasnow, 1999; Panman and Zeller, 2003; Saxén, 1987).

1. Molecular control of vertebrate limb bud morphogenesis

Limb bud development is controlled by reciprocal interactions between the mesoderm and the ectoderm. These interactions are mediated by two main signaling centers, the zone of polarizing activity (ZPA) and the apical ectodermal ridge (AER; Fig. 1A). The embryonic limb is first visible as a small bud that protrudes from the body and contains morphologically homogenous mesenchymal cells that are covered by a layer of ectoderm. As the bud grows, cells initiate their differentiation program and limb cartilage elements form. The skeletal elements are positioned along the proximo-distal axis with the stylopod (humerus) being most proximal and becoming apparent first, then the zeugopod (radius and ulna) and finally the distal-most autopod (metacarpals and digits).

1.1. The AER: induction and function

The apical ectodermal ridge (AER) is a group of columnar epithelial cells running along the distal tip of the developing limb bud. The AER is positioned at the interface of the ventral and dorsal limb bud ectoderm. Classical experiments have established the requirement of the AER for limb bud morphogenesis. Removal of the AER at an early stage causes apoptosis and distal limb truncation. Removal of the AER at successively later stages results in progressively more distal truncations, depending on the time of AER removal. These experiments suggest that the AER produces factors that promote limb bud outgrowth and survival of mesenchymal cells (Saunders, 1948; Summerbell, 1974). The discovery that a bead soaked in FGF4 can substitute the AER lead to the realization that FGF signaling mediates AER functions (Niswander and Martin, 1993; Vogel and Tickle, 1993). Indeed, several FGF signals are produced by the AER in a dynamic pattern, including *Fgf2, 4, 8, 9* and *17* (Martin, 1998; Tickle, 2003). *Fgf8* is the first FGF to be expressed by the ectoderm during initiation of limb bud outgrowth and *Fgf8*-expressing cells are restricted to the tip of the limb bud as the

AER forms (Capdevila and Izpisua Belmonte, 2001; Niswander, 2003). *Fgf8* and *2* are expressed along the entire AER during limb development, while expression of *Fgf4*, *9* and *17* is restricted to the posterior AER, indicating that the posterior AER is functionally different from the anterior compartment. Finally, analysis of mouse embryos lacking one or several FGFs in the AER has demonstrated that FGF4 and 8 are both required for AER function and limb bud morphogenesis (Lewandoski et al., 2000; Moon et al., 2000; Moon and Capecchi, 2000; Sun et al., 2000; 2002; Fig. 1C).

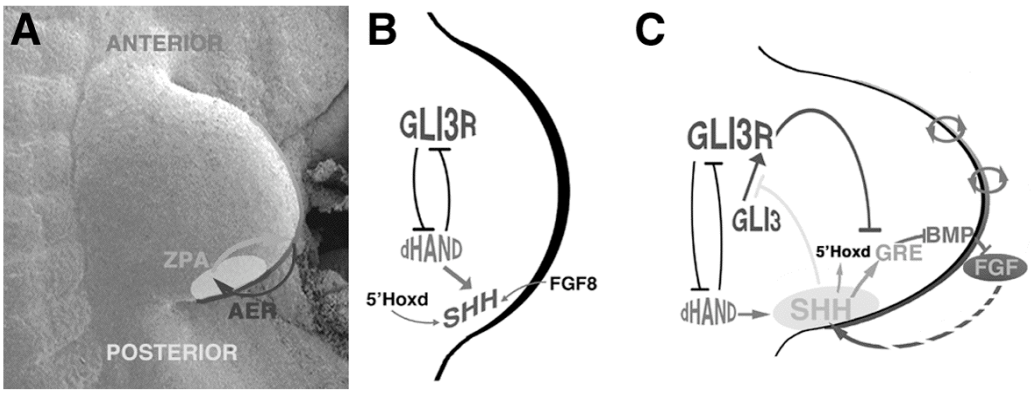

Fig.1 Limb bud development is controlled by epithelial-mesenchymal signaling interactions.
Limb bud outgrowth and patterning is controlled by reciprocal interactions between the zone of polarizing activity (ZPA) and the apical ectodermal ridge (AER). (B) The limb bud mesenchyme is pre-patterned before SHH activation. Activation of *Shh* expression domain depends on GLI3R/dHAND interactions, 5'Hoxd genes in the posterior limb bud mesenchyme and FGF8 signaling from the AER. (C) The SHH/FGF feedback loop controls distal limb bud outgrowth.

1.2 The ZPA: function and establishment

The polarizing region (ZPA) was discovered when Saunders and Gasseling (1968) grafted the posterior part of the limb bud mesenchyme to an ectopic anterior location. Such ectopic grafting of posterior ZPA mesenchyme induces mirror image duplications of the distal limb skeletal elements (Panman and Zeller, 2003). These experiments suggest that the ZPA functions as a classical organizer to regulate distal limb bud morphogenesis (Spemann, 2001, reprinted). In 1993, Sonic Hedgehog (SHH) was identified as the molecule mediating polarizing activity (Riddle et al., 1993). The analysis of *Shh* deficient mice has shown that SHH is essential for vertebrate development (Chiang et al., 1996). In particular, *Shh* deficient mice exhibit severe distal limb truncations as only a rudimentary zeugopod is present and the autopod forms only one rudimentary digit (Chiang et al., 2001).
Several lines of evidence support the notion that retinoic acid activity is required for distal limb bud patterning. In particular, analysis of *Raldh2* deficient mouse embryos shows that retinoic acid participates in activation of *Shh* expression by the ZPA (Niederreither et al., 1999). Limb bud development in *Raldh2* deficient embryos can be rescued in a dose-dependent fashion by administration of retinoic acid (Niederreither

et al., 2002). Recently, Zakany et al. (2004) demonstrated that 5'Hoxd genes are restricted posteriorly in the emerging limb bud and that misexpression of 5'Hoxd genes causes activation of *Shh* expression in the anterior limb bud mesenchyme. Therefore, 5'Hoxd genes have been implicated in positioning the *Shh* expression domain in the posterior limb bud mesenchyme (Zakany et al., 2004; Fig. 1B).
The transcription factor dHAND is required for activation of *Shh* expression (Charite et al., 2000). Indeed, *dHand* is initially expressed throughout the lateral plate mesoderm, but is restricted to the posterior limb bud mesenchyme during onset of limb bud outgrowth (Charite et al., 2000; Fernandez-Teran et al., 2000). Concurrently, expression of the *Gli3* transcriptional regulator is activated in the anterior limb bud. Inactivation of *Gli3* causes polydactyly and establishment of an anterior ectopic *Shh* expression domain. te Welscher et al. (2002a) established that mutual genetic repression between posterior dHAND and anterior GLI3 in the early limb bud pre-patterns the mesenchyme prior to and independent of *Shh* expression (te Welscher et al., 2002a). This antagonistic interaction most likely directs *Shh* activation in the posterior limb bud mesenchyme (Fig. 1B). Once *Shh* expression is correctly activated in the posterior mesenchyme, SHH signaling coordinates limb bud outgrowth and patterning in concert with FGF signaling by the AER (Fig. 1C).

1.3. Limb bud outgrowth is controlled by the SHH/FGF feedback loop

It was demonstrated that SHH signaling from the ZPA and FGF signaling from the AER interact to promote and maintain limb bud development (Laufer et al., 1994; Niswander et al., 1994). It was also postulated that the mesenchyme produces a factor that is required to maintain the AER in an active state (Saunders, 1977). Using a classical mutation called *limb deformity* (*ld*), Zuniga et al., (1999) proposed that the BMP antagonist Gremlin is the apical ectodermal ridge maintenance factor (AEMF; Fig. 1C). This conclusion is based on several observations: first of all, *Gremlin* is expressed in the posterior mesenchyme underlying the AER and SHH signaling is able to up-regulate *Gremlin* expression in wild type limb buds (Zuniga et al., 1999). Secondly, *Gremlin* expression, like expression of FGFs in the posterior AER, is absent from *ld* mutant limb buds (Zuniga et al., 1999). However, *Shh* expression is still induced but fails to be maintained in *ld* deficient limb buds, which corroborates the role of FGF signaling in maintaining *Shh* expression in the posterior limb bud mesenchyme. Interestingly, grafts of *Gremlin*-expressing cells into *ld* mutant limb buds are sufficient to re-activate *Fgf4* expression in the posterior AER and to restore the SHH/FGF feedback loop (Zuniga et al., 1999).

1.4. Distal limb bud patterning by the morphogenetic SHH signal

The observations discussed above suggest that SHH signaling is required to maintain a functional AER that allows distal progression of limb bud morphogenesis. In fact, SHH signaling primes the distal limb bud mesenchyme to form digits, and activation of BMP2 signaling in response to SHH in the posterior mesenchyme specifies digit identities in a graded fashion (Drossopoulou et al., 2000). Furthermore, Dahn and Fallon (2000) showed that manipulation of interdigital BMP levels during later limb bud development disrupts digit identities despite the fact that previous studies indicated that they were supposedly specified much earlier. These studies suggested that initial

positional information is set by SHH signaling and digit identities are determined by combined SHH and BMP signaling (Niswander, 2003; Panman and Zeller, 2003; Tickle, 2003).
However, recent unexpected results question the proposed role of SHH signaling in determination of digit identities. *Gli3* deficient mouse embryos display polydactyly with associated loss of digit identities. Interestingly, *Gli3* is present in the limb bud mesenchyme as both activator and repressor forms. Processing of the Gli3 protein from an activator (Gli3A) to a repressor form (Gli3R) is controlled by SHH signaling (Wang et al., 2000). This results in a gradient of Gli3R versus Gli3A in the limb bud mesenchyme with high Gli3R levels in the anterior limb bud (Wang et al., 2000). Genetic analysis established that inactivation of one or both *Gli3* alleles in *Shh* deficient mouse embryos restore distal limb bud development progressively. The digit phenotypes of the *Shh*/*Gli3* double mutant embryos phenocopies the one of *Gli3* mutant embryos, indicating that digit formation and identity is controlled by mutual antagonistic interaction of SHH with Gli3R function (Litingtung et al., 2002; te Welscher et al., 2002b). Interestingly, in *Shh* mutant embryos, *Gli3* is present as repressors throughout the limb bud, confirming the need to repress Gli3R formation in the mesenchyme to enable distal progression of limb bud morphogenesis (te Welscher et al., 2002b; Tickle, 2003). Finally, Chen et al. (2004) showed that Hoxd proteins, in particular Hoxd12, genetically and physiologically interact with the Gli3R form. The [Gli3R-Hoxd] protein complex now acquires an activator potential that enables digit morphogenesis (Chen et al., 2004).

1.5. BMP signaling during limb bud development

BMPs are expressed during all stages of limb development in dynamic patterns (Hogan, 1996) and BMP signaling has been implicated in regulating limb development from AER induction onwards. During initiation of limb bud development, expression of several BMP ligands, including *Bmp2, 4* and *7* in the ventral ectoderm together with the transcription factor *Engrailed1* (*En1*) establishes ventral fate by restricting *Wnt7a* expression to the dorsal ectoderm. Fate map and misexpression studies indicate that En1 is also required for AER formation. In mouse embryos lacking *En1*, a broad and flattened AER is formed (Loomis et al., 1996; Tickle and Munsterberg, 2001). Interestingly, perturbation of BMP signaling during limb bud initiation causes dorso-ventral limb patterning defects due to loss of *En1* expression in the ventral ectoderm (Ahn et al., 2001; Pizette et al., 2001). Furthermore, inactivation of the BMP receptor isoform IA disrupts AER formation as revealed by the loss of *Fgf8* expression from the early limb bud ectoderm (Ahn et al., 2001). Misexpression of the BMP targets *Msx1* in the limb bud ectoderm causes formation of an ectopic AER-like structure that expresses *Fgf8* (Pizette et al., 2001). In summary, these results demonstrate that BMP signaling is required for dorso-ventral patterning through activation of *En1* and participates in AER formation through activation of *Msx* and subsequently *Fgf8* expression in the ventral ectoderm.
During SHH-mediated progression of limb bud morphogenesis, inhibition of BMP activity is crucial to allow establishment and maintenance of the SHH/FGF feedback loop (see before). During late limb bud morphogenesis SHH/FGF feedback signaling is terminated and the AER begins to regress. The mechanism of AER regression is

largely unknown, but an involvement of BMP signaling is likely (Pizette and Niswander, 1999). Finally, BMP ligands also participate in late limb morphogenesis where they seem to fulfill dual functions. In particular, they induce programmed cell death of the undifferentiated interdigital mesoderm, which is necessary to shape individual digits (Merino et al., 1999a; Rodriguez-Leon et al., 1999; Zuzarte-Luis and Hurle, 2002). However, BMPs also promote growth of the differentiating cartilage elements (Li and Cao, 2003; Macias et al., 1997; Mariani and Martin, 2003; Reddi, 2000). During chondrogenesis, BMP ligands are required to initiate cartilage formation and regulate chondrocytes differentiation (Li and Cao, 2003; Zhao, 2003).

2. Molecular control of branching morphogenesis during lung development

The developing lung is used as a model system to study the molecular mechanism controlling branching morphogenesis and epithelial-mesenchymal signaling interactions during organogenesis. In mouse embryos, the two lung buds, which originate as an epithelial outgrowth from the ventral foregut, undergo stereotypic dichotomous and lateral branching as the epithelium invades the surrounding splanchnic mesenchyme. The formation of the bronchiolar tree is completed at the end of the pseudoglandular stage. During this period, epithelial cell differentiation and formation of air sac structures (future alveoli) is initiated and will proceed during the subsequent stages, called canalicular and saccular stages. After birth, the pre-alveolar structures expand considerably and are further subdivided into alveoli by secondary septation. The terminal differentiation of the distal respiratory epithelium is associated with the production of surfactant proteins and continues until about four weeks after birth (Ten Have-Opbroek, 1991; Fig. 2).

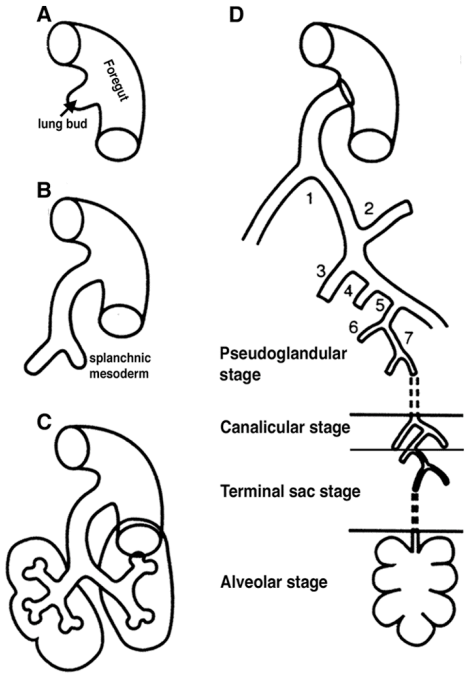

Fig.2 Key events during the mouse lung organogenesis.
(A) The primitive lung anlagen emerging from the ventral surface of the primitive foregut at E9.5.
(B) The two primary bronchial buds elongate and branch as they interact with the splanchnic mesoderm at E10.5.
(C) The primitive lobar bronchi branching from the primary bronchi at E11.5.
(D) A schematic rendering of the four developing stages of mouse embryonic lungs. (From *Warburton et al., 2000*).

2.1. Key regulators of lung branching morphogenesis

Genetics analysis of the FGF10 signaling molecule has revealed its essential functions during branching morphogenesis. *Fgf10* is specifically expressed in the distal lung mesenchyme and signals to the epithelium through the ubiquitously expressed FGF receptor 2. During the pseudoglandular stage, *Fgf10*-expressing cells locate the prospective sites of budding (Bellusci et al., 1997b). The resulting "turn on and off" pattern indicates that FGF10 is involved in the spatial control of lung bud formation. Indeed, *Fgf10* deficient mice lack lungs, due to a defect in primary branching (Min et al., 1998; Sekine et al., 1999). Furthermore, *in vitro* experiments indicate that FGF10 is the major signal regulating bud formation (Bellusci et al., 1997b; Park et al., 1998; Sekine et al., 1999; Fig. 3). FGF10 was proposed to determine where and when buds are induced, as it exerts a chemo-attractant effect on the epithelium and induces buds locally in lung epithelial explants separated from their mesenchyme (Park et al., 1998; Weaver et al., 2000). Moreover, FGF10 beads implanted into cultured lung organ rudiments induce ectopic budding, which indicates that tight regulation of mesenchymal *Fgf10* at the tip of the growing epithelial bud is essential for correct branching. Recently, two studies have shown that the transcription factor Tbx4 plays a critical role in regulating FGF10 signaling. Electroporation of *Tbx4* into foregut mesenchymal cells induces *Fgf10* expression and ectopic lung bud formation (Sakiyama et al., 2003). Conversely, inactivation of *Tbx4* by anti-sense oligonucleotides inhibits *Fgf10* expression and branching morphogenesis (Cebra-Thomas et al., 2003). Interestingly, *Tbx4* is expressed in the splanchnic mesoderm at the prospective site of lung bud initiation. During subsequent lung development, *Tbx4* is expressed similar to *Fgf10*. Collectively; these data support the idea that a local source of FGF10 in the distal lung mesenchyme temporally and spatially controls outgrowth and branching of the lung bud epithelium (Fig. 3).

BMP4 appears to be another important regulator of branching morphogenesis. *Bmp4* is expressed in the distal epithelium and adjacent mesenchyme of the branching airways. Epithelial *Bmp4* expression is activated after lung bud formation and expression levels increase during elongation of the lung bud (Weaver et al., 2000). BMP4 signals through its serine threonine kinase receptors ALK3 and ALK6, which are expressed by both mesenchyme and epithelium. Over expression of *Bmp4* in the distal endoderm of transgenic mice severely impairs lung development through inhibition of both epithelial and mesenchymal cell proliferation (Bellusci et al., 1996). Over expression of a dominant negative form of *ALK6* (*dnALK6*) or the BMP antagonist *Noggin* in the distal lung epithelium also disrupts lung morphogenesis as proximal markers (e.g. *CC10* and *Hfh4*) are up regulated and distal markers (e.g. *SpC*) are inhibited. These studies indicate that high levels of BMP4 actively promote distal lung morphogenesis (Weaver et al., 1999). Similar results where obtained applying the BMP antagonist Gremlin both *in vitro* and *in vivo* (Lu et al., 2001; Shi et al., 2001). Collectively, these data establish that BMP4 is part of a distal signaling center controlling cell proliferation, branching and proximo-distal differentiation (Fig. 3). Furthermore, FGF10 beads implanted into proximal lung explants up-regulate epithelial *Bmp4* expression (Lebeche et al., 1999; Weaver et al., 2000). Experimental evidence shows that BMP4 inhibits epithelial cell proliferation and prevents lung bud formation, thus antagonizing the effects of FGF10 signaling on epithelial explants

(Weaver et al., 2000). In contrast, mesenchymal *Bmp4* seems to be regulated by SHH signaling (Litingtung et al., 1998; Weaver et al., 2003). In conclusion, epithelial and mesenchymal *Bmp4* expression appears to be regulated differentially during its function in regulating lung branching morphogenesis.

Shh is expressed in the mouse lung epithelium from E9.5 onwards, with expression being highest at the distal tip. *Shh* deficient mouse embryos display severely hypoplastic lungs, which establish SHH signaling as essential for lung branching morphogenesis but not for induction of lung organogenesis. Furthermore, the primary cellular defect seems to reside in the *Ptc*-expressing mesenchyme as mesenchymal cell death is increased and cell proliferation is decreased. Finally, branching of the lung bud epithelium, but not proximo-distal axis specification is disrupted in *Shh* deficient mouse embryos (Litingtung et al., 1998; Pepicelli et al., 1998). Interestingly, Pepicelli and coworkers (1998) also reported that *Fgf10* is no longer locally restricted in the mesenchyme of *Shh* deficient embryonic lungs. Conversely, *Shh* over expression in lungs increases mesenchymal cell proliferation and inhibits *Fgf10* expression (Bellusci et al., 1997a; b; Lebeche et al., 1999; Weaver et al., 2000; Fig. 3). In addition, inactivation of *Fgf9* by gene targeting results in decreased branching morphogenesis and lung hypoplasia, most likely due to decreased *Fgf10* expression and reduced mesenchymal proliferation (Colvin et al., 2001).

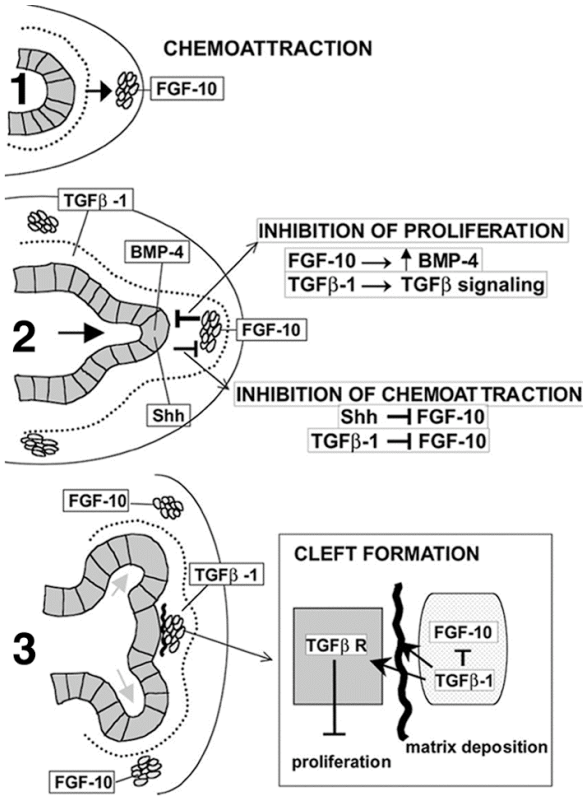

Fig.3 Control of bud formation during lung branching morphogenesis.
(1) Local expression of *Fgf10* in the mesenchyme results in chemo-attraction and epithelial growth.
(2) As the bud is induced, *Fgf10* is inhibited by *Shh* expressed at the tips and by *Tgfβ1* expressed in the sub-epithelial region. Concomitantly, proliferation is inhibited at the tips by Fgf10-mediated up regulation of *Bmp4*.
(3) These mechanisms limit lung bud outgrowth and result in cleft formation. *Fgf10*-expressing cells appear at other sites to induce a new generation of buds. At the cleft, low levels of *Fgf10* are maintained by sub-epithelial *Tgfβ1*, which also induces synthesis of extra-cellular matrix components deposited in the epithelial-mesenchymal interface and prevents local budding. (From *Cardoso, 2001*).

Another key regulatory signal of lung branching morphogenesis is TGFß1. *Tgfß1* is expressed uniformly by the sub-epithelial mesenchyme and TGFß1 proteins accumulate later at sites of cleft formation and along the proximal airways. TGFß1 promotes synthesis of extra-cellular matrix that, upon deposition at the epithelial-mesenchymal interface, may prevent local branching (Heine et al., 1990). Ectopic TGFß1 signaling inhibits epithelial branching, while expression of a dominant negative *TGFß* receptor stimulates branching morphogenesis in cultured lung organ rudiments (Zhao et al., 1996). Conversely, recombinant TGFß1 inhibits *Fgf10* expression and branching in lung culture explants (Lebeche et al., 1999; Serra and Moses, 1995; Fig. 3).

2.2. Proximo-distal lung axis specification

The proximal airways are lined with ciliated columnar epithelial cells, mucus-secreting cells and Clara cells, while the distal alveolar epithelium consists of squamous (AEC1) and cuboidal (AEC2) cells (Warburton et al., 2000). This proximo-distal axis is established during the progression of lung organogenesis. The first morphological differences between proximal and distal epithelium appear during the pseudoglandular stages. Hfh4 is a transcription factor belonging to the Hepatocyte nuclear factor family, which is expressed by the basal and ciliated cells of the proximal airways (Tichelaar et al., 1999b). *Hfh4* over expression and loss-of-function studies in the mouse show that Hfh4 is required for differentiation of columnar and ciliated epithelial cells. *Hfh4* deficient mice completely lack ciliated epithelial cells. In contrast, ectopic expression of *Hfh4* in the distal epithelium induces transdifferentiation of distal into proximal ciliated epithelial cells (Chen et al., 1998; Tichelaar et al., 1999a). Nkx2.1 is a homeodomain protein essential for lung branching morphogenesis (Kimura et al., 1996; Minoo et al., 1995; 1999). In particular, the lung epithelium of *Nkx2*.1 deficient mice lacks distal identities and is composed of proximal cells (Minoo et al., 1999). This genetic analysis shows that Nkx2.1 is essential for early branching morphogenesis and epithelial lineage determination, which occurs prior to specification of peripheral lung cell types. At the molecular level, Nkx2.1 seems to positively regulate expression of BMP4, one of the key morphoregulatory signals (see before; Zhu et al., 2004).

3. Epithelial-mesenchymal signaling controls induction of metanephric kidney development

The metanephric kidney or metanephros is the functional adult kidney in mammals. The metanephros is comprised of two main parts: the so-called nephrons, which are the mesenchymal-derived structures regulating secretion and the epithelium-derived collecting duct system, which connects the nephrons to the ureter (Saxén, 1987). In mammals, the complete urogenital system is derived from the intermediate mesoderm and three types of embryonic kidneys form in a spatially and temporally controlled manner. Around embryonic day 8 (E8.0), kidney development is initiated by formation of the Wolffian duct, an epithelial structure derived from the rostral intermediate mesoderm. Subsequently, Wolffian duct development progresses caudally and induces the pro-, meso- and metanephros successively through reciprocal epithelial-mesenchymal signaling interactions. Around E10.5, when the Wolffian duct reaches the caudal part of the embryo, the ureter buds out at about the level of the mid-hind

limb. This Wolffian duct-derived epithelium elongates towards the metanephric blastema. At this stage, the metanephric blastema, a group of undifferentiated mesenchymal cells is located in the caudal region of the nephrogenic cord. In summary, the induction and formation of the metanephros depends on the formation of the pro- and mesonephros. In particular, genes expressed by the intermediate mesoderm, which are required for formation and/or maintenance of the Wolffian duct, are also essential for metanephric development. For example, *Lim1* is expressed by the intermediate mesenchyme (Fujii et al., 1994) and *Lim1* deficient mouse embryos fail to activate *Pax2*, which is in turn also essential for metanephric kidney development (Torres et al., 1995). *Pax2*, a paired box transcription factor, is initially expressed by the intermediate mesoderm and later the Wolffian duct, the mesonephros and both compartments of the metanephros. Inactivation of *Pax2* in the mouse causes bilateral agenesis due to complete absence of the caudal Wolffian duct and thereby ureteric bud (Torres et al., 1995). Normally, the ureter elongates and invades the metanephric mesenchyme to induce its condensation. In turn, the mesenchyme triggers ureteric bud outgrowth and branching. A failure to induce metanephric mesenchyme results in an early arrest of development and elimination of the mesenchyme by apoptosis. During progression of kidney organogenesis, the ureter grows and repeatedly branches in concert with condensation of the mesenchyme (Fig. 4). Such coordination of growth and branching creates the characteristic structure of the definitive metanephric kidney. The condensing mesenchyme adjacent to the tips of the ureter aggregates and epithelializes to form the tubular structure of the nephron. During progression of tubules morphogenesis a glomerulus is formed at the end of the proximal tubule and its distal end fuses with the collecting duct system (Saxén, 1987; Fig. 4).

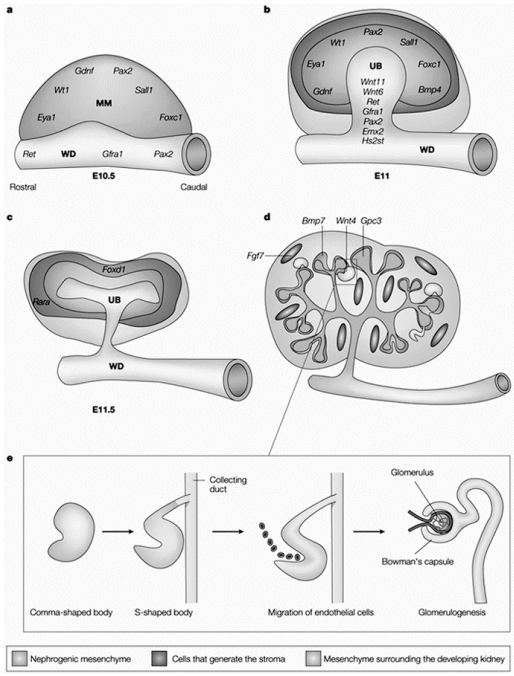

Fig.4 Morphological stage of kidney development and some of the key regulator genes involved in its development.
(a) Metanephric kidney development starts when the ureteric bud (UB) forms at about E10.5.
(b) The UB grows into the metanepheric mesenchyme (MM) and induces its condensation. (c) The condensed MM induces the UB to branch from E11.5 onwards.
(d) Metanephric kidney development proceeds through repetitive branching of the UB and MM condensation followed by mesenchymal to epithelial transformation to form the tubule of the nephron.
(e) Nephrogenesis leads to the formation of a Glumerulus. (From *Vainio and Lin, 2002*).

3.1. Molecular control of metanephric kidney induction

It remains to be established if ureteric bud formation in the caudal part of the Wolffian duct initiates metanephric development or if signals from either the Wolffian duct or the metanephric blastema trigger metanephric morphogenesis prior to appearance of a morphologically distinct ureteric bud. However, recent studies indicate that the metanephric mesenchyme is already pre-patterned prior to formation of a morphologically distinct ureteric bud (Vainio and Lin, 2002). To date, several transcription factors including Wt1, Lim1, Six1, Eya1, Pax2 and Sall1 have been found as essential for ureteric bud induction (Fig. 5). Prior to ureteric bud formation, the Wolffian duct expresses *Pax2, Lim1 and Sall1*, whereas expression of *Pax2*, *Six1*, *Eya1* and *Wt1* is activated in the metanephric blastema. Following ureteric bud formation, these mesenchymal genes are all up regulated in the induced mesenchyme and *Sall1* is activated in the mesenchyme around the tip of the ureteric bud. Mouse embryos lacking the Wilms tumor-suppressor gene (Wt1) fail to form a ureteric bud, which results in massive mesenchymal cell death and complete renal agenesis (Kreidberg et al., 1993). However, *Pax2*, *Six2* and *Gdnf* remain expressed normally in the uninduced mesenchyme (Donovan et al., 1999), indicating that the mesenchyme has been specified as nephrogenic. In contrast, the metanephric mesenchyme of *Eya1* deficient embryos lacks *Gdnf* and *Six* genes (*Six1*, *Six2*) indicating that Eya1 acts downstream of Wt1, Pax2 and upstream of Six and Gdnf (Xu et al., 1999; 2003). In *Six1* deficient metanephric mesenchyme, *Sall1* fails to be expressed indicating that Six1 is required for *Sall1* activation (Xu et al., 2003; see Fig. 5 for gene hierarchies). In *Sall1* deficient embryos, the ureteric bud is defective, as the mutant mesenchyme is able to promote tubulogenesis when recombined with wild type inducing tissues (Nishinakamura et al., 2001). Finally, analysis of *Empty spiracles 2* (*Emx2*) deficient mouse embryos provides evidence that signals from the ureteric bud are required for tubulogenesis. The mutant ureteric bud invades the metanephric mesenchyme initially but fails to branch and therefore, the mesenchyme fails to undergo condensation and tubule formation (Miyamoto et al., 1997). The ureter seems to provide signals that instruct the mesenchyme to condense and initiate tubulogenesis (Fig. 5).

One of the major mesenchymal signals controlling ureteric bud formation and outgrowth is GDNF (Glial-derived Neurotrophic Factor). GDNF was shown to signal through a receptor complex consisting of the proto-oncogene RET and its co-receptor GRFα (Cacalano et al., 1998; Durbec et al., 1996). The GDNF ligand is initially expressed by the uninduced metanephric mesenchyme and subsequently by the condensing mesenchyme. Its receptors RET and GRFα are expressed by the Wolffian duct and the invading ureteric bud (Avantaggiato et al., 1994; Hellmich et al., 1996; Pachnis et al., 1993; Towers et al., 1998). During subsequent metanephric organogenesis *Ret* expression becomes restricted to the tip of the branching ureter. Inactivation of all three genes in the mouse results in bilateral renal agenesis due to a failure to induce ureteric bud outgrowth. These results establish that the GDNF/RET/GRFα signaling pathway is required for early metanephric organogenesis (Cacalano et al., 1998; Pichel et al., 1996; Sanchez et al., 1996; Schuchardt et al., 1994; 1996; Vega et al., 1996). Moreover, tissue recombination experiments have shown that the ureteric bud epithelium of *Ret* deficient mouse embryos is not competent to respond to the metanephric mesenchyme. Moreover, misexpression or

inhibition of RET-mediated signal transduction causes defects in branching morphogenesis (Ehrenfels et al., 1999; Srinivas et al., 1999), while ectopic activation increases cell motility and migration towards a source of GDNF ligand (Tang et al., 1998). Local application of GDNF in proximity to the caudal Wolffian duct induces supranumerary ureteric buds, indicating that GDNF is sufficient to induce ureteric bud formation and branching (Pepicelli et al., 1997; Sainio et al., 1997). Interestingly, inactivation of the transcription factor *Foxc1* (*Forkhead box C1*) results in formation of a duplicated ureter. *Foxc1* is expressed in the mesenchyme and restricts *Gdnf* expression indirectly through regulation of the Eya1 transcription factor. Expression of both *Eya1* and *Gdnf* is expanded anteriorly in *Foxc1* deficient mice, and thereby additional ureteric buds are induced (Kume et al., 2000). Recently, Grieshammer and coworkers (2004) established that the SLIT/ROBO signaling pathway is also required to restrict ureteric bud formation to a single site along the Wolffian duct. The SLIT2 ligand is normally expressed throughout the Wolffian duct and its receptor *Robo2* is expressed locally by the prospective metanephric mesenchyme (Grieshammer et al., 2004). In either *Slit2* or *Robo2* deficient mouse embryos *Gdnf* is expressed broadly, which results in aberrant ectopic ureteric bud formation.

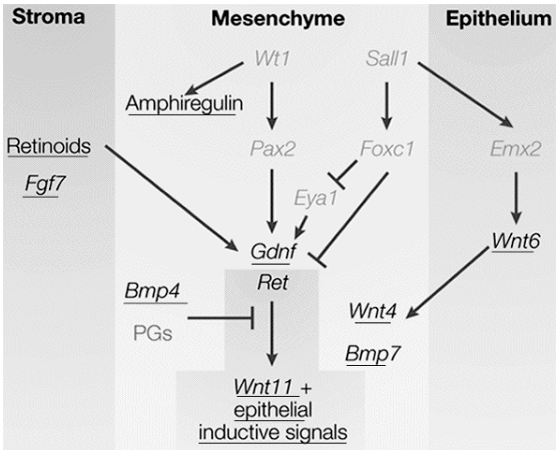

Fig.5 Model of genetic interactions during early kidney development.
Possible interactions between the different transcription factors and signaling molecules (underlying) leading to the competence of the metannephric mesenchyme and induction of ureteric bud outgrowth. These interactions are hypothetical and are based on in vivo expression data and mouse knockout mutants. (From *Vainio and Lin, 2002*).

Experimental evidence suggests that signals others than GDNF are required for ureteric bud formation and branching (Vainio and Lin, 2002). For example, BMP signaling seems critical during early kidney development. Several BMPs, including *Bmp2*, *4*, *5* and *7* are expressed during metanephric kidney development (Dudley and Robertson, 1997; Martinez and Bertram, 2003; Miyazaki et al., 2000). In particular, *Bmp7* is expressed by the Wolffian duct, the ureteric bud and subsequently by the condensing mesenchyme, suggesting a potential role in metanephric kidney induction. Ureteric bud formation and mesenchymal induction are initially normal in *Bmp7* deficient embryos. However, at E13.0, the *Bmp7* deficient metanephric mesenchyme undergoes apoptosis, revealing that BMP7 is a survival factor that allows the mesenchyme to undergo nephrogenesis (Dudley et al., 1995; Luo et al., 1995). Analysis of mice lacking one functional *Bmp4* allele revealed a role for BMP4 in

ureteric bud formation. Heterozygote mouse embryos display a low frequency of ectopic ureteric buds and collecting duct defects indicative of BMP4 activity critical for ureteric bud initiation (Miyazaki et al., 2000; 2003). Furthermore, BMP4 activity inhibits formation of supranumerary ureteric buds as induced by GDNF (Raatikainen-Ahokas et al., 2000). In contrast, over expression of a constitutively active form of the epithelial BMP receptor *ALK3* partially inhibits ureter branching and tubule formation (Gupta et al., 2000). Taken together, these studies support a critical role of BMP signaling during ureteric bud formation and branching morphogenesis. In conclusion, it is clear that metanephric kidney induction does not only depend on GDNF/RET-mediated epithelial-mesenchymal signaling but seems to involve additional signals. This issue will be addressed in the course of my studies.

4. Molecular interactions regulating BMP activity

As analysis of the BMP pathway is quite central to my studies, some of its key features are summarized in this section. BMPs are multifunctional proteins with a wide range of biological activities in various cell types. They regulate diverse processes such as growth, differentiation, chemotaxis and apoptosis and play critical roles during morphogenesis of various tissues and organs (Chang et al., 2002; Hogan, 1996; Zhao, 2003). BMPs belong to the Transforming Growth Factor ß (TGFß) superfamily (Kingsley, 1994; Zhao, 2003). BMPs were originally identified as molecules that induce bone and cartilage formation when implanted or expressed ectopically (Reddi, 1997). BMP-like signals have been identified in various species, including invertebrates such as *Drosophila* and *C. elegans*. Interestingly, the *Drosophila* homologue DPP can also induce bone and cartilage formation in mammals and conversely, mammalian BMP4 can rescue genetic defects caused by *Dpp* mutations in fruit flies (Kawabata et al., 1998). Thus, mammalian BMP and *Drosophila* DPP are functionally interchangeable. BMPs are disulfide-linked proteins, most of which encode seven cysteine residues conserved among all TGFß superfamily members. BMP ligands are produced as large precursor proteins and the C-terminal peptide forms the mature and active BMP signal following proteolitic cleavage. So far, more than 20 BMP family members have been identified in mammals (Hogan, 1996; Massague, 1998; Zhao, 2003).

4.1. BMP Receptors

BMP ligand dimers activate their cognate serine threonine kinase receptors, which are divided into BMP type I and type II receptors (BMPRI, BMPRII), both of which are required for signal transduction. To date, only one type II receptor (BMPRII) has been identified in mammals. The BMPRII binds BMP dimers only weakly in absence of BMPRI. In addition to BMPRII, Activin type II receptors (ActRIIA and ActRIIB) are also targets for certain BMP ligands such as BMP2 and BMP7. Two different type I BMP receptors, namely BMPRIA (ALK3) and BMPRIB (ALK6) have been isolated. Different BMP dimers bind BMPRIA and BMPRIB with different affinities. For example, BMP4 binds both type I receptors with similar affinities, while BMP7 binds more strongly to BMPRIB. In contrast, another BMP-like ligand, GDF5, binds only to BMPRIB. Furthermore, like Activin type II receptors, Activin type I receptors (ALK2) also interact with certain BMP ligands, such as BMP6 and 7 (Attisano and Wrana, 2002; Canalis et al., 2003; Derynck and Zhang, 2003; Kawabata et al., 1998; Massague, 1998;

Massague and Chen, 2000). BMPRII is constitutively active and activate the type I receptor by phosphorylation of its intracellular domain upon ligand binding. Signal transduction is then mediated through the type I receptor, which thus determines specificity. Subsequently, the type I receptors recruit and activate intracytoplasmic receptor-regulated SMAD proteins (Fig. 6A).

4.2. Intracellular signal transduction by SMAD proteins

The SMAD family is defined by the first members identified in invertebrates, which are the *Drosophila* MAD protein and *C. elegans* SMA protein (Derynck et al., 1996). SMAD proteins are direct substrates of type I receptor kinase and share conserved N-terminal (MH1) and C-terminal (MH2) domains connected by a proline-rich linker region. SMAD1, 5 and 8 (receptor-SMAD) belong to the same subgroup and mediate BMP signaling, whereas SMAD2, 3 transduces TGFß and activin signals. SMAD4 is common to all TGFß- and BMP-mediated signal transduction processes. Furthermore, SMAD6 and 7 lack the MH1 domain and are intracellular inhibitors of SMAD-mediated signal transduction. SMAD6 preferentially inhibits BMP signaling, while SMAD7 inhibits both TGFß and BMP signaling (Attisano and Wrana, 2002; Fig. 6A). Once a complex between receptor-SMAD and SMAD4 is formed, it translocates into the nucleus where it interacts with transcription factors responsible for regulation of targeted genes (Fig. 6A). However, TGFß and BMP ligands not only activate the classical canonical SMAD pathway but also the MAPK pathway (Fig. 6B). Currently, the functional differences between these two alternate signaling pathways remain largely unknown (Attisano and Wrana, 2002; Derynck and Zhang, 2003; von Bubnoff and Cho, 2001).

Fig.6 The BMP signaling pathway.

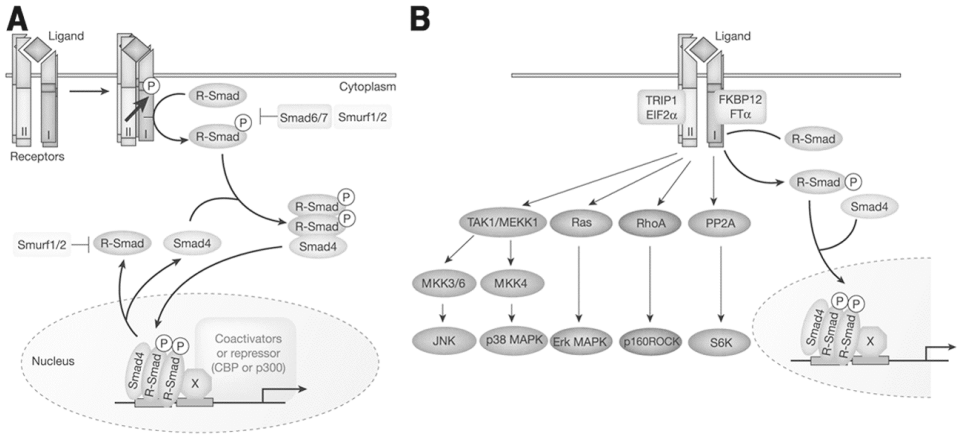

(A) Schematic representation of the canonical BMP-SMAD pathway. (B) Alternative SMAD-independent signaling pathways induce in response of BMP ligands. (From *Derynck and Zhang, 2003*).

4.3. Modulation of BMP signaling by extra-cellular antagonists

Over the last ten years much progress has been made in understanding the complex modulation of BMP signaling activity. One major finding was the realization that BMP signaling is regulated by extra-cellular BMP ligand-binding proteins that modulate BMP activity by directly competing with receptor-ligand interactions. BMP antagonists are also divided into several subgroups according to their structural similarities (Avsian-Kretchmer and Hsueh, 2003; Balemans and Van Hul, 2002; Fig. 7A).

The first of these antagonists identified, Noggin, is a secreted protein produced by the Spemann-Mangold organizer during gastrulation. Noggin antagonizes BMP activity to dorsalize ventral mesoderm and induce neural tissue (Zimmerman et al., 1996). Noggin binds directly to BMP2 and 4 with high affinity and BMP7 and GDF5 with lower affinity (Merino et al., 1999b; Zimmerman et al., 1996). A *Noggin* loss-of-function mutation in mice causes perinatal lethality due to a severely shortened body axis, a loss of caudal vertebra and limb malformations. *Noggin* deficient mice also display excess bone and cartilage formation and fail to initiate joint formation (Brunet et al., 1998). The BMP antagonist Chordin is the vertebrate orthologue of the *Drosophila* short gastrulation gene (*Sog*). Chordin binds several BMPs (Piccolo et al., 1996) and *Chordin* deficient mice exhibit inner and outer ear malformations as well as abnormalities in pharyngeal and cardiovascular organization (Bachiller et al., 2000). Mice lacking both *Noggin* and *Chordin* display severe defects in formation of the main body axes, revealing the redundant roles of these two antagonists during early development (Bachiller et al., 2000).

An additional class of BMP antagonists has recently emerged (Avsian-Kretchmer and Hsueh, 2003; Hsu et al., 1998; Pearce et al., 1999; Fig. 7A,B). All members of the CAN domain family share the CAN domain located in the C-terminal part of the protein (Pearce et al., 1999; Fig. 7B). This domain consists of 6 conserved cysteine residues that form a cystine-knot, similar to the cystine-knot of the BMP ligands, and an additional 2 cysteine residues that could form a disulfide bond (Avsian-Kretchmer and Hsueh, 2003). Interestingly, members of the CAN domain family of BMP antagonist are localized in syntenic chromosomal regions in mice and humans, pointing to their orthologous relationship (Avsian-Kretchmer and Hsueh, 2003; Fig. 7B).

Fig.7 Extra-cellular BMP antagonists.

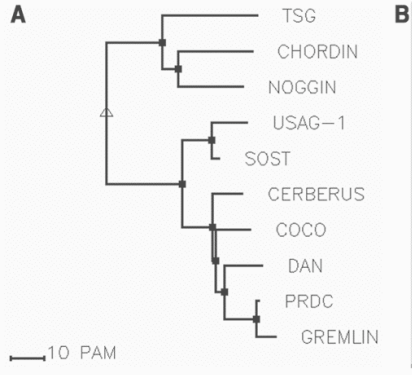

B

Gene	Human	Mouse
Gremlin/Drm/IHG-2	15q13-15 NP_037504.1	2 E4 NP_035954.1
PRDC	1q43 NP_071914.1	1 H3 NP_035955.1
Cerberus	9p22 NP_005445.1	4 C3 NP_034017.1
Coco	19 NP_689867.1	8 predicted
DAN	1p36.12 NP_005371.1	4 D3 Q61477
USAG-1	7p21 XP_166501	11 NP_079588.1
SOST	17q12 NP_079513.1	11 D AF326737_1

(A) Phylogenetic relationship of the BMP antagonists. Phylogenetic tree of human BMP antagonists based on the alignment of cystine-knot sequences.

(B) Identification of the CAN domain family. The chromosomal locations of the CAN domain family members are shown for human and mouse.

(From *Asvian-Kretchmer and Hsueh, 2003*).

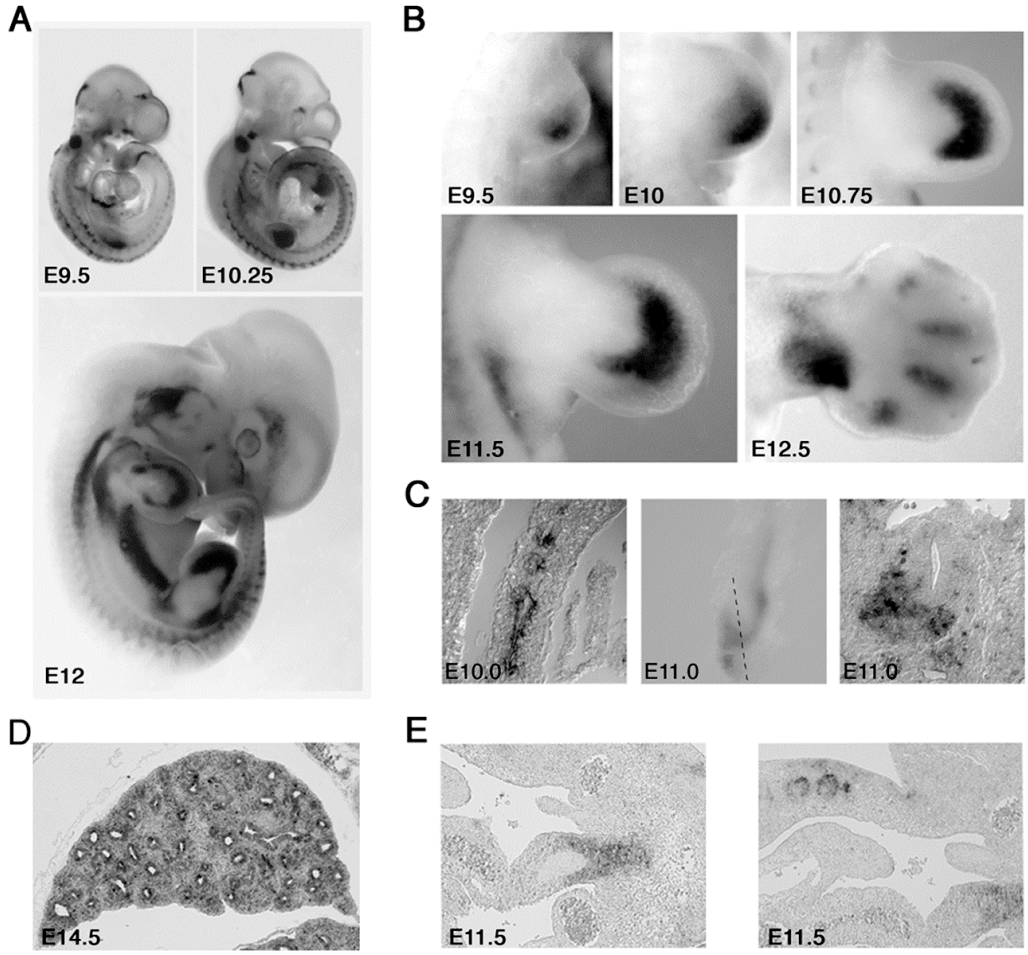

Fig.8 Gremlin expression during mouse development.
(A) Whole mount *in situ* hybridization showing the dynamic expression pattern of *Gremlin* during development. (B) Kinetics of *Gremlin* expression during limb bud development. (C) *Gremlin* is expressed during initiation of metanephric development in the Wolffian duct and metanephric mesenchyme.
(D) During lung development, *Gremlin* is expressed by both the epithelium and the mesenchyme.
(E) *Gremlin* is expressed by the mesenchyme of the hindgut and the dermamyotome of the developing somites.

The BMP antagonist Gremlin was first identified as a gene down-regulated in cells transformed by the proto-oncogene v-mos (DRM = Down-Regulated in Mos transformed cells; Topol et al., 1997). Hsu and coworkers (1998) identified the DRM homologue, *Gremlin*, from *Xenopus Leavis* as a protein capable of inducing a secondary axis in embryos. Despite the fact that Gremlin can act as a dorsalizing factor, this antagonist is only expressed from the tail bud stage onwards in neural crest lineages. In addition, in *Xenopus Leavis Gremlin* is expressed during pronephric development, and experimental evidence supports an important involvement in pronephric development in *Xenopus Leavis* embryos. In the mouse, *Gremlin* is

expressed from about embryonic day 8.5 onwards in a dynamic pattern during somitogenesis and in various tissues and organs, including genitalia tubercle, intestine, brain, limb buds, lungs and kidneys (Fig. 8). The BMP antagonist Gremlin is a secreted protein of 184 amino acids, which is encoded by an intron less open reading frame (ORF). However, the Gremlin gene is comprised of two exons, the first one is non-coding and is located about 10kb upstream of coding exon 2 on mouse chromosome 2 (Zhang et al., 2000). Evidence for a critical role of the BMP antagonist Gremlin during limb bud morphogenesis was obtained prior to the start of my PhD thesis (Capdevila et al., 1999; Merino et al., 1999c; Zuniga et al., 1999). In particular, limb bud outgrowth and patterning is controlled by the SHH/FGF feedback loop (see above). Zuniga et al. (1999) proposed that Gremlin is most likely required to relay the SHH signal from the posterior mesenchyme to the AER. Furthermore, evidence for an involvement of Gremlin in lung morphogenesis (Lu et al., 2001; Shi et al., 2001) has also been suggested. Experimental evidence suggest that BMP signaling can induce *Gremlin* expression pointing to a possible auto-regulatory loop involving activation of this BMP antagonist (Pereira et al., 2000).
Interestingly, *Gremlin* is not expressed in transformed cells and over expression of *Gremlin* in tumor cells reduces their *in vivo* tumorigenicity (Chen et al., 2002; Topol et al., 1997; 2000). Moreover, Gremlin induces transcription of the cell cycle inhibitor $p21^{Cip1}$, which suggests that Gremlin may act as a tumor suppressor gene (Chen et al., 2002). Human Gremlin maps on chromosome 15 in a locus that is associated with metastatic carcinomas and breast cancer (Topol et al., 2000). Human Gremlin has been identified as a gene induced by high glucose in mesanglial cells and *Gremlin* expression is also increased during diabetic nephropathy (Lappin et al., 2000; McMahon et al., 2000).

5. Aim of the thesis

The BMP signaling pathway is one of the major signaling pathways required for vertebrate organogenesis. BMP signaling activity is fine-tuned in a temporally and spatially regulated manner. Several extra-cellular BMP antagonists play a major role in this fine-tuning by modulating BMP activity negatively by binding to the BMP ligands and sequestering them from the receptor (see above).
In my studies, I have analyzed the functions of the BMP antagonist Gremlin during embryonic development and organogenesis. To address this question, I have generated a loss-of-function mutation using homologous recombination in mouse ES cells. *Gremlin* deficient mouse embryos have allowed me to analyze BMP signaling activity during epithelial-mesenchymal signaling in development. Analysis of *Gremlin* mutant embryos reveals that this BMP antagonist is not required for early development, but is essential for epithelial-mesenchymal signaling during organogenesis. *Gremlin* deficient mouse embryos display pleiotropic phenotypes affecting limb, kidney and lung organogenesis. My results reveal that Gremlin is required for propagation of morphogenetic signals during progression of organogenesis. Finally, in chapter 4 we demonstrate that, unlike previously published, the *ld* limb phenotype is not caused directly by disruption of the *Formin* gene but is due to disruption of a novel type of cis-regulatory region that controls transcription of *Gremlin* expression in the posterior limb mesenchyme.

CHAPTER 2
Roles Of Gremlin During Early Limb And Kidney Development

Gremlin-mediated BMP antagonism induces the epithelial-mesenchymal feedback signaling controlling metanephric kidney and limb organogenesis

Odyssé Michos[1,2], Lia Panman[2], Kristina Vintersten[3,5], Konstantin Beier[4], Rolf Zeller[1] and Aimée Zuniga[1]

[1]Developmental Genetics, Dept. of Clinical-Biological Sciences (DKBW), University of Basel Medical School, c/o Anatomy Institute, Pestalozzistrasse 20, CH-4056 Basel, Switzerland, [2]Dept. of Developmental Biology, Utrecht University, Padualaan 8, NL-3584CH Utrecht, The Netherlands, [3]Transgenic Service, EMBL, Meyerhofstrasse 1, D-69117 Heidelberg, Germany, [4]Dept. of Histology, Anatomy Institute, Pestalozzistrasse 20, CH-4056 Basel, Switzerland.
[5]Present address: Mount Sinai Hospital, Samuel Lunenfeld Research Institute, Stem Cell Mutagenesis Laboratory, 600 University Avenue, Toronto, Ontario M5G1X5, Canada.

Development. 2004 Jul;131(14):3401-10. Epub 2004 Jun 16.

1. Summary

Epithelial-mesenchymal feedback signaling is key to diverse organogenetic processes such as limb bud development and branching morphogenesis in kidney and lung rudiments. This study establishes that the BMP antagonist Gremlin is essential to initiate these epithelial-mesenchymal signaling interactions during limb and metanephric kidney organogenesis. A *Gremlin* null mutation in the mouse generated by gene targeting causes neonatal lethality due to lack of kidneys and lung septation defects. In early limb buds, mesenchymal Gremlin is required to establish a functional apical ectodermal ridge and the epithelial-mesenchymal feedback signaling that propagates the Sonic Hedgehog morphogen. Furthermore, Gremlin-mediated BMP antagonism is essential to induce metanephric kidney development as initiation of ureter growth, branching and establishment of RET/GDNF feedback signaling are disrupted in *Gremlin* deficient embryos. As a consequence, the metanephric mesenchyme is eliminated by apoptosis like the core mesenchymal cells of the limb bud.

2. Introduction

Vertebrate organogenesis is orchestrated by signaling centers with organizer properties that coordinate cell proliferation and survival with cell specification and differentiation. Signaling by cells with special organizer properties instructs undetermined neighboring cells with respect to their fate and differentiation potential. Such reciprocal epithelial-mesenchymal signaling interactions control growth and patterning of morphologically very diverse embryonic structures including limbs, kidneys and lungs in vertebrates. In particular, the molecular epithelial-mesenchymal signaling interactions regulating branching morphogenesis have recently provided novel insights into how tissues are organized in space as organogenesis proceeds (Affolter et al., 2003). Two models of paradigmatic value to study morphogenetic epithelial-mesenchymal signaling interactions in vertebrate embryos are the limb bud (Tickle, 2003) and branching morphogenesis of the ureter during kidney organogenesis (Vainio and Lin, 2002). In particular, two main signaling centers control limb bud development, the *Sonic Hedgehog* (*Shh*)-expressing polarizing region, which is located in the posterior limb bud mesenchyme, and the apical ectodermal ridge (AER), a differentiated columnar epithelium expressing different types of signaling peptides. SHH signaling by the polarizing region controls patterning of distal limb structures and its expression is regulated by Fibroblast growth factor (FGF) signaling from the AER (SHH/FGF feedback loop; Panman and Zeller, 2003). Genetic analysis in the mouse indicates that the AER expressed FGF, such as FGF8 and FGF4, cooperate to activate and positively regulate *Shh* expression in the posterior limb bud mesenchyme (Lewandoski et al., 2000; Moon and Capecchi, 2000; Sun et al., 2002). The bone morphogenetic protein (BMP) antagonist Gremlin (Hsu et al., 1998) is a cystine-knot protein belonging to the CAN domain family that antagonizes preferentially BMP2 and BMP4 (Avsian-Kretchmer and Hsueh, 2003). *Gremlin* is expressed by a subset of SHH responsive mesenchymal cells and has been implicated in transducing the SHH signal to the posterior AER. This results in activation of *Fgf4* expression and establishment of the SHH/FGF4 feedback loop (Capdevila et al., 1999; Zuniga et al., 1999).

In addition to the limb bud, *Gremlin* is expressed by a variety of embryonic structures including lung and kidney rudiments (Chapter 1, Fig. 8). Development of the definitive metanephric kidney is initiated by formation and growth of the ureteric bud. As the ureteric bud invades the metanephric mesenchyme, it induces condensation and nephrogenesis through reciprocal interactions (Saxén, 1987). Genetic analysis in the mouse shows that the Wt1 and Pax2 transcription factors (Kreidberg et al., 1993; Torres et al., 1995) control the induction of metanephric development. In contrast, the extra-cellular signals that trigger ureteric bud formation in the posterior part of the Wolffian duct and initiate ureter growth and branching have so far remained largely elusive. The tips of the invading ureter express the tyrosine kinase receptor RET (Pachnis et al., 1993; Towers et al., 1998), whereas RET ligand GDNF is expressed in the condensing metanephric mesenchyme (Hellmich et al., 1996; Towers et al., 1998). Genetic analysis has established that the epithelial-mesenchymal signaling interactions mediated by RET and GDNF are essential for metanephric development (Vainio and Lin, 2002). BMP signaling has also been implicated in metanephric development as potential regulator of ureter growth, branching and nephrogenesis (Dudley et al., 1995; Luo et al., 1995; Martinez and Bertram, 2003; Miyazaki et al., 2000; Raatikainen-Ahokas et al., 2000). In particular *Bmp4*, which is expressed by the mesenchyme surrounding the Wolffian duct and ureter stalk seems to fulfill a dual function during early metanephric development. Heterozygous *Bmp4* mutant mouse embryos display a variable kidney phenotype characterized by defects in ureteric epithelium growth and induction of ectopic ureter branching (Miyazaki et al., 2000; Raatikainen-Ahokas et al., 2000). These studies have also provided evidence that BMP signaling regulates ureteric bud initiation and branching. An involvement of BMP antagonism has been postulated, but the relevant antagonist(s) remained to be identified (Miyazaki et al., 2000). To study the essential functions of the BMP antagonist Gremlin, we have deleted the Gremlin open reading frame (ORF) by homologous recombination in mouse ES cells. Here, we report that *Gremlin* deficient mice die shortly after birth due to disruption of kidney and lung organogenesis. During limb bud development, Gremlin is required for survival of core mesenchymal cells and to establish a functional AER expressing different types of signals, which regulate *Shh* expression and progression of limb bud morphogenesis. During kidney organogenesis, Gremlin is required to initiate ureter growth and branching that in turn induces metanephric nephrogenesis. Together, these results reveal a common and essential role of Gremlin-mediated BMP antagonism in initiating dynamic epithelial-mesenchymal signaling.

3. Materials and methods

3.1. Generation of the *Gre*$^{\Delta ORF}$ null allele

We generated the targeting vector using a 4.8kb NdeI-XbaI and a 5.6kb NsiI-NsiI *Gre* genomic fragment isolated from a 129/SvJ Lambda FIXII library (Stratagene). We inserted an IRES-*LacZ* gene and a PGK-*Neo*^{R} cassette flanked by two *lox*P sites in the same transcriptional orientation as the Gremlin gene. R1 ES cells were electroporated with the NotI linearized targeting vector and screened by genomic Southern with an NsiI-EcoRI probe mapping outside the 3'homology arm (Fig. 1A). 35 homologous recombined ES-cell clones were obtained at a frequency of 10.8%. Correct

recombination resulting in the deletion of the entire 552 bases Gremlin ORF encoded by exon 2 and of 132 bases of the 3'UTR was confirmed by extensive Southern blot and PCR analysis. ES cells carrying the *Gre*$^{\Delta ORF}$ null allele were injected into C57BL/6 blastocysts and following germline transmission, the mice were maintained in mixed B6;129S and CD1 backgrounds. PCR genotyping was used for all subsequent studies to allow specific detection of both the wild type and *Gre*$^{\Delta ORF}$ alleles. The floxed PGK-*neo*^{R} gene was removed by crossing *Gre*$^{\Delta ORF}$ heterozygous mice with the *Cre* deleter strain. The sequence of the murine Gremlin locus was obtained from the UCSC Genome Bioinformatics Website (http://genome.ucsc.edu/) and analyzed using the DNA Strider 1.3^{TM} program. The *Gre*$^{\Delta ORF}$ mutation was crossed into 129S3/SvImJ, C57BL/6 and CD1 strains as the penetrance of the kidney phenotype depends on genetic background. In the 129S and CD1 backgrounds, the kidney phenotype is fully penetrant (Fig. 2B).

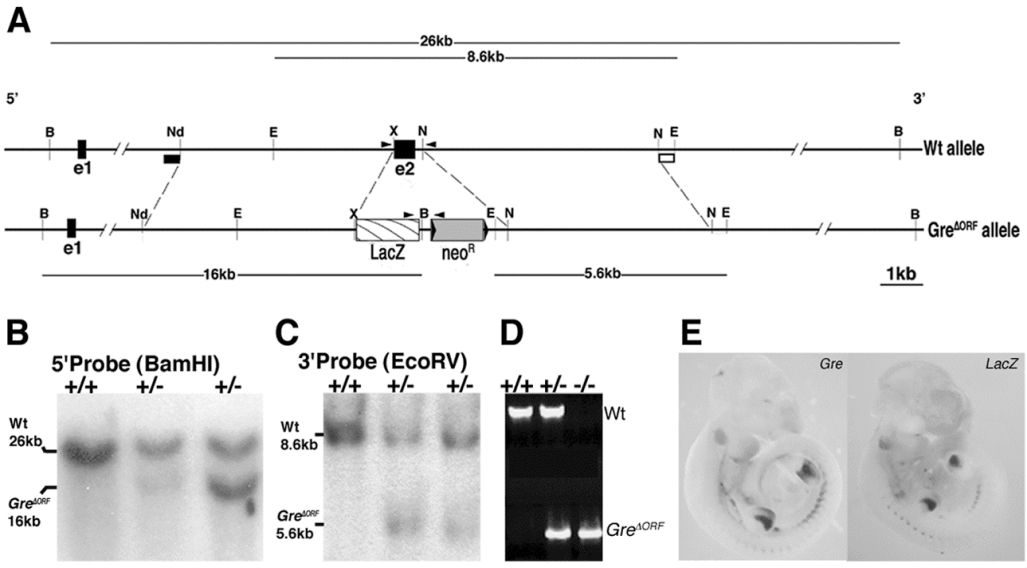

Fig.1 Generation of a Gremlin loss-of-function mutation by gene targeting.
Scheme: The *Gre*$^{\Delta ORF}$ loss-of-function allele was generated by homologous recombination in ES cells. The entire ORF encoded by exon 2 (e2) was replaced with an IRES-LacZ gene and the Neo^{R} cassette (flanked by *lox*P sites indicated by black triangles). Exon 1 (e1) is non-coding and located 8.5kb upstream of exon 2 (UCSC). The 5' and 3'genomic probes used to screen ES-cell clones by Southern blotting are indicated by black and white boxes, respectively. Thin black lines indicate the sizes of the expected genomic bands detected by these probes. Arrowheads indicate the primers used to detect both wild type (Wt) and mutant alleles (*Gre*$^{\Delta ORF}$). The relevant restriction enzyme sites are indicated as follows: B: BamHI, E: EcoRV, N: NsiI, Nd: NdeI, X: XbaI. (B,C) Analysis of wild type (+/+) and correctly targeted heterozygous (+/-) ES-cell clones by Southern blotting using 5' and 3'genomic probes. (D) PCR genotyping of embryos of F2 littermate embryos. (E) Whole mount in situ hybridization using *Gre*$^{\Delta ORF/+}$ embryos at embryonic day 11.0 reveals the identical distribution of *Gremlin* and *LacZ* transcripts.

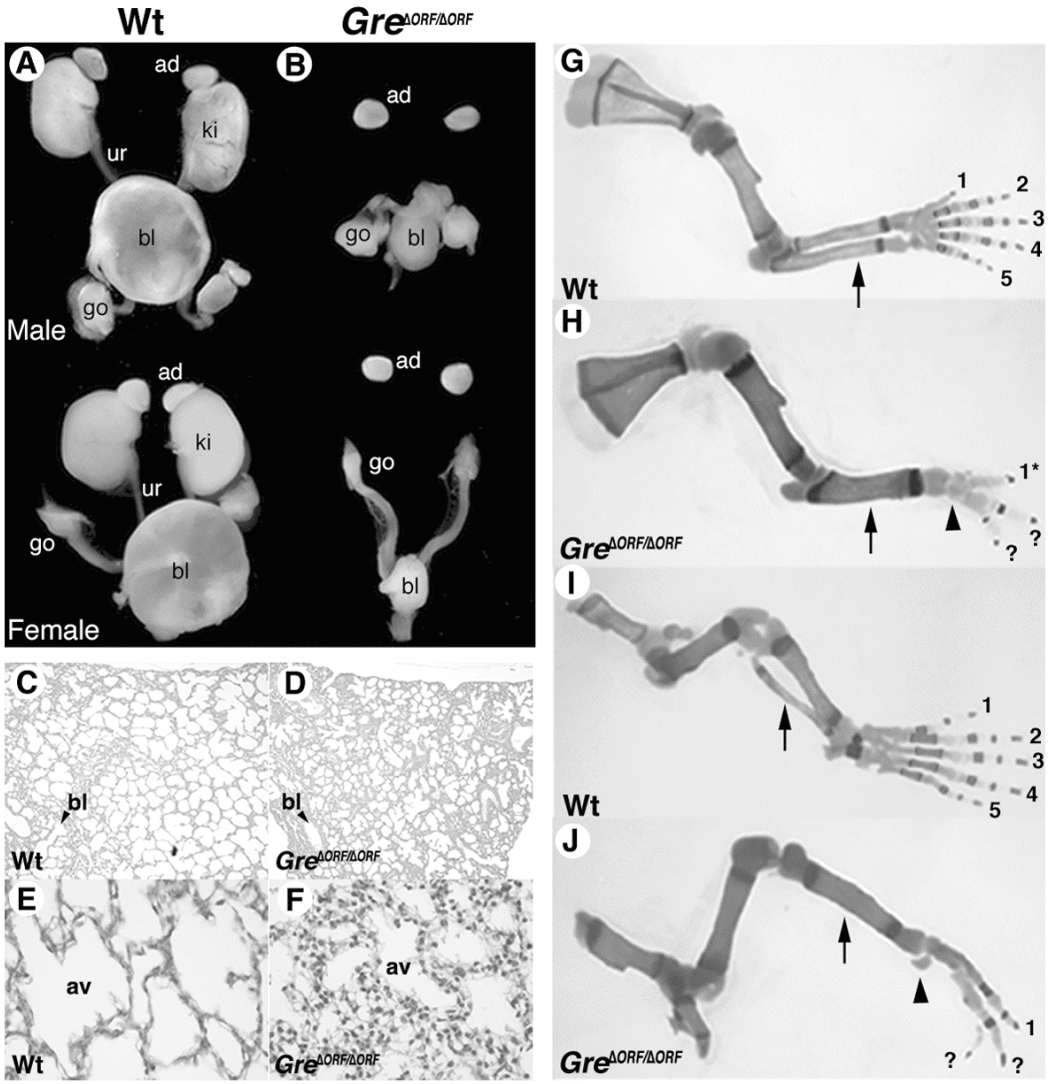

Fig.2 *Gremlin* deficiency causes neo-natal lethality due to renal agenesis and lung defects in combination with distal limb defects.

(A,B) Urogenital defects in *Gre*$^{\Delta ORF}$ newborn mice. Mutant mice display bilateral agenesis of the kidney (ki) and ureter (ur). Note that gonads (go) and adrenal glands (ad) form correctly, while the bladder (bl) is not filled in mutant mice. (C-F) Lung defects in newborn *Gremlin* deficient mice. (C,D) Transversal histological section through the lung of a newborn wild type mouse and *Gremlin* deficient mouse at the level of the heart. (E,F) High magnification view of a longitudinal section through the lung of a wild type newborn mouse and a *Gremlin* deficient newborn mouse. av: alveoli, bl: bronchiole. (G-J) Limb skeletal abnormalities in *Gre*$^{\Delta ORF}$ newborn mice. (G,H) fore limbs, (I,J) hind limbs. Arrows point to the zeugopod and arrowheads to the metacarpal bones. Digit numbers are reduced and identities lost in *Gre*$^{\Delta ORF/\Delta ORF}$ limbs. Asterisk indicates a fused digit 1; question marks indicate posterior digits with unclear identities.

3.2. Molecular and morphological analysis of embryos and newborn mice

Embryos and newborn mice were PCR genotyped and accurately staged by determining their somite numbers. Whole mount and section RNA *in situ* hybridization were performed as previously described (Dono et al., 1998; Zuniga et al., 1999) using digoxygenin-UTP labeled anti-sense riboprobes. Apoptotic cells were detected *in situ* by incorporating fluorescein-dUTP into fragmented DNA using terminal transferase (Roche Diagnostics). For histological analysis, sections were cut from formalin-fixed and paraffin-embedded material and stained with haematoxylin and eosin using standard protocols. For scanning electron microscopy, embryos were fixed in 1% gluteraldehyde (Sigma) for one hour at 4°C and processed for SEM.

3.3. *In vitro* grafting and culturing of mouse limb buds (trunk cultures)

Mouse fore limb buds were cultured and grafted as described (Zuniga et al., 1999) with the following modifications. Trunks with attached fore limb buds were isolated from either wild type, heterozygous or *Gremlin* deficient embryos. Embryos were staged by counting somites and genotyped by PCR. Spherical cell aggregates were grafted into the fore limb buds and trunks and were cultured for 15hours in serum free medium in 6.5% CO_2 at 37°C. The culture medium was prepared by supplementing high glucose DMEM (GIBCO BRL) medium, with L-glutamine, penicillin/streptomycin, non-essential amino acids, sodium pyruvate, D-glucose, L-ascorbic acid, lactic acid, D-biotin, vitamin B12 and PABA. QT6 fibroblast cells expressing *Shh* and *Gremlin* under control of the CMV promoter were prepared using standard calcium phosphate transfection (Zuniga et al., 1999). One day after transfection, spherical cell aggregates were prepared by plating cells at high density on bacterial plates. The following day cells were treated with mitomycin-C for one hour to block proliferation. After washing the cell aggregates extensively, they were grafted into recipient limb buds (a detailed protocol for media preparation, limb bud grafting and culturing is available upon request).

4. Results

4.1. Disruption of the *Gremlin* ORF results in multiple organ defects causing neonatal lethality

The second exon of the *Gremlin* gene, which encodes the complete ORF, was inactivated by homologous recombination in R1 ES cells as shown in Fig. 1A. The complete *Gremlin* coding exon 2 was deleted and replaced by a *LacZ* marker and a *Neomycin* resistance (Neo^R) gene flanked by two *lox*P sites. Correctly targeted ES-cell clones were identified by Southern blot screening (Fig. 1B,C) and 2 independent clones were used to generate $Gre^{\Delta ORF}$ mice (Fig. 1D). Heterozygous mice of both strains appear normal and the distribution of *Gremlin* and *Gre-LacZ* fusion transcripts (Fig. 1A) are identical (Fig. 1E). In contrast, $Gre^{\Delta ORF}$ homozygous newborn mice display limb defects (Fig. 2G-J) and die shortly after birth. Autopsy at birth reveals that $Gre^{\Delta ORF}$ homozygous newborn mice lack metanephric kidneys and ureters (compare Fig. 2A to 2B and data not shown), while the remainder of the urogenital system appears normal. In addition, newborn *Gremlin* deficient mice display respiratory

problems (dyspnoe and cyanosis) that probably contribute significantly to their early death. Indeed, septation of the lung airway epithelium is affected as numbers of differentiated alveoli are reduced in *Gremlin* deficient newborn mice (compare Fig. 2C to 2D). Furthermore, the airway epithelium remains multi-layered in comparison to wild type embryos (compare Fig. 2E to 2F). Cre recombinase-mediated removal of the Neo^R gene does not alter the phenotypes, confirming that they are due to the *Gremlin* deficiency (data not shown). As initial analysis indicated that the lung septation defects arise only during advanced lung organogenesis, the present study focuses on analyzing the early pattern defects that disrupt limb bud and kidney organogenesis.
The limb phenotypes observed in *Gremlin* deficient mice correspond to a strong and fully penetrant *ld* limb phenotype (Fig. 2G-J). The zeugopods of *Gremlin* deficient newborn mice are differentially affected as ulna and radius fuse during onset of ossification, while only one skeletal element forms in hind limbs (arrows, Fig. 2G-J). The autopods are severely truncated due to metacarpal fusions (arrowheads, Fig. 2H,J), reductions in digit numbers and loss of posterior identities together with soft tissue webbing (Fig. 2H,J and data not shown).

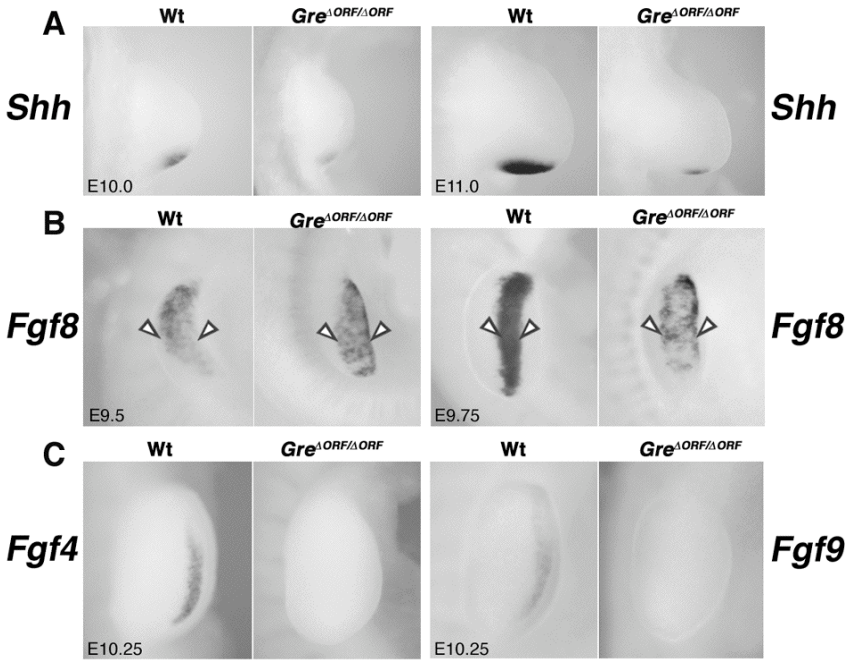

Fig.3 Gremlin is required for propagation of *Shh* in the limb bud mesenchyme and for *Fgf* expression in the AER.
(A) *Shh* expression in wild type and *Gremlin* deficient limb buds during E10.0 and E11.0. The *Shh* expression domain is activated but not propagated in mutant limb buds. Posterior is to the bottom and distal to the right. (B) *Fgf8* is activated normally, but the domain remains broader and patchy in mutant limb buds (arrowheads). (C) Neither *Fgf4* nor *Fgf9* expression is activated in mutant limb buds (E10.25). All limb buds shown are fore limb buds. In panels (B,C) posterior is to the bottom and dorsal to the left.

4.2. Mesenchymal Gremlin-mediated BMP antagonism is required for proper AER formation and epithelial-mesenchymal signaling in limb buds

During limb bud morphogenesis, the number of *Shh*-expressing cells and transcript levels increase progressively in wild type embryos (Fig. 3A; Riddle et al., 1993). In contrast, the *Shh* expression domain remains small and levels stay low in limb buds of $Gre^{\Delta ORF}$ homozygous embryos (Fig. 3A and data not shown). This failure to propagate SHH signaling has been attributed to the disruption of the SHH/FGF4 feedback loop (Haramis et al., 1995; Khokha et al., 2003; Zuniga et al., 1999). However, analysis of $Gre^{\Delta ORF}$ homozygous embryos reveals a general disruption of AER morphology and function (Fig. 3,4). Activation of *Fgf8* in the limb bud ectoderm and thereby initiation of AER formation occur normally in *Gremlin* deficient limb buds (Fig. 3B, E9.5). However, the *Fgf8*-expressing AER cells remain more spread out along the dorso-ventral ectoderm, revealing the early disruption of AER morphology in *Gremlin* deficient limb buds (Fig. 3B, E9.75). As development proceeds, *Fgf8*-expressing cells become restricted to the apex, but the domain remains patchy in mutant limb buds (Fig. 6E,G and data not shown), owing to the defects in AER morphology (Fig. 4E,F). Also, FGF signaling by the posterior AER (Martin, 1998) is completely disrupted as neither *Fgf4*, nor *9* or *17* are activated in *Gremlin* deficient limb buds (Fig. 3C and data not shown).

This general alteration of AER morphology and function could be a direct consequence of enhanced BMP signaling as it has been shown that BMP, although required to induce the AER, interfere with formation of the mature and fully functional AER (Pizette and Niswander, 1999). *Msx1* and *Msx2* are targets of BMP signaling in the limb bud and can be used as *in situ* indicators of enhanced and/or ectopic BMP signaling (Pizette et al., 2001). *Msx1* and *Msx2* are activated normally (Fig. 4A and data not shown), but subsequently ectopically expressed in the distal to anterior sub-AER limb bud mesenchyme of *Gremlin* deficient embryos (Fig. 4B and data not shown). This up regulation is indicative of enhanced BMP signaling in the sub-AER mesenchyme due to lack of Gremlin-mediated BMP antagonism. Indeed, expression of both *Bmp4* and *7* is maintained in the limb bud mesenchyme of *Gremlin* deficient embryos, while *Bmp2* is reduced from early stages onwards (Fig. 4C and for details see Fig. 5). Therefore, overall *Bmp* transcript levels appear unaffected in the sub-AER mesenchyme, where BMP signaling is enhanced due to lack of Gremlin function (compare Fig. 4B to 4C). Furthermore, *Bmp* expression is activated in the mutant AER, but not maintained during progression of limb bud morphogenesis (compare Fig. 4D to Fig. 5). Morphological analysis by scanning electron microscopy reveals that the apical ectodermal cells of $Gre^{\Delta ORF}$ homozygous limb buds fail to adopt the characteristic ridge-like morphology (Fig. 4E), although AER-type cells are present (Fig. 4F). Taken together, these results establish that induction of *Fgf8*-expressing AER cells occurs normally, while formation of a morphologically distinct and functional AER depends critically on Gremlin-mediated antagonism of BMP signaling in the distal sub-AER mesenchyme.

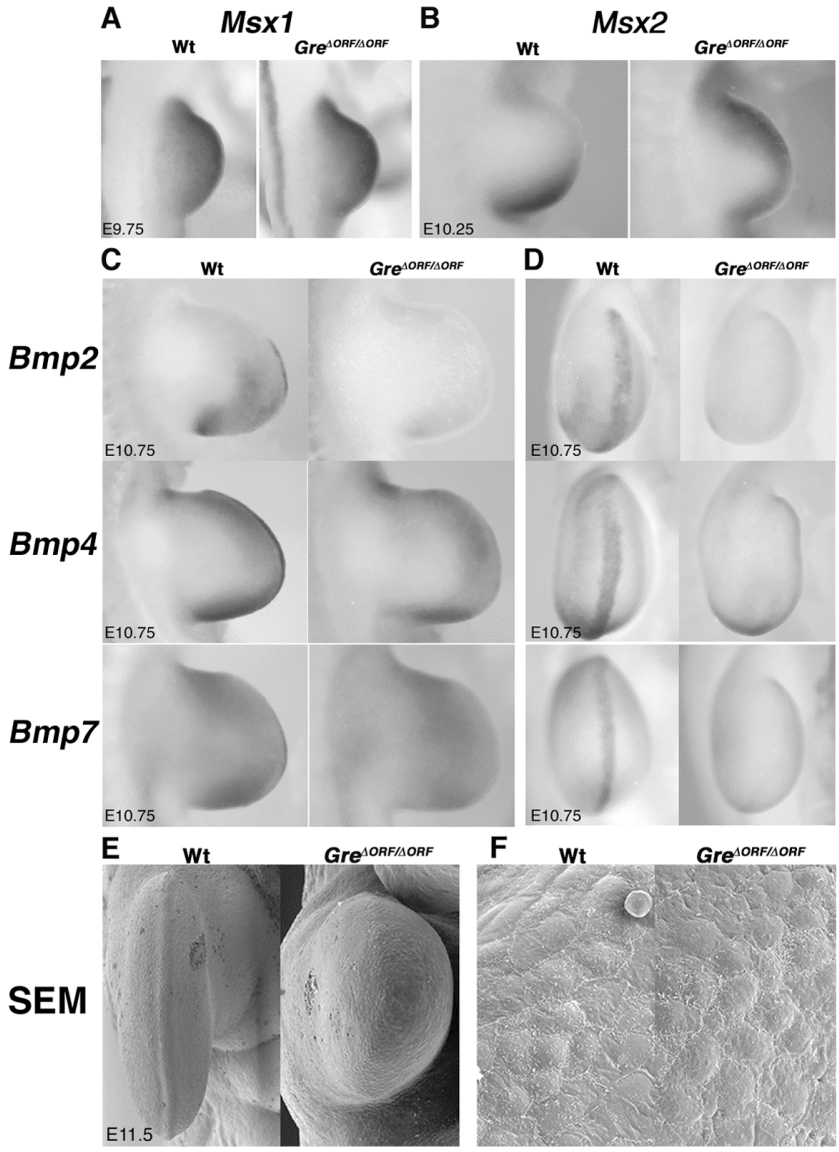

Fig.4 BMP signaling and expression in *Gremlin* deficient limb buds.
(A,B) Expression of the BMP targets *Msx1* and *Msx2* during early of limb bud development. Note ectopic *Msx2* expression in the distal to anterior limb bud mesenchyme of *Gremlin* deficient embryos. (C) Expression of *Bmp2, 4* and *7* in the limb bud mesenchyme. Mesenchymal *Bmp2* expression is significantly reduced at this stage in *Gremlin* deficient limb buds, while *Bmp4* and *7* are maintained at normal levels. (D) Expression of *Bmp2, 4* and *7* in the AER of wild type and *Gremlin* mutant fore limb buds. Expression of all three BMP is lacking from the AER of mutant limb buds. (E) Scanning electronic microscopy analysis of wild type and *Gremlin* deficient fore limb buds. Note that the AER of mutant limb buds is poorly differentiated and the antero-posterior limb bud axis is shortened in comparison to the wild type. In panel (D,E), posterior is to the bottom and dorsal is to the left. (F) High power SEM to reveal the morphology of AER-type ectodermal cells.

Particularly *Bmp2* has been considered a direct transcriptional target of SHH signaling in the mesenchyme (Drossopoulou et al., 2000). Therefore, reduced *Bmp2* expression could be a consequence of reduced SHH signaling and thus secondary to disrupting Gremlin. However, posterior grafts of *Shh*-expressing fibroblasts, capable of rescuing gene expression (Zuniga et al., 1999), fail to up-regulate *Bmp2* expression in limb buds of $Gre^{\Delta ORF}$ homozygous embryos (Fig. 6A,B). In contrast, grafts of *Gremlin*-expressing fibroblasts enhance mesenchymal *Bmp2* transcription and restore *Bmp2* expression in the AER of mutant limb buds (Fig. 6C,D). Similarly, Gremlin (Fig. 6G,H) but not SHH grafts (Fig. 6E,F) restore *Fgf8*, *Fgf4* (Zuniga et al., 1999) and *Fgf9* (data not shown) expression in the AER of mutant limb buds. These results establish that mesenchymal Gremlin modulates *Bmp2* and *Fgf8* expression positively and is required for activation of FGF in the posterior AER.

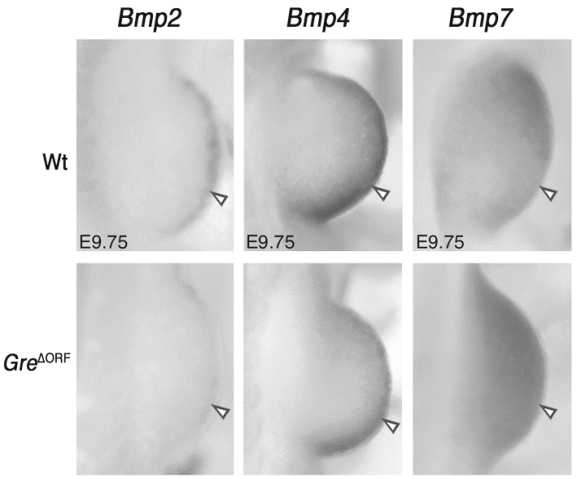

Fig.5 Bmp expression is activated normally in *Gremlin* deficient limb buds.
During embryonic day 9.5, *Bmp2* is expressed only in the AER of both wild type and $Gre^{\Delta ORF/\Delta ORF}$ limb buds. *Bmp4* and *7* are activated in both mesenchyme and AER in wild type and $Gre^{\Delta ORF/\Delta ORF}$ limb buds. Arrowheads mark the position of the AER.

4.3. Gremlin is essential for metanephric kidney organogenesis

The bilateral renal agenesis in $Gre^{\Delta ORF}$ homozygous newborn mice in the context of an otherwise normal urogenital system (Fig. 2B) points to an unexpected essential role of Gremlin during metanephric kidney organogenesis. Metanephric kidney development is initiated by invasion and induction of the metanephric mesenchyme by the ureter between embryonic days 10.5 to 11.0 in mouse embryos (Vainio and Lin, 2002). *Gremlin* is initially expressed by the intermediate mesenchyme (Pearce et al., 1999) and from about embryonic day 9.5 onwards by the Wolffian duct and mesonephric tubules (Fig. 7A and data not shown). During onset of metanephric development, *Gremlin* is rapidly down regulated and restricted posteriorly in the Wolffian duct (Fig. 7B and data not shown). At this stage, *Gremlin* is expressed locally in the condensing metanephric mesenchyme, which surrounds the ureteric bud (Fig. 7C). The Pax2 transcription factor is essential for urogenital l development and acts upstream of the signal(s) initiating metanephric development (Torres et al., 1995). During ureteric bud formation, *Pax2* expression is not affected in $Gre^{\Delta ORF}$ homozygous embryos (data not shown). In contrast, invasion of the metanephric mesenchyme by the ureter and up

regulation of *Pax2* expression in the induced mesenchyme fail to occur in *Gremlin* deficient embryos (Fig. 7D). The failure to induce metanephric development becomes more apparent as development progresses. *Pax2* expression is lost from the mutant metanephric mesenchyme by embryonic day 12.5, while nephrogenesis progresses in wild type embryos (Fig. 7E). In addition, *Bmp2*, *7* (Fig. 7F,G) and *Wnt4* transcripts (data not shown) are absent from the mutant metanephric mesenchyme. These results are indicative of a possible failure to induce condensation of the metanephric mesenchyme.

4.4. The failure to induce metanephric organogenesis is due to a complete disruption of ureter growth and branching

The tyrosine kinase receptor RET and its ligand GDNF are expressed by the ureter epithelium and mesenchyme, respectively (Fig. 8A, Hellmich et al., 1996; Pachnis et al., 1993; Towers et al., 1998). In *Gre*$^{\Delta ORF}$ homozygous embryos, both *Ret* and *Gdnf* expression are activated and the ureteric bud forms (Fig. 8B and data not shown), possibly as a consequence of activating RET/GNDF signaling. However, initiation of ureter growth (arrow, Fig. 8A) and *Gdnf* up regulation are completely blocked in *Gremlin* deficient embryos (compare Fig. 8A to 8B). The ureter branches (arrowheads, Fig. 8C) as it invades the metanephric mesenchyme. The branching tips of the wild type ureter express high levels of *Ret* and *Gdnf* is up regulated in the surrounding, condensing mesenchyme (Fig. 8E). In contrast, the ureteric bud does not branch in *Gremlin* deficient embryos (Fig. 8D) and mesenchymal *Gdnf* expression is rapidly lost, despite continued *Ret* expression by the arrested epithelium (Fig. 8D,F).

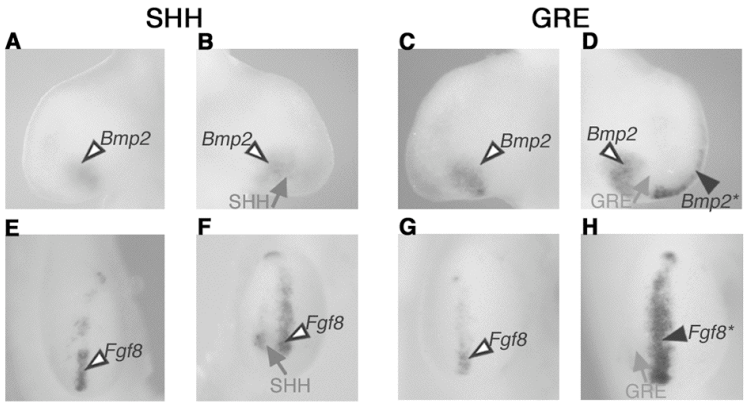

Fig.6 Gremlin, but not Shh, rescues *Fgf8* and *Bmp2* expression in the AER of *Gre*$^{\Delta ORF/\Delta ORF}$ limb buds.
All grafted limb buds are fore limb buds (E10.5) of *Gremlin* mutant embryos. Limb buds either received *Shh*- or *Gremlin*-expressing cell aggregates or were cultured for 15hrs prior to analysis.
Open arrowheads indicate the endogenous expression domains, filled arrowheads the induced expression. (A) *Bmp2* expression in a non-grafted control limb bud of a mutant embryo. (B) Posterior grafts of *Shh*-expressing cell aggregates fail to rescue *Bmp2* expression. (C,D) Posterior grafts of *Gremlin*-expressing cells induce *Bmp2* expression in the AER (D), while no *Bmp2* transcripts are detected in the AER of non-grafted mutant limb buds (C). Note also the enhancement of mesenchymal *Bmp2* expression (D). (E,F) Posterior grafts of *Shh*-expressing cells do not rescue *Fgf8* expression in the AER (F) in comparison to a non-grafted mutant limb buds (E). (G,H) Posterior grafts of *Gremlin*-expressing cells induce up regulation of *Fgf8* expression in the AER (H) in comparison to endogenous *Fgf8* expression in non-grafted mutant limb buds (G). Panels (A) to (D) are dorsal views with posterior to the bottom and distal to the right, in panels (E) to (H) posterior is to the bottom and dorsal to the left.

4.5. Gremlin-mediated BMP antagonism promotes survival of mesenchymal cells

To understand how the molecular alterations give rise to the distal limb defects and result in elimination of the metanephric kidney, potential effects on programmed cell death were assayed. Massive cell death is observed in the core mesenchyme of *Gremlin* deficient limb buds by embryonic day 11.0 (Fig. 9A). However, the superficial dorsal and ventral limb bud mesenchymal cells normally expressing *Gremlin* (Merino et al., 1999c) survive in limb buds of $Gre^{\Delta ORF}$ homozygous embryos as indicated by the continued presence of *LacZ*-expressing cells (Fig. 9B). Similarly, *LacZ*-expressing cells remain in the Wolffian duct and mesenchyme of *Gremlin* deficient embryos (data not shown) in spite of massive aberrant cell death at embryonic day 11.5 (Fig. 9C). Analysis of parallel sections shows that the metanephric mesenchyme, which expresses *Pax2* (Fig. 9D) is eliminated by apoptosis.

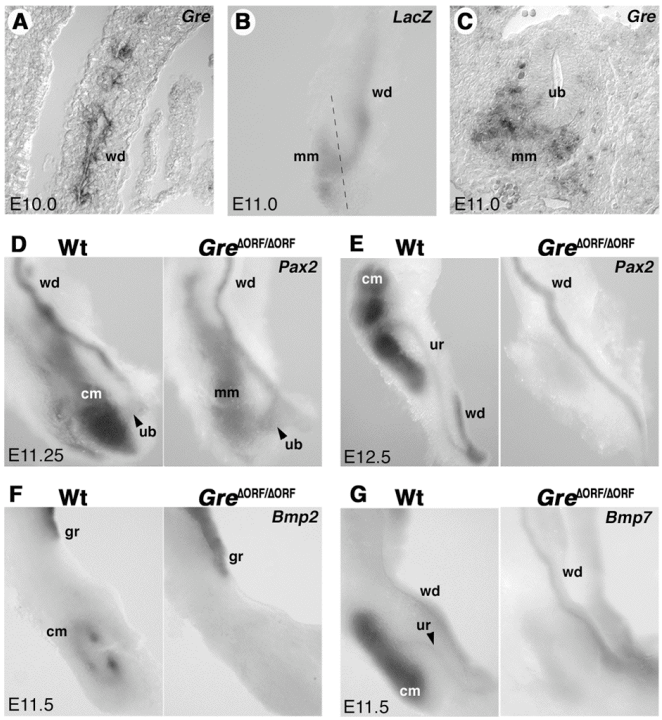

Fig.7 Disruption of metanephric kidney morphogenesis. (A-C) Distribution of *Gremlin* transcripts during kidney morphogenesis. (A) *Gremlin* expression in the Wolffian duct and mesonephric tubules E10.0. (B) Distribution of *Gremlin* transcripts during initiation of metanephric development (E11.0). The distribution of *LacZ* transcripts in a $Gre^{\Delta ORF}$ heterozygous embryonic kidney is shown. Note expression by both posterior Wolffian duct and metanephric mesenchyme. The dotted line indicates the approximate position corresponding to the section shown in panel (C). (C) *In situ* analysis on section reveals *Gremlin* expression locally in the metanephric mesenchyme surrounding the ureter tips. (D) Growth of the ureter and invasion of the metanephric mesenchyme in wild type embryos by E11.25. As a consequence, *Pax2* expression is up regulated in the induced mesenchyme while it remains low in mutant mesenchyme. (E) In contrast to the wild type, *Pax2* expression is lost from mutant mesenchyme by E12.5, while it remains similar to the wild type in the Wolffian duct. (F) In contrast to the wild type, *Bmp2* fails to be expressed by the nephrogenic regions of mutant embryos. (G) In wild type embryos *Bmp7* expression is induced to high levels within the condensing mesenchyme. This induction is completely disrupted in *Gremlin* deficient embryos. cm: condensing metanephric mesenchyme, gr: genital ridge, mm: metanephric mesenchyme, ub: ureteric bud, ur: ureter, wd: Wolffian duct.

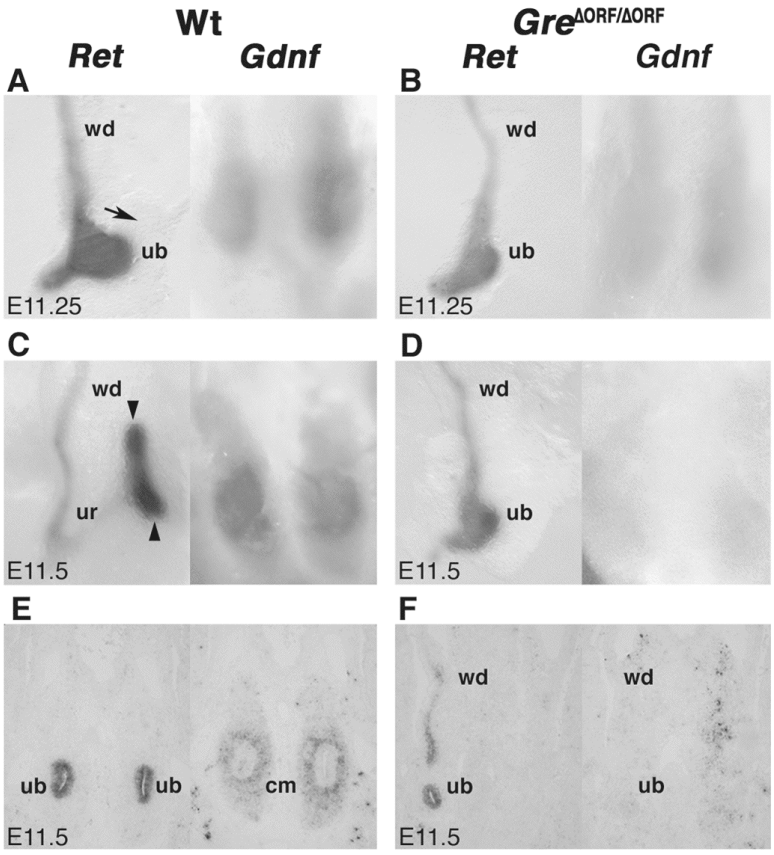

Fig.8 Disruption of ureter growth and RET/GDNF feedback signaling during metanephric organogenesis. During onset of ureter growth (arrow) in wild type embryos, *Gdnf* transcription is up regulated in the induced metanephric mesenchyme. (B) Ureter growth and *Gdnf* up regulation are not induced in mutant embryos (E11.25). (C) By E11.5, the ureter has branched once and expresses high levels of *Ret* (arrowheads) and *Gdnf* is maintained in the induced metanephric mesenchyme. (D) In contrast, ureter development is arrested and *Gdnf* expression lost in *Gremlin* deficient embryos. (E,F) Analysis of *Ret* and *Gdnf* expression on sections of E11.5 embryos confirms the disruption of RET/GDNF epithelial-mesenchymal feedback signaling in mutant embryos. cm: condensing mesenchyme, ub: ureteric bud, wd: Wolffian duct. Panels (E,F) show transverse sections at the level of hind limb buds.

5. Discussion

We show that inactivation of *Gremlin* in the mouse causes a limb phenotype in combination with complete renal agenesis and lung airway defects. In particular, the gross morphological appearance of the limb and kidney phenotypes is strikingly similar to newborn mice homozygous for the strongest *ld* alleles (Maas et al., 1994). Indeed, Khokha et al. (2003) reported allelism between their *Gremlin* loss-of-function mutation and the ld^{J} allele as trans-heterozygous mice display limb defects at birth. We have now identified the molecular lesions in both the ld^{J} and ld^{OR} alleles and shown that they disrupt, respectively delete the *Gremlin* ORF (Zuniga et al., 2004). These rather unexpected results prompted us to re-evaluate the other *ld* alleles and the proposed function of *Formin* in regulating *Gremlin* expression in the limb bud mesenchyme (Zuniga et al., 1999) using extensive reverse genetic analysis of the two genes. These studies reveal that disruption a cis-regulatory element within *Formin*, which is required for limb bud mesenchymal expression of *Gremlin,* causes the *ld* limb phenotype

(Zuniga et al., 2004). In conclusion, these studies show that the existing *ld* alleles are either complete or limb bud specific *Gremlin* loss-of-function mutations and that the *ld* phenotype is not caused by disruption of the C-terminal Formin domain as so far assumed (Evangelista et al., 2003; Zeller et al., 1999).

The present study establishes that Gremlin-mediated antagonism of BMP signaling is required for proper AER formation and function. However in *Gremlin* deficient limb buds, the expression of genes controlling dorso-ventral axis formation is normal (A. Z., unpublished results) and both the AER and *Fgf8* expression are induced indistinguishable form wild type limb buds (this study). The AER and *Fgf8* expression are induced by *Wnt3*/β-*catenin* and BMP signaling activities in the ectoderm during initiation of limb bud development and establishment of dorso-ventral polarity (Barrow et al., 2003; Kawakami et al., 2001; Pizette et al., 2001; Soshnikova et al., 2003). Gremlin functions subsequently by antagonizing BMP signaling in the distal limb bud mesenchyme, which is obviously essential for progression of AER formation and establishment of multi-factorial AER signaling. In *Gremlin* deficient limb buds, enhanced mesenchymal BMP signaling blocks AER maturation and signaling at an early stage and disrupts distal limb bud morphogenesis, last but not least through apoptosis of core mesenchymal cells (see also below). These results corroborate previous studies in chicken embryos, which showed that mesenchymal BMP antagonism maintains the AER and promotes distal limb bud morphogenesis (Capdevila et al., 1999; Pizette and Niswander, 1999).

Furthermore, Gremlin-mediated BMP antagonism has been implicated in regulating *Shh* expression through its role in establishment of the SHH/FGF4 feedback loop (Capdevila et al., 1999; Zuniga et al., 1999). During initiation of limb bud development, *Shh* expression is activated in the posterior mesenchyme under the influence of FGH8 signaling by the AER, likely in combination with FGF4 (Lewandoski et al., 2000; Moon and Capecchi, 2000; Sun et al., 2002). In particular, SHH is not activated in hind limb buds lacking both *Fgf8* and *4* despite continued expression of *Gremlin* in the mesenchyme and *Fgf9*, *17* and *Bmp* in the mutant AER (Sun et al., 2002). These results together with our studies (Zuniga et al., 1999) also show that Gremlin functions initially independent of SHH in AER formation and FGF activation in the posterior AER**.** During progression of limb bud morphogenesis, Gremlin induced FGF signaling by the posterior AER participates in dynamic SHH regulation as Gremlin rescues *Shh* expression with kinetics similar to *Fgf4* in *ld* mutant limb buds (Panman et al., manuscript in preparation). The general disruption of AER-FGF signaling underlies the failure to up-regulate SHH signaling in *Gremlin* deficient limb buds. Through establishment of feedback signaling, Gremlin mediates the dynamic regulation of both limb bud-signaling centers. For example, the distal anterior progression of mesenchymal *Gremlin* expression during limb bud morphogenesis causes anterior expansion of FGF signaling in the AER, which in turn regulates SHH signaling by the polarizing region (Zuniga et al., 1999). These dynamic changes alter the ratios of different peptide signals received by both AER cells and the underlying limb bud mesenchyme. Sanz-Ezquerro and Tickle (2000) showed that the size and signaling strength of the *Shh* expression domain in limb buds is tightly regulated by apoptosis. Taken together, the analysis of epithelial-mesenchymal signaling in limb buds indicates that *Shh* expression is not regulated by a mere SHH/FGF feedback loop, but through complex and dynamic feedback signaling involving different types of

mesenchyme and AER signals and their antagonists belonging to the FGF, BMP and WNT gene families.

In *Gremlin* deficient mouse limb buds, prominent apoptotic cell death is observed in the core mesenchyme from about embryonic day 11.0 onwards. This cell death pattern is rather distinct from the ones observed in *Shh* deficient (te Welscher et al., 2002b) and *Fgf4/8* double mutant (Sun et al., 2002) mouse embryos and following AER removal (Dudley et al., 2002). In addition, experiments in chicken embryos have provided evidence for a role of Gremlin-mediated BMP antagonism in cell survival during digit formation and chondrogenesis (Merino et al., 1999c). During the onset of chondrogenesis, Gremlin acts in a paracrine fashion on the adjacent core mesenchyme to protect it from undergoing programmed cell death (this study). Therefore, this anti-apoptotic function of Gremlin could provide an explanation for the reductions and fusions of distal limb skeletal elements observed in *Gremlin* deficient mouse embryos. It is possible that the effect of Gremlin-mediated BMP antagonism on cell survival is direct and does not involve feedback signaling between mesenchyme and AER.

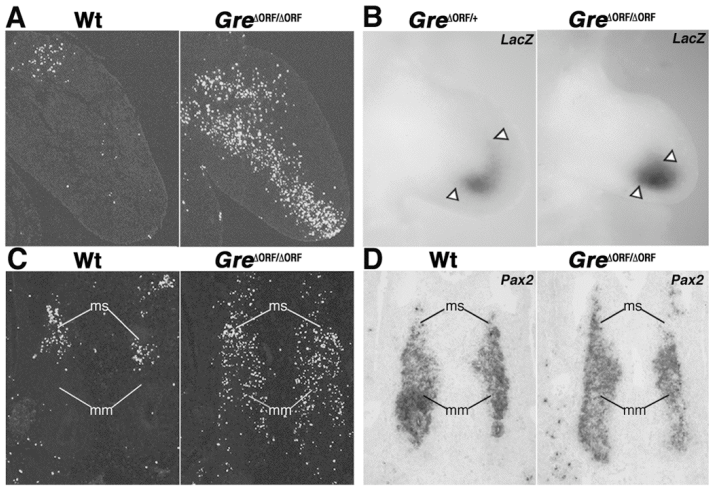

Fig.9 Gremlin is required for cell survival during both limb and kidney organogenesis.
TUNEL assay to reveal apoptotic cell death on histological sections. In the absence of Gremlin, cells in core limb bud mesenchyme undergo massive cell death by E11.0.
(B) *LacZ* transcripts are detected in E11.0 fore limb buds to follow the fate of cells normally expressing *Gremlin* in both heterozygous and homozygous mutant limb buds. Note that *LacZ*-expressing cells survive in $Gre^{\Delta ORF/\Delta ORF}$ limb buds. Open arrowheads indicate the anterior and posterior domain boundaries. Fore limb buds in (A,B) are shown with ventral to the bottom and distal to the right. (C) Massive abnormal cell death is detected by TUNEL assay in the metanephric mesenchyme (mm) of *Gremlin* mutant kidneys by E11.5. Note that both wild type and *Gremlin* mutant mesonephric mesenchyme (ms) undergoes normal apoptosis at this stage. (D) *Pax2* expression in the nephrogenic tissue of a wild type and $Gre^{\Delta ORF/\Delta ORF}$ embryo. The sections shown are adjacent to the ones shown in panel (C). *Pax2* expression fails to be up regulated in the metanephric mesenchyme of mutant kidneys, while expression in mesonephric mesenchyme (ms) is similar to Wt. Posterior is to the bottom, ventral view in (C,D).

The complete renal agenesis in *Gremlin* deficient mice reveals that the BMP antagonist Gremlin is required for metanephric development. This study identifies Gremlin as the essential extra-cellular signal, which initiates metanephric kidney development by enabling the ureter to invade the metanephric mesenchyme.

However, establishment of the two signaling centers controlling metanephric development, the ureteric bud (expressing *Ret*) and metanephric mesenchyme (expressing *Gdnf*), occurs without Gremlin, while initiation of the ureter growth and branching depend on Gremlin function. In analogy to its function in limb buds, Gremlin regulates the transition to dynamic signaling interactions to enable induction of metanephric organogenesis. During set-up of RET/GDNF signaling and ureteric bud formation, *Gremlin* is expressed by the Wolffian duct and locally by the metanephric mesenchyme, but the primary tissue affected in *Gremlin* deficient embryos could be the ureteric epithelium as is the case in *ld* homozygous embryos (Maas et al., 1994). Such impairment of epithelium to mesenchyme signaling disrupts up regulation of *Gdnf*, *Pax2* and *Ret* expression in the mesenchyme and tips of the invading ureter, respectively. This disruption in turn leads to complete elimination of the metanephric mesenchyme by apoptotic cell death. This phenotype is strikingly similar to the one caused by inactivation of *Sall1*, a transcription factor expressed by the metanephric mesenchyme (Nishinakamura et al., 2001). However, *Sall1* remains expressed in Gremlin mutant embryos (O.M. and A.Z., unpublished results), which indicates that it is not a direct target.

Several BMP genes are expressed during initiation of metanephric kidney development and have been implicated in the early inductive events (Martinez and Bertram, 2003; Vainio and Lin, 2002). In particular, analysis of *Bmp4* heterozygous embryos has provided evidence for its essential roles during ureter morphogenesis (Miyazaki et al., 2000; Raatikainen-Ahokas et al., 2000). BMP4, possibly similar to BMP2, (Gupta et al., 1999) inhibits ectopic branching of the ureteric bud and is required for growth of the ureter stalk. These studies (Miyazaki et al., 2000; Raatikainen-Ahokas et al., 2000) together with ours reveal the likely mechanism by which metanephric development is initiated. Ureteric bud formation by the Wolffian duct is independent of Gremlin-mediated BMP antagonism, while it is required to induce ureter growth, branching and propagation of RET/GDNF feedback signaling. During branching morphogenesis, *Gremlin* is expressed locally in the mesenchyme surrounding the invading ureter (this study) and *Bmp4* in mesenchyme adjacent to the ureter stalk (Dudley and Robertson, 1997; Miyazaki et al., 2000). Dynamic local changes in BMP activity as mediated by antagonistic Gremlin-BMP2/4 interactions may regulate the temporal and spatial kinetics of ureter branching, while BMP signaling alone promotes ureter stalk elongation (Miyazaki et al., 2000; Raatikainen-Ahokas et al., 2000). In summary, the present study reveals that Gremlin-mediated BMP antagonism regulates the dynamic interactions of diverse epithelial and mesenchymal signaling centers during progression of vertebrate organogenesis.

Acknowledgements

The authors are grateful to I. Ginez, H. Goedemans, N. Lagarde, C. Lehmann and H. Schaller for technical assistance and mouse husbandry. We thank S. Kuc for performing the *LacZ in situ* analysis, the Zentrum für Mikroskopie der Universität Basel, M. Dürrenberger and M. Düggelin for assistance with SEM analysis and K. O'Leary for help in preparation of the manuscript. We thank S. Vainio for expert advice concerning metanephric kidney development and F. Maina, M. Torres and S. Vainio for providing probes for *in situ* hybridization. We are grateful to J. Deschamps, R.

Dono, A. Galli, G. Holländer, F. Meijlink, I. Mattaj and C. Torres de los Reyes for helpful discussions and comments on the manuscript. This research was supported by the Swiss National Science Foundation (to R.Z.), both cantons of Basel (to R.Z. and K.B.), the Faculty of Biology at Utrecht University, and grants from KNAW (to A.Z.) and NWO (to R.Z.).

CHAPTER 3
Roles Of Gremlin During Lung Development

The BMP antagonist Gremlin regulates epithelial morphology and branching morphogenesis during mouse lung development

Odyssé Michos[1], Konstantin Beier[2], Rolf Zeller[1] and Aimée Zuniga[1]

[1]Developmental Genetics, Dept. of Clinical-Biological Sciences (DKBW), University of Basel Medical School, c/o Anatomy Institute, Pestalozzistrasse 20, CH-4056 Basel, Switzerland, [2]Dept. of Histology, Anatomy Institute, Pestalozzistrasse 20, CH-4056 Basel, Switzerland.

(Manuscript in preparation)

1. Summary

Lung morphogenesis is regulated by complex stereotypical branching of the epithelium that ultimately leads to the formation of the characteristic tree-like respiratory tracts and alveoli that are required for gas exchange. Bone morphogenetic protein (BMP) signaling and in particular BMP4 have been implicated as regulators of lung branching morphogenesis and differentiation of lung epithelial cells. However, the critical functions of the BMP signaling pathway and possible modulation by BMP antagonists during lung development have remain unclear. We have previously shown that *Gremlin* deficient mice die shortly after birth due to lung defects and complete renal agenesis. Therefore, *Gremlin* deficient mice provide a model to study the importance of modulating BMP activity during lung organogenesis. Morphological and molecular analysis establishes that lungs of *Gremlin* deficient embryos display an abnormal epithelial branching pattern and defects in epithelial cell differentiation, which may be the primary cause of respiratory failure. Analysis of newborn mice indicates that Gremlin-mediated BMP antagonism is required for epithelial cell maturation during advanced embryogenesis.

2. Introduction

Lung development is initiated by the appearance of an epithelial bud from the ventral endoderm of the primitive foregut, which invades the surrounding splanchnic mesenchyme at about mouse day embryonic 9.5 (E9.5). Subsequently, the prospective trachea and primary bronchi become apparent as first distinct lung epithelial structures. The two primary buds elongate and undergo stereotypical branching to form the characteristic bronchial and respiratory tree of the lung epithelium. As development proceeds, formation of acini and alveoli creates epithelial structures critical for gas exchange, a pre-requisite for respiration during postnatal life. The histological development of mouse lung organogenesis is divided into four stages: (1) pseudoglandular stage (E9.5-E16.5): development of the bronchial and respiratory tree and formation of the undifferentiated lung primordia; (2) canalicular stage (E16.5-E17.5): development of terminal sacs and onset of vascularization; (3) terminal sac stage (E17.5 to postnatal day 5 P5): continuing morphogenesis resulting in an increase of terminal sacs and the vascular system together with differentiation of alveolar cells (type I and II); and (4) alveolar stage (P5-P30): differentiation of the terminal sacs into mature alveolar ducts and alveoli (Ten Have-Opbroek, 1991).

The proximal epithelium is columnar in morphology and is composed of Clara cells expressing *CC10* and ciliated cells expressing *Hfh4*, while the distal epithelium is composed of cuboidal alveolar type I and squamous alveolar type II epithelial cells (expressing *SpC*; Warburton et al., 2000). Classical recombination and transfilter experiments revealed the importance of epithelial-mesenchymal signaling interactions during branching morphogenesis. For example, recombination of distal mesenchyme with tracheal epithelium induces ectopic budding and branching. In contrast, proximal mesenchyme inhibits branching when recombined with distal epithelia. Among the signals regulating these epithelial-mesenchymal interactions are BMPs. BMPs are secreted growth factors belonging to the TGFß superfamily. BMPs transduce their signal via serine threonine kinase BMP receptors. Upon activation, the BMP receptor activates SMAD proteins, which dimerize and translocate to the nucleus to regulate

gene expression in target cells. Several BMP ligands are expressed during lung morphogenesis including *Bmp5* and *7,* which are expressed in the mesenchyme and the epithelium, respectively (Bellusci et al., 1996; King et al., 1994). In contrast, *Bmp4* is expressed in a dynamic pattern at the distal tip of the epithelial bud and the surrounding mesenchyme and has been implicated in epithelial-mesenchymal signaling during lung morphogenesis. Over expression of *Bmp4* in the distal lung bud epithelium of transgenic mice results in small lungs with dilated distal buds. Furthermore, the number of type II alveolar cells is reduced in such transgenic lungs in concert with a general inhibition of cell proliferation and aberrant mesenchymal cell death (Bellusci et al., 1996). In agreement, over expression of either a dominant negative form of the BMP4 receptor or the BMP antagonist Noggin also disrupts embryonic lung development. Reduced BMP4 activity shifts the balance from distal to proximal epithelial cell types (Weaver et al., 1999). These studies indicate that in particular BMP4 is part of a distal signaling center together with FGF10 and SHH (Cardoso, 2001; Hogan, 1999). However, the exact role of BMP4 signaling in lung morphogenesis remains to be established. Addition of BMP4 to whole lung explants promotes branching morphogenesis (Bragg et al., 2001; Shi et al., 2001), while its addition to isolated lung epithelia inhibits branching (Hyatt et al., 2002; Weaver et al., 2000).

An important aspect of modulating BMP activity is local extra-cellular binding and sequestration of ligands by means of extra-cellular antagonists. Gremlin is one such extra-cellular BMP antagonist able to bind and inhibit both BMP2 and BMP4 ligands (Hsu et al., 1998). Gremlin belongs to the CAN domain family of BMP antagonists, which also include Cerberus and DAN (Avsian-Kretchmer and Hsueh, 2003). Recently, we have shown that Gremlin is essential for lung, kidney and limb morphogenesis using gene targeting in the mouse (Michos et al., 2004). We also showed that Gremlin is required for establishment of the epithelial-mesenchymal signaling interactions controlling limb bud and kidney development, while disruption of lung morphogenesis remained to be analyzed. Over expression of *Gremlin* in the distal lung epithelium disrupts proximo-distal axis specification. Lungs of such transgenic mice exhibit an expansion of proximal makers into the distal epithelium, together with expression of smooth muscle α-actin around the distal airway epithelia, which is indicative of proximalized distal lung epithelia (Lu et al., 2001). In contrast, reduction of *Gremlin* using anti-sense oligonucleotides enhances epithelial branching morphogenesis, epithelial cell proliferation and *SpC* expression in cultured organs rudiments (Shi et al., 2001).

In the present study, we show that the proximo-distal axis is established correctly in lung primordia of *Gremlin* deficient mouse embryos. Proximal markers such as *CC10* and *Hfh4*, and distal markers such as *SpC*, are still expressed normally. However, more *SpC*-expressing cells are detected in the distal lung epithelium. Molecular and morphological analysis establishes that early branching morphogenesis is not affected, but an increase in lateral branching is observed during later stages. Lungs of *Gremlin* deficient mouse embryos display a thickened epithelium in association with collapsed alveoli at birth, which is the most probable cause of the neonatal lethality.

3. Materials and methods

3.1. *Gremlin* deficient mice

The generation of *Gremlin* deficient mice was previously described (Michos et al., 2004; Zuniga et al., 2004). Mice were kept in a mixed B6;129S genetic background.

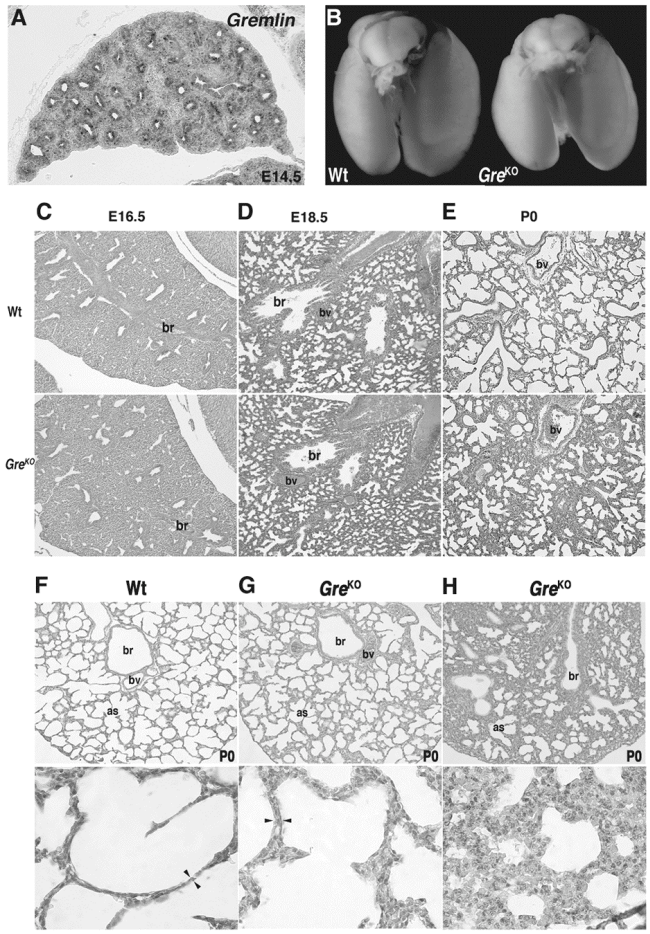

Fig.1 Histological defects in lungs of *Gremlin* deficient mouse embryos.
Gremlin in situ hybridization on transversal section at E14.5 showing its expression in both epithelial and mesenchymal compartment.
(B) Dissected E18.5 lungs showing the external normal appearance of *Gremlin* mutant lungs in comparison to a wild type littermate.
(C-H) Transverse histological sections through wild type and *Gremlin* deficient lungs of different development stages. Note the similarity between mutant and wild type lungs at E16.5 (C) and E18.5 (D) and the excess tissue in mutant lung at birth (E,H). (F-H) Two mutant lungs with varying penetrance of the phenotype (G,H) are shown in comparaison to the normal wild type appearance (F). Arrowheads in (F,G) point to the epithelium. br: bronchi; bv: blood vessel; as: alveolar sac.

3.2. Molecular and morphological analysis of embryos and newborn mice

Embryos and newborn mice were PCR genotyped. Whole mount and section *in situ* hybridization was performed as previously described (Michos et al., 2004) using digoxygenin-UTP labeled anti-sense riboprobes. After whole mount *in situ* hybridization, dissected lungs were dehydrated through methanol/PBS series and cleared using a Benzyl Benzoate/Benzyl Alcohol (2:1) solution. For histological analysis, sections were cut from formalin-fixed and paraffin-embedded material and stained with haematoxilin and eosin using standard protocols. Detection of elastic fibers (elastin) was performed as described (Luna, 1968). Anti-SMA-Cy3 conjugated

antibody (Sigma) was used at 1/200 in PBT/5% goat serum to detect smooth muscle cells. Sections were mounted in vectashield for analysis by immunofluorescence.

4. Results and discussion

4.1. Abnormal lung morphogenesis in *Gremlin* deficient mouse embryos

During lung morphogenesis, *Gremlin* is expressed in a dynamic pattern from embryonic day 11 (E11.0) onwards (Lu et al., 2001; Shi et al., 2001; data not shown). In particular, *Gremlin* is expressed in both the epithelial and mesenchymal compartment during lung branching morphogenesis (Fig. 1A). The size and external morphology of lung rudiments in *Gremlin* deficient embryos is comparable to wild type lungs at E18.5 (Fig. 1B). However, the majority of isolated lungs (n= 7/12) do not float when transferred into an aqueous solution, indicative of respiratory failure at birth. No phenotypic differences are observed between the mutant and the wild type lungs during the pseudoglandular stage, when branching morphogenesis occurs (Fig. 2A, 1C). After E16.5, the architecture of lung primordia undergoes radical changes as development progresses through the canalicular stage and the characteristic sac-like pre-alveolar structures are formed. Up to E18.5, no striking differences are observed between mutant and wild type lung rudiments (Fig. 1D), while clear differences are apparent in lungs of newborn *Gremlin* deficient mice (Fig. 1E).

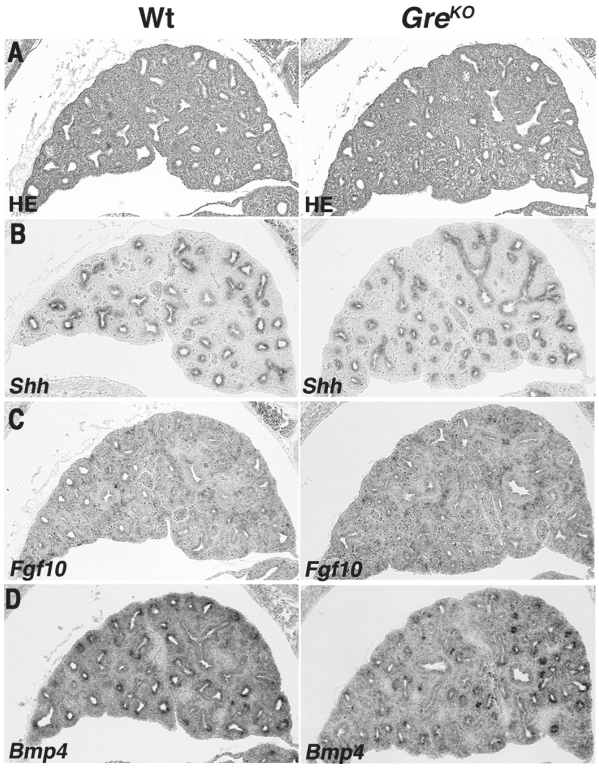

Fig.2 Expression of key regulators of lung branching morphogenesis.
Transverse sections of wild type and *Gremlin* deficient lungs at E18.5.
(A) Haematoxilin-eosin staining.
(B-D) *In situ* hybridization of *Shh* (B), *Fgf10* (C) and *Bmp4* (D) showing their normal expression.

In wild type newborn mice, the peripheral air spaces are drained of fluid and filled with air, so that they can then be separated by a thin ectodermal layer. The size of the alveoli is increased considerably (Fig. 1E, panel "Wt"; Fig. 1F). In *Gremlin* deficient newborn mice, severe lung defects are observed at birth. The airspaces are not properly dilated and appear more collapsed than in wild type littermates (Fig. 1E, panel "*Gre*^{KO}"; Fig. 1G). Furthermore, the lung epithelium is much thicker than normal and appears multi-layered (compare Fig. 1F to 1G; see also Fig. 5A,C). However, the severity of the lung phenotype at birth varies considerably from an almost normal morphology (Fig. 1G, n= 7/11) to severely affected lungs with few developed terminal sacs (Fig. 1H, n= 4/11). *Gremlin* deficient mice displaying the most severe phenotype are highly dyspnotic and cyanotic and die within a few hours after birth (data not shown). Histological analysis of lungs of newborn mice displaying a weak (Fig. 1G) or severe phenotype (Fig. 1H) reveals the presence of a thickened and multi-layered epithelium (Fig. 1G; see also Fig. 5C, panel *"Gre*^{KO}") in contrast to wild type littermates (Fig. 1F; see also Fig. 5C, panel "Wt"). Taken together, these results reveal that the neonatal lethality of *Gremlin* deficient mice is caused by respiratory failure due to lack of alveolar differentiation and function in combination with bilateral renal agenesis (Michos et al., 2004).

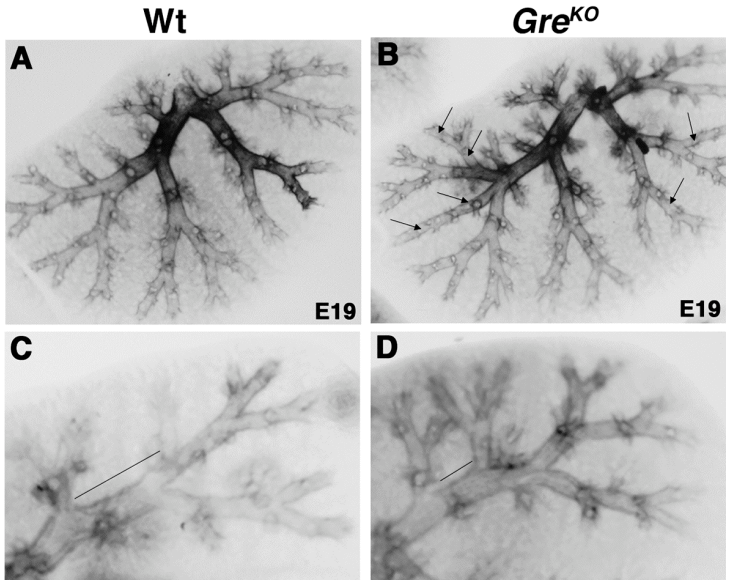

Fig.3 Lung branching defects in *Gremlin* deficient embryos.
The whole mount distribution of the proximal marker *CC10* illustrates the branching pattern of the bronchial trees. Note the additional branches (arrows) in mutant lungs (B) in comparison to a wild type littermate (A). The bars in panels (C,D) indicate the reduced branch length in the mutant (D) in comparison to a wild type littermate (C).

4.2. Molecular analysis of lung branching morphogenesis in *Gremlin* deficient mouse embryos

Embryonic lung branching occurs mainly during the pseudoglandular stage. During this period, the tree-like structure of the respiratory system develops by a highly reproducible pattern of dichotomous and lateral branching. This process seems controlled by a distal signaling center and involves signals such as BMP4, FGF10,

SHH and WNT (Cardoso, 2001; Hogan, 1996; Shannon and Hyatt, 2004). Therefore, the expression of select signals was analyzed in *Gremlin* deficient embryos by section *in situ* hybridization. These studies show that the early branching pattern is not altered and *Bmp4* and *Fgf10* remain expressed normally in lungs of *Gremlin* deficient embryos (data not shown). By E14.5 branching morphogenesis is well advanced and *Gremlin* deficient embryos express *Bmp4*, *Fgf10* and *Shh* in their lungs in a pattern similar to wild type littermates (Fig. 2). *Shh* remains expressed by all epithelial cells and *Fgf10* by the mesenchyme (Fig. 2B,C), while *Bmp4* is expressed at the distal tip of the epithelium and by the adjacent mesenchyme (Fig. 2D).

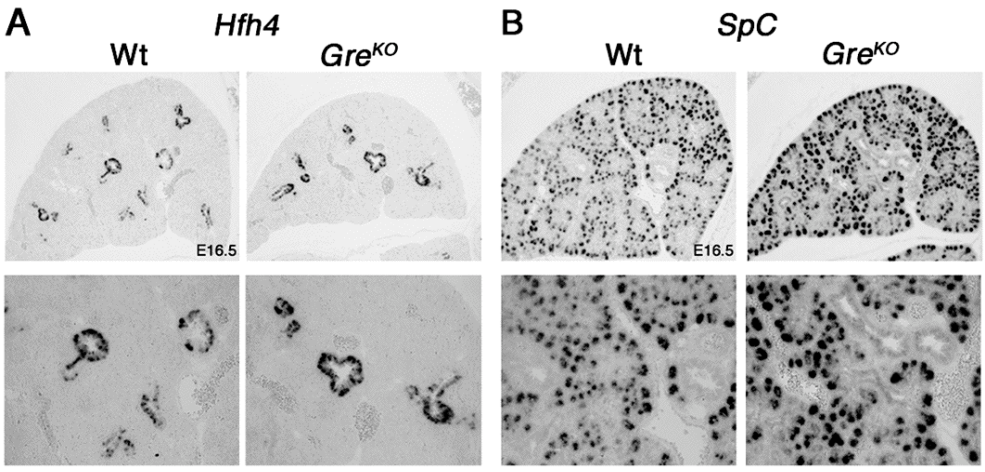

Fig.4 Early proximo-distal lung axis specification is normal in *Gremlin* deficient embryos.
(A) *In situ* hybridization of the proximal marker *Hfh4* at E16.5. (B) *In situ* hybridization of the distal marker *SpC* at E16.5. Note the very similar expression of both markers in wild type (Wt) and mutant (Gre^{KO}) lungs.

Previous studies provided evidence that inhibition of *Gremlin* expression by anti-sense oligonucleotides enhances branching morphogenesis in cultured lung organ rudiments (Shi et al., 2001). Therefore, the 3-D branching pattern was comparatively analyzed (Fig. 3). *CC10* expression was used to mark the bronchial tree as all Clara epithelial cells express *CC10* during mouse lung morphogenesis. Indeed, additional lateral branches are observed in *Gremlin* deficient mouse embryos (compare Fig. 3A to 3B, arrows in Fig. 3B; n= 4/11) and the length of individual branches seems reduced (compare bar in Fig. 3C,D). This phenotype is in accordance with previous reports showing that addition of BMP4 to cultured lung rudiment explants increases branching (Bragg et al., 2001; Shi et al., 2001). In contrast, Bragg and coworkers (2001) provided evidence that BMP4 produced by epithelial cells does not alter branching morphogenesis and that the surrounding mesenchyme provides factors that modulate BMP4 activity. Furthermore, Hyatt et al. (2002) and Weaver et al. (2000) established that BMP4 inhibits epithelial cell proliferation in mesenchyme-free culture. Together with our results, these studies indicate that *Gremlin* expressed by the lung

mesenchyme (Fig. 1A) may modulate BMP activity so as to direct the pattern of epithelial branching morphogenesis.

4.3. Gremlin is required for lung epithelial cell differentiation but not proximo-distal axis specification

It has been previously established that BMP4 is critical for proximo-distal axis specification of the lung primordia. For example, inhibition of BMP activity, using a dominant negative form of the BMP4 receptor results in reduction of distal and augmentation of proximal cell fates (Weaver et al., 1999). Furthermore, over expression of *Gremlin* or *Noggin* causes a decrease in *SpC*-expressing cells and increased *CC10* and *Hfh4* expression in the maturing distal epithelium, suggesting that balanced BMP signaling and antagonism may be critical to proximo-distal axis specification (Lu et al., 2001; Weaver et al., 1999). Therefore, we assessed whether the proximo-distal axis is altered in lung rudiments of *Gremlin* deficient embryos. By E16.5, no differences in *Hfh4* or *SpC* expression are detected when comparing wild type and mutant lungs (Fig. 4A,B). These results indicate that proximo-distal epithelial cell fates are established correctly in mutant lung primordia. At birth, the expression of *CC10* (Fig. 5A) and *Hfh4* (Fig. 5B) in mutant lungs is comparable to wild type, indicating that specification of the proximal airway epithelium occurs normally in *Gremlin* deficient mouse embryos. In contrast, the expression of *SpC* in type II alveolar epithelial cells is increased in mutant lungs at birth (Fig. 5C).

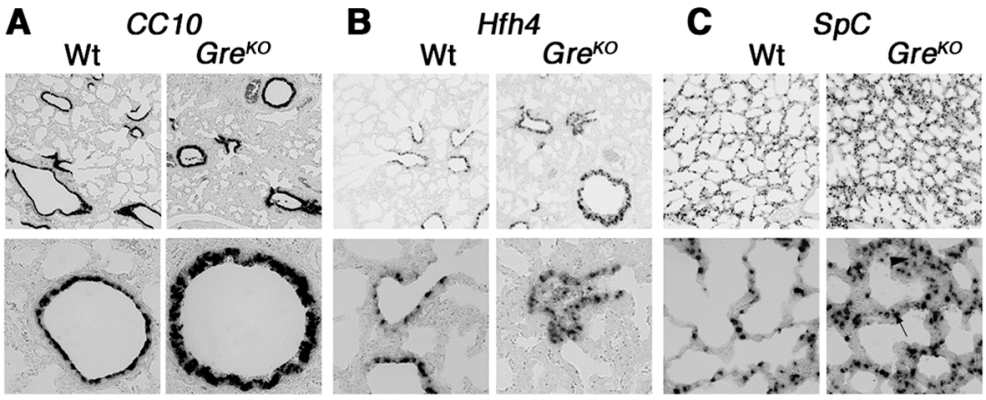

Fig.5 Proximo-distal axis specification in *Gremlin* deficient newborn mice.
In situ hybridization of the proximal markers *CC10* (A) and *Hfh4* (B) and the distal marker *SpC* (C) using transversal sections of lungs of wild type and *Gremlin* deficient newborn mice. In panel (C), arrow point to *SpC*-expressing cells lining collapsed airspaces, arrowhead point to *SpC* expression within the interstitial compartment. Note the thickened and multi-layered lung epithelium of *Gremlin* deficient newborn mice.

The majority of *SpC*-expressing cells do not line differentiated airspaces, but are located either within collapsed airspaces (arrows, Fig. 5C) or within the interstitial compartment in *Gremlin* deficient mouse embryos (arrowheads, Fig. 5C). These

results point to possible primary dysplasia of the alveolar epithelium. In conclusion, no changes in the proximo-distal restriction of *CC10, Hfh4* and *SpC* are detected (Fig. 5), which establishes that Gremlin-mediated BMP antagonism is not essential for proximo-distal axis specification. In contrast however, Gremlin-mediated BMP antagonism is critical for alveolar epithelial cell differentiation as lungs become functional at the time of birth (Fig 1G,H and Fig. 5C). These results seem to contradict previous reports indicating that over expression of *Gremlin* in the distal lung bud epithelium induces proximalization (Lu et al., 2001). One possible explanation for this discrepancy could be functional redundancy with other BMP antagonists such as Noggin (Weaver et al., 2003; 1999).

In the present study we establish that loss of Gremlin causes a dramatic change in epithelial morphology in both distal and proximal lung compartments. The proximal lung epithelium of *Gremlin* mutant mice is at least 2 to 4-fold thicker than the wild type (Fig. 5A,B and data not shown). Normally, the distal epithelium is lined by alveolar epithelial type II cells (AEC2), which have a characteristic elongated morphology that can span several alveoli, allowing exchange of gases (Fig. 1F and Fig. 5C, panel "Wt"). Unlike wild type AEC2 cells, the mutant epithelium is not lined by such cyto-differentiated cells, but rather by AEC2 cells lacking the characteristic elongated morphology, and packed in multiple layers that most likely have a severe impact on proper gas exchange (Fig. 1G,H and Fig. 5C, panel *"Gre*^{KO}*"*). No changes in cellular apoptosis were observed during lung organogenesis (data not shown). Interestingly, the differentiation of the mature AER in limb buds of *Gremlin* deficient embryos is blocked as epithelial cells also fail to adopt the characteristic polarized morphology (Michos et al., 2004). These results suggest that Gremlin-mediated epithelial-mesenchymal signaling interactions regulate differentiation and/or polarization of different types of epithelial cells.

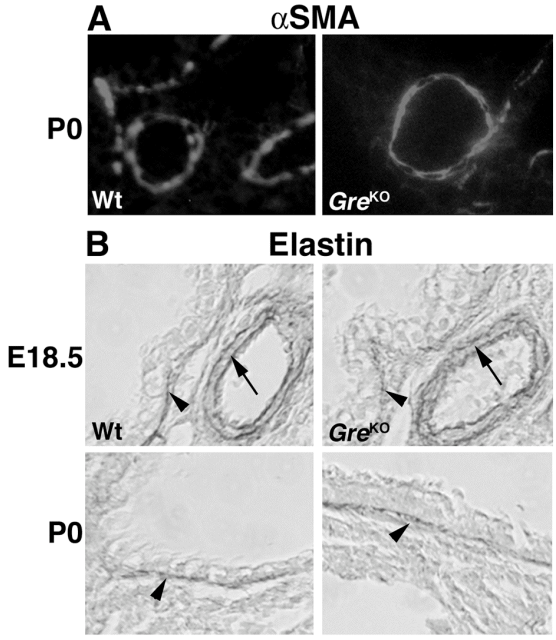

Fig.6 Staining for mesenchymal markers.
(A) Immunohistochymistry to reveal smooth muscle a-actin (aSMA) in wild type and *Gremlin* deficient newborn lungs (P0).
(B) Staining for elastin at E18.5 and P0. Note the similarity of the elastin and aSMA distribution around the proximal epithelium (arrowheads) and blood vessel (arrows).

4.4. Possible effects of the lack of *Gremlin* on smooth muscle and connective tissue differentiation

As *Gremlin* is expressed by both mesenchymal and epithelial lung compartments (Fig. 1A), we assessed whether the possible excess of cells in neonatal lungs lacking *Gremlin* (Fig. 1H) is due to aberrant mesenchymal cell specification and/or differentiation. However, both smooth muscle α-actin (αSMA; Fig. 6A) and the mesenchymal marker elastin (Fig. 6B) are expressed normally in lungs of *Gremlin* deficient newborn mice. To date, we have however not been able to test if smooth muscle function is normal in lungs of newborn mice lacking the BMP antagonist Gremlin.

5. Conclusion

Taken together, the present study demonstrates that Gremlin is not essential for proximo-distal axis specification during lung organogenesis. Rather, this BMP antagonist regulates branching morphogenesis and is required for epithelial cell differentiation, an essential step in the formation of functional alveoli and initiation of normal respiration at birth.

Acknowledgements

The authors are grateful to I. Ginez, H, N. Lagarde, C. Lehmann and H. Schaller for technical assistance and mouse husbandry. We thank D. Warburton for expert advice concerning lung development and B. Hogan and D. Warburton for providing probes for *in situ* hybridization. This research was supported by the Swiss National Science Foundation (to R.Z.), both cantons of Basel (to R.Z. and K.B.).

CHAPTER 4
Regulation Of Gremlin Expression: The ld Story

Mouse *limb deformity* mutations disrupt a global control region within the large regulatory landscape required for *Gremlin* expression

Aimée Zuniga[1,2], **Odyssé Michos**[1,2], François Spitz[3], Anna-Pavlina G. Haramis[4,5], Lia Panman[2], Antonella Galli[1], Kristina Vintersten[4,6], Christian Klasen[4], William Mansfield[4], Sylwia Kuc[2], Denis Duboule[3], Rosanna Dono[2,7] and Rolf Zeller[1]

[1]Developmental Genetics, Dept. of Clinical-Biological Sciences, University of Basel Medical School, c/o Anatomy Institute, Pestalozzistrasse 20, CH-4056 Basel, Switzerland, [2]Dept. of Developmental Biology, Utrecht University, Padualaan 8, NL-3584CH Utrecht, The Netherlands, [3]Dept. of Zoology and Animal Biology, NCCR 'Frontiers in Genetics' University of Geneva, 30 Quai Ernest-Ansermet, CH-1211 Geneva, Switzerland, [4]EMBL, Meyerhofstrasse 1, D-69117 Heidelberg, Germany, [5]present address: NIOB/KNAW Hubrecht Laboratorium, Uppsalalaan 8, NL-3584 CT Utrecht, The Netherlands, [6]present address: Mount Sinai Hospital, Samuel Lunenfeld Research Institute, Stem Cell Mutagenesis Laboratory, 600 University Avenue, Toronto, Ontario M5G1X5, Canada, [7]present address: INSERM UMR 623, Development and Pathology of the Nervous System, IBDM Campus de Luminy, Case 907, F-13288 Marseille CEDEX 09, France.

Genes Dev. 2004 Jul 1;18(13):1553-64. Epub 2004 Jun 15.

1. Summary

The mouse *limb deformity* (*ld*) mutations cause limb malformations by disrupting epithelial-mesenchymal signaling between the polarizing region and the apical ectodermal ridge. Formin was proposed as the relevant gene because three of the five *ld* alleles disrupt its C-terminal domain. In contrast, our studies establish that the two other *ld* alleles directly disrupt the neighboring Gremlin gene, corroborating the requirement of this BMP antagonist for limb morphogenesis. Further doubts concerning an involvement of Formin in the *ld* limb phenotype are cast, as a targeted mutation removing the C-terminal Formin domain by frame shift does not affect embryogenesis. In contrast, the deletion of the corresponding genomic region reproduces the *ld* limb phenotype and is allelic to mutations in Gremlin. We resolve these conflicting results by identifying a cis-regulatory region within the deletion that is required for *Gremlin* activation in the limb bud mesenchyme. This distant cis-regulatory region within Formin is also altered by three of the *ld* mutations. Therefore, the *ld* limb bud patterning defects are not caused by disruption of Formin, but by alteration of a global control region (GCR) required for *Gremlin* transcription. Our studies reveal the large genomic landscape harboring this GCR, which is required for tissue-specific co-expression of two structurally and functionally unrelated genes.

2. Introduction

The mouse is the genetic model of choice to study mammalian development and diseases. In addition to alteration of specific genes by gene targeting and transgenesis, mutant mouse strains identified by phenotypic screens are commonly used to analyze developmental and disease processes (Justice, 2000; Perkins, 2002). A significant fraction of spontaneous mutations in mice and humans cause congenital limb malformations and have proven crucial to unravel the molecular mechanisms regulating vertebrate limb bud morphogenesis (Gurrieri et al., 2002). In particular, several alleles of the recessive mouse *limb deformity* (*ld*) mutation disrupt patterning of the distal limb skeleton. Over the years, a total of five *ld* alleles have been identified by phenotypic and genetic complementation analysis. All *ld* homozygous newborn mice display limb patterning defects characterized by synostosis of the zeugopod in combination with oligo- and syndactyly of metacarpal bones and digits (Zeller et al., 1999). In addition, *ld* homozygous newborn mice display varying degrees of uni- and bilateral renal aplasias depending on allele "strength" (Maas et al., 1994). Molecular analysis showed that the two *ld* alleles (ld^{TgHd}, ld^{TgBri}), which arose by chance insertional mutagenesis disrupt the C-terminal region of the Formin gene (Wang et al., 1997). The ld^{In2} allele arose by an about 40Mb inversion with breakpoints in the C-terminal region of Formin and the Agouti locus (Woychik et al., 1990). To date the molecular lesions in the two first identified *ld* alleles, ld^{OR} and ld^{J} (Zeller et al., 1999), remained obscure as there are no alterations in the Formin open reading frame (ORF; Wynshaw-Boris et al., 1997). Formin (or Formin1) is the founding member of a multi-gene family that mediates cytoskeletal rearrangements in response to signals that induce, for example, cell polarization (Evangelista et al., 2003). The Formin proteins are encoded by at least 24 exons spread over about 400kb, and alternative splicing gives rise to several protein isoforms of about 180kDa. All Formin isoforms share a proline-rich FH1 domain (interacting with SH3 domains and Profilin) and a highly

conserved C-terminal FH2 domain, which is required to stimulate polymerization of linear actin filaments (Kobielak et al., 2004; Zeller et al., 1999). However, inactivation of specific Formin isoforms by gene targeting in the mouse resulted in partial renal agenesis phenotypes, but failed to reproduce the *ld* limb phenotype as limb morphogenesis was normal (Chao et al., 1998; Wynshaw-Boris et al., 1997).

In *ld* homozygous embryos, the epithelial-mesenchymal signaling interactions regulating limb bud development are disrupted (Panman and Zeller, 2003). Limb bud growth and patterning are coordinately controlled by two main signaling centers, the *Sonic Hedgehog* (*Shh*)-expressing polarizing region, located in the posterior limb bud mesenchyme and the apical ectodermal ridge (AER), which expresses several types of signals including Fibroblast growth factors (FGFs) and Bone morphogenetic proteins (BMPs). Molecular analysis of *ld* mutant limb buds revealed that activation of *Fgf4* expression in the posterior AER, establishment of the SHH/FGF4 feedback loop and thereby up regulation of *Shh* expression by the polarizing region are disrupted (Panman and Zeller, 2003). A functional screen for mesenchymal signals able to relay SHH to the AER resulted in identification of the BMP antagonist Gremlin as the signal lacking from *ld* mutant limb bud mesenchyme. Grafts of *Gremlin*-expressing cells into *ld* mutant limb buds restore *Fgf4* expression and the SHH/FGF4 feedback loop (Zuniga et al., 1999). Analysis of *Gremlin* deficient mouse embryos generated by gene targeting has confirmed its essential functions during limb bud development (Khokha et al., 2003; Michos et al., 2004). Induction of *Fgf8*-expressing AER cells occurs normally, but a morphologically distinct and functional AER fails to form in *Gremlin* deficient embryos. Gremlin-mediated BMP antagonism is required in the limb bud mesenchyme to enable expression of various types of AER signals such as FGF and BMP and for survival of core mesenchymal cells (Michos et al., 2004). The general disruption of AER function in *Gremlin* deficient embryos in turn blocks propagation of *Shh* expression by the polarizing region as is also observed in *ld* mutant limb buds. In addition, the induction of metanephric kidney organogenesis and complete differentiation of lung airway epithelia fail to occur, which causes neonatal lethality (Chapter 2,3). The studies by Michos et al. (2004; Chapter 2) reveal a more general role of Gremlin-mediated BMP antagonism in epithelial-mesenchymal signaling during vertebrate organogenesis. Interestingly, the *Gremlin* transcription unit maps only about 40kb downstream of the Formin gene on mouse chromosome 2 and is transcribed in opposite orientation (University of California at Santa Cruz Genome Browser, http://genome.ucsc.edu). Finally, Khokha et al. (2003) established allelism between one of the *ld* alleles (ld^{J}) and a *Gremlin* null allele generated by gene targeting, but did not analyze the genetic and molecular basis for these rather unexpected findings.

In the present study we establish that the ld^{J} mutation is a point mutation affecting splicing of *Gremlin* transcripts that results in truncation of the 5'part of the Gremlin ORF. Furthermore, the complete *Gremlin* ORF encoded by exon 2 is deleted by the ld^{OR} mutation. Therefore, these two *ld* alleles are spontaneous *Gremlin* loss-of-function alleles, which also establishes that the *ld* complementation group encompasses both the Gremlin and Formin loci. Using gene targeting we show that disruption of the Formin FH2 domain by deleting coding exon 10 ($Fmn^{\Delta 10}$ mutation) does not reproduce the *ld* phenotype. In contrast, deletion of the genomic region encompassing exon 10 to 24 ($Fmn^{\Delta 10.24}$ mutation) results in the characteristic *ld* limb phenotype. Interestingly, the $Fmn^{\Delta 10.24}$ deletion, but not the $Fmn^{\Delta 10}$ mutation, is allelic to *Gremlin* loss-of-function

mutations. Further analysis establishes that the deleted region encodes regulatory elements required to activate both *Formin* and *Gremlin* expression in the posterior limb bud mesenchyme and mediate responsiveness to SHH, but not to FGF signaling. BAC transgenic analysis positively identifies this cis-regulatory region and shows that it is required to activate *Gremlin* transcription in the posterior distal limb bud mesenchyme. The features of this large cis-regulatory landscape are reminiscent of a recently discovered global control region, a novel type of chromosomal regulatory element that controls expression of 5'Hoxd genes in the distal limb bud mesenchyme (Spitz et al., 2003). Taken together, our studies establish that the *ld* limb phenotype is a direct consequence of losing *Gremlin* expression in the limb bud mesenchyme and not due to disrupting Formin functions. We also discuss how such large regulatory landscapes that control tissue-specific co-expression of functionally unrelated genes may have arisen.

3. Materials and methods

3.1. Mapping and identification of the *ld*^{OR} and *ld*^{J} mutations

The deletion of the Gremlin ORF in the *ld*^{OR} allele was initially detected by Southern blotting (Fig. 1B) and mapped using a combination of Southern blot and long-range PCR analysis (Jansen et al., 1997). A PCR fragment spanning the deletion breakpoints in the *ld*^{OR} allele was isolated. This fragment was sequenced and the extent of the deletion identified by sequence comparison to the wild type *Gremlin* locus. The *ld*^{OR} allele was crossed into 129S3/SvImJ, C57BL/6 and CD1 strains as the penetrance of the kidney phenotype depends on genetic background. In the 129S and CD1 backgrounds, the kidney phenotype is fully penetrant (Fig. 1D). The point mutation affecting splicing of *Gremlin* in the *ld*^{J} allele was identified as follows. Total RNAs were isolated from wild type and *ld*$^{J/J}$ mouse embryos (embryonic day 12) using the RNeasy kit (Qiagen) and cDNAs synthesized using standard procedures. *Gremlin* transcripts were amplified using specific primers in exon 1 and 2. The *Gremlin* locus was analyzed comparing genomic DNA from wild type and *ld*$^{J/J}$ embryos. The genomic region containing the intron-exon 2 boundary was amplified by PCR and PCR products separated on a 1.0% agarose gel and in all cases (cDNAs and genomic DNAs) only one specific fragment was amplified (data not shown). These amplified DNA bands were cloned and their sequences analyzed using the CLUSTAL-X program (http://www.ebi.ac.uk/clustalw/). Sequences of all primers used for these studies are available upon request.

3.2. Generation of *Fmn* mutant alleles

The *Fmn*$^{\Delta 10}$ allele was obtained by successive targeting in R1 ES cells (Nagy et al., 1993). Initially, Fmn exon 10 (151 bases) was completely replaced by a PGK-*Neo*^{R} expression cassette with an SV40 poly-adenylation site and a *Lox*P site was inserted further downstream in the intron (Fig. 3B). One of three correctly recombined ES-cell clones was selected for additional gene targeting. A PGK-*Hygro*^{R} cassette flanked by two *lox*P sites and an *En2* splice acceptor-IRES-*LacZ* expression cassette (Mountford et al., 1994) was inserted into Fmn exon 24 using a Spe1 site 86 bases downstream of the translational stop codon. 53 correctly targeted ES-cell clones were obtained and characterized extensively by genomic Southern blot analysis to confirm correct

alterations of both targeted genomic sites. To identify clones carrying both targeting sites in cis, 25 ES-cell clones were electroporated with a *Cre* expression vector. For 14 ES-cell clones, the correct Cre-mediated excision patterns were obtained for all possible combinations between the three *Lox*P sites (Fig. 3B). ES-cell clones carrying the $Fmn^{\Delta 10}$ allele were injected into C57BL/6 blastocysts and germline transmission was obtained. $Fmn^{\Delta 10}$ mice were maintained by breeding a mixed B6;129S background. The $Fmn^{\Delta 10.24}$ allele was generated by intercrossing $Fmn^{\Delta 10/+}$ mice with the Cre deleter mouse strain (Schwenk et al., 1995). PCR analysis was used to show that excision had occurred between the two most distant *Lox*P sites, causing deletion of the genomic region spanning *Fmn* exons 10 to 24 (170kb).

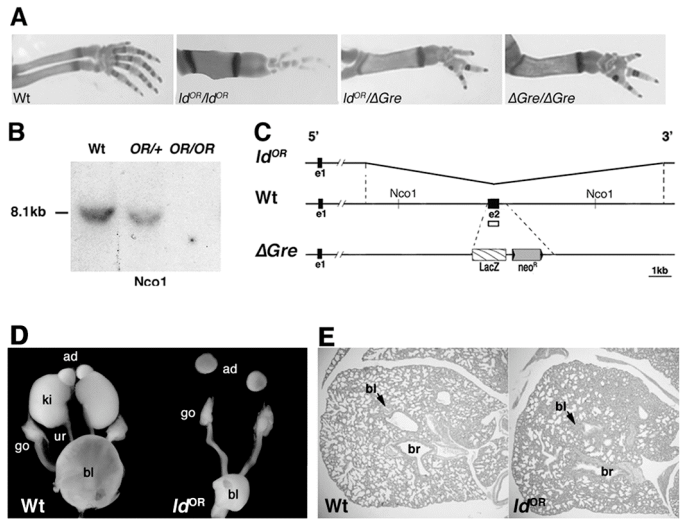

Fig.1 The ld^{OR} is a *Gremlin* loss-of-function alleles.
(A) The ld^{OR} mutation is allelic to the *Gremlin* null allele generated by gene targeting (Chapter 2). (B) Southern blot analysis reveals that the Gremlin ORF encoded by exon 2 is deleted in the ld^{OR} mutation. Genomic DNA isolated from embryos was digested by NcoI and probed with a Gre e2 probe (open box in scheme, panel C). Wt: wild type littermate; OR/+; heterozygous embryo; OR/OR: homozygous embryo. (C) Schematic representation of the Gremlin locus on chromosome 2 in the ld^{OR} allele, wild type and Δ*Gre* mutation. ld^{OR}: kinked line indicates the 12.7kb region deleted in the ld^{OR} mutation. Wt: Open box indicates the probe used for the Southern blot analysis shown in panel B. Δ*Gre*: *LacZ* and the Neo^{R} replace coding e2 in the *Gremlin* null allele generated by gene targeting. e1: exon 1; e2: exon 2. (D,E) Bilateral renal agenesis and lung defects in $ld^{OR/OR}$. (D) Dissected urogenital system of wild type and $ld^{OR/OR}$ newborn female. Note the absence of both kidneys and ureter in the mutant. ad: adrenal gland; ki: kidney; ur: ureter; go: gonade; bl: bladder. (E) Haematoxylin-eosin staining of transversal sections of newborn lungs and $ld^{OR/OR}$ newborn mouse. Note the reduced number of alveoli in mutant's lungs. bl: blood vessel; br: bronchiole.

3.3. RT-PCR analysis of *Formin* expression

Total RNA from wild type, $Fmn^{\Delta 10}$ and $Fmn^{\Delta 10.24}$ homozygous embryos was isolated using the RNeasy extraction kit (Qiagen). First strand cDNAs were synthesized according to standard procedures by using 17μg of total RNA. Subsequently, PCR was performed to detect *Formin* transcripts. The following primer pairs were used: forward primer in exon 9 (e9: 5' GCTCTTCCTAACAGTGGAGGTCC 3') and reverse primer in exon 15 (e15: 5' CACACTCTTCATGTGCAACAA 3') or exon 23 (e23L1: 5' CTTTGTCTCCACTTTCTTCTCTGATGTC 3') for wild type and $Fmn^{\Delta 10/\Delta 10}$ cDNAs, forward primer in exon 9 and reverse primer in IRES (IRES1: 5' GCTTCCTTCACGACATTCAACAGACC 3') for $Fmn^{\Delta 10.24/\Delta 10.24}$ cDNAs. PCR products

were separated on a 1.0% agarose gel and cloned for sequence analysis and alignment using the CLUSTAL-X program (http://www.ebi.ac.uk/clustalw/).

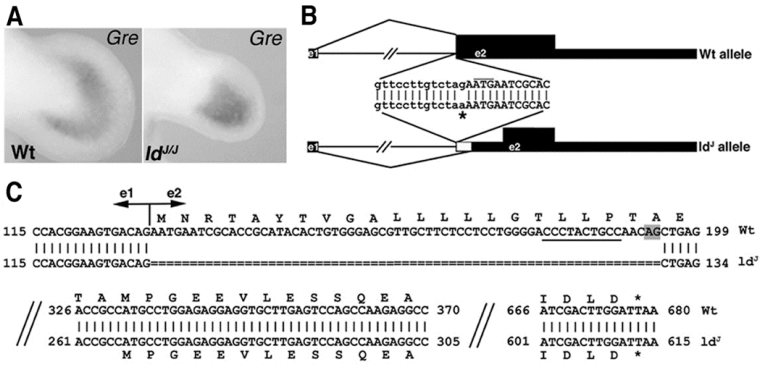

Fig.2 The *ld*^{J} mutation is a *Gremlin* loss-of-function allele.
(A) *Gremlin* remains expressed in *l d*^{J} homozygous embryos. Shown are limb buds of a wild type (Wt) and *ld*^{J} homozygous (*ld*$^{J/J}$) mouse embryo at embryonic day 11.5. (B) The G to A mutation at the intron-exon 2 junction of the Gremlin gene (indicated by an asterisk) disrupts splicing. Lower cases indicate intronic, upper cases exonic sequences. Thick black boxes indicate the Gremlin ORF, thin boxes the 5' and 3'non-coding regions. The thin white box indicates the deletion of mRNA due to aberrant splicing. Thin black lines indicate intronic sequences and splices. (C) Aberrant pre-mRNA splicing deletes the first 65 bases of the Gremlin ORF. Shown is an alignment of the cDNA sequences of Wt and *ld*^{J} alleles with the respective ORFs. The truncated *ld*^{J} *Gremlin* transcript could potentially encode a Gremlin protein of 117 amino acids (instead of 184) lacking the signal peptide (Avsian-Kretchmer and Hsueh, 2003). The AG dinucleotide used for splicing in the *ld*^{J} allele is shaded grey. The required upstream poly-pyrimidine tract is underlined (Faustino and Cooper, 2003).

3.4. Culture of mouse limb buds (trunk cultures) and inhibition of FGF signaling

Shh-expressing cells were grafted into mouse limb buds (30-33 somites, E10.0-10.25) cultured as described (Zuniga et al., 1999). Alternatively, FGF signaling was blocked by supplementing the culture medium with 10μM SU5402 (final concentration), an efficient inhibitor of FGF signal transduction (Mohammadi et al., 1997). SU5402 (Calbiochem) was dissolved in 100% DMSO at 10mg/ml (stock solution). Experimental controls were treated with an equal concentration of DMSO in culture medium (0.03% final). The SU5402 concentration blocking FGF signaling efficiently was established in pilot experiments and is well within the commonly used range of concentrations. Both grafted and SU5402 treated limb buds were cultured for 14-16hrs prior to analysis by *in situ* hybridization.

3.5. Skeletal preparations, whole mount *in situ* hybridization and LacZ staining

Skeletal preparations and whole mount *in situ* hybridization assays were carried out as previously described (Zuniga and Zeller, 1999). β-galactosidase (LacZ) activity was detected in whole mounts (Knittel et al., 1995) with the following modification: embryos were stained in the dark at 37°C in 1mg/ml X-Gal, 0.25mM $K_3Fe(CN)_6$, 0.25mM $K_4Fe(CN)_6$, 0.01% NP40, 0.4mM $MgCl_2$ in 1X PBS.

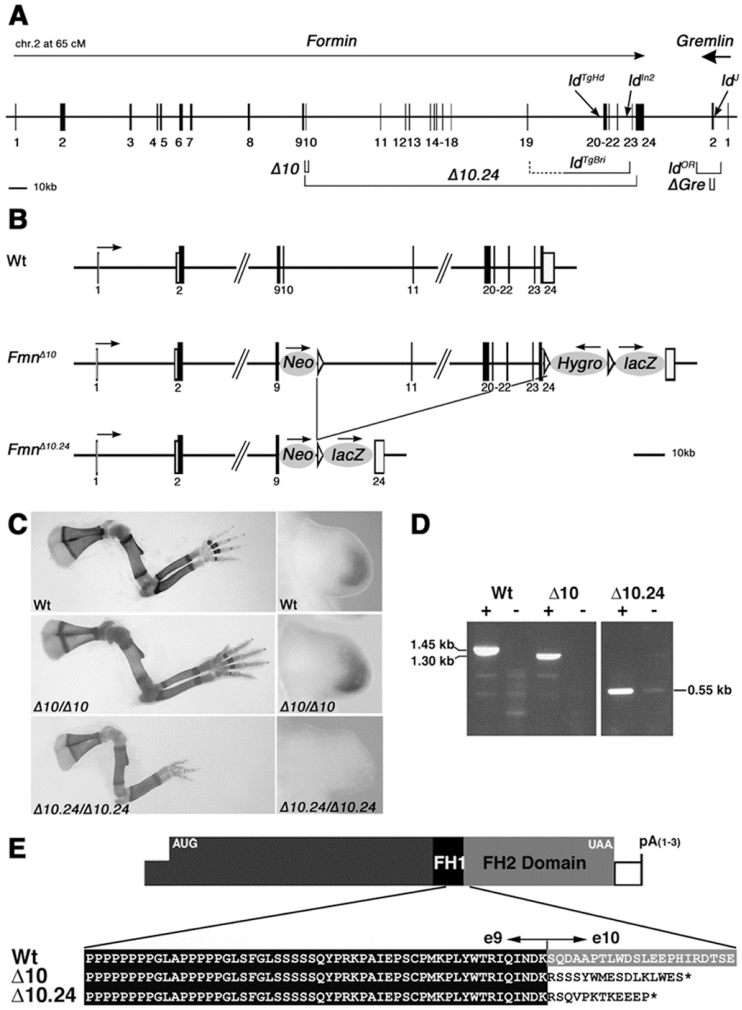

Fig.3 Not disruption of the Formin FH2 domain, but deletion of the corresponding genomic region causes the *ld* limb phenotype. (A) Representation of the *ld* complementation group consisting of Formin (Fmn) and Gremlin (Gre) loci. The Fmn gene is encoded by at least 24 exons (transcriptional direction indicated by arrow), while the Gre gene is transcribed in reverse orientation (bold arrow) and contains only two exons. The intergenic region separating the 2 genes is about 38kb. The Fmn FH2 domain is encoded by exons 10 to 24 and is present in all Fmn protein isoforms (Wang et al. 1997). The following genetically engineered mutations are indicated: Δ10: *Fmn*$^{\Delta 10}$ allele; Δ10.24: *Fmn*$^{\Delta 10.24}$ allele; ΔGre: *Gre*$^{\Delta ORF}$ null allele (Chapter 2). The spontaneous *ld* alleles are indicated: *ld*^{TgBri}: transgene induced deletion of genomic region between exon 19 and 23 (Vogt et al. 1992); *ld*^{TgHd}: transgene insertional mutagenesis (Woychik et al. 1985); *ld*^{In2}: 40Mb inversion involving Fmn and Agouti loci (Woychik et al. 1990); *ld*^{OR}: deletion of the *Gre*$^{\Delta ORF}$; *ld*^{J}: point mutation disrupting *Gre* pre-mRNA splicing. (B) Representation of the genetically engineered *Fmn*$^{\Delta 10}$ and *Fmn*$^{\Delta 10.24}$ alleles. Neo: PGK-*Neo*^{R} gene used to select ES-cell clones (first round of gene targeting), Hygro: PGK-*Hygro*^{R} gene used to select ES-cell clones (second round of gene targeting), lacZ: IRES-*LacZ* gene used to tag *Fmn* transcripts. Arrows indicate direction of transcription. Fmn exons are numbered as in panel A. (C) Left panels: limb skeletal phenotypes of wild type and homozygous mice. Genotypes are indicated in the panels. Right panels: *Gre* expression in limb buds of wild type and homozygous embryos (E10.75). (D) RT-PCR of *Fmn* transcripts isolated from wild type (Wt), *Fmn*$^{\Delta 10}$ (10/10) and *Fmn*$^{\Delta 10.24}$ (10.24/10.24) homozygous embryos. Wild type and *Fmn*$^{\Delta 10}$ mRNAs extending downstream of exon 9 were detected using primers in exons 9 and 23, *Fmn*$^{\Delta 10.24}$ mRNAs extending downstream of exon 9 were detected using primers in exon 9 and the IRES-*LacZ* tag (see Methods). +: reverse transcriptase included, -: reverse transcriptase omitted (control). Note that the difference in size between wild type (Wt) and *Fmn*$^{\Delta 10}$ transcripts is 150 bases, as expected. (E) Amino acid sequence deduced from the sequences of the *Fmn* transcripts arising from wild type, *Fmn*$^{\Delta 10}$ and *Fmn*$^{\Delta 10.24}$ alleles.

3.6. BAC constructs and generation of transient transgenic mouse embryos

The genomic organization of the Gremlin and Formin loci and the appropriate BAC were identified using sequences from the Mouse Genome Sequencing Consortium (Waterston et al., 2002) and analyzed with the UCSC Genome Browser (http://genome.ucsc.edu). Mouse BAC clones were obtained from BacPac Resources (Children' s Hospital Oakland, USA) and modified by ET recombination as described (Spitz et al., 2003). Construct A was engineered by inserting a LacZ reporter gene in frame into the Gremlin ORF encoded by BAC RP23-113H17 (Fig. 8A) using a Zeocin resistance cassette (Invitrogen). Construct B (Fig. 8B) was obtained by deleting the region between exons 19 to 23 from construct A using a Kanamycin resistance cassette. Construct C (Fig. 8C) was generated by targeted replacement of Fmn exon 23 and all downstream 3'sequences from BAC RP23-113H17 by a LacZ reporter gene driven by a *β-globin* minimal promoter (Spitz et al., 2003). This cassette is flanked by 50 bases of BAC DNA sequence, which borders the region to be deleted by homologous recombination. All BAC constructs were injected into the pronucleus of fertilized mouse eggs according to standard procedures (Nagy et al., 2002; Spitz et al., 2001) and embryos were collected during embryonic day 10 (E10.5) and analyzed by LacZ staining.

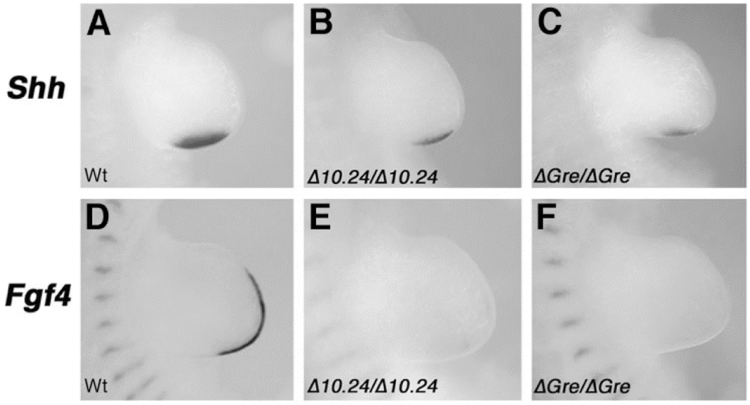

Fig.4 Epithelial-mesenchymal signaling in limb buds of $Fmn^{\Delta 10}$, $Fmn^{\Delta 10.24}$ and $Gre^{\Delta ORF}$ homozygous embryos (E10.5).
(A-C) *Shh* expression in the posterior limb bud mesenchyme. (D-F) *Fgf4* expression in the posterior AER. Genotypes are indicated as defined in the legend to Fig. 3A.

4. Results

4.1. The ld^{J} and ld^{OR} alleles are loss-of-function mutations directly disrupting the Gremlin gene products

In contrast to the three independent alleles of the mouse *ld* mutation that truncate Formin (see Introduction), no molecular alterations of the Formin ORF were identified for the ld^{OR} and ld^{J} alleles (Wynshaw-Boris et al., 1997). However, both these *ld* mutations are allelic to null mutations in the neighboring Gremlin gene (generated by gene targeting; Michos et al., 2004) as compound heterozygous mice display the characteristic *ld* limb phenotype (Fig. 1A; Khokha et al., 2003). Furthermore, newborn ld^{OR} homozygous mice lack kidneys and ureters (Fig. 1D) similar to *Gremlin* deficient

(Michos et al., 2004; Chapter 2) and *ld*^{J} homozygous mice (Maas et al., 1994). This renal agenesis in combination with lung defects (Fig. 1D,E) causes death shortly after birth identical to *Gremlin* null mutant mice (Michos et al., 2004). Molecular analysis of the *ld*^{OR} allele indeed reveals a 12.7kb genomic deletion removing the complete Gremlin ORF (Fig. 1B,C), which establishes the *ld*^{OR} mutation as a spontaneous *Gremlin* null allele. In sharp contrast, *Gremlin* transcripts remain expressed in embryos homozygous for the *ld*^{J} allele (Fig. 2A), despite the fact that activation of *Fgf4* in the posterior AER is disrupted and the *Shh*-expressing polarizing region is not maintained (Haramis et al., 1995). Sequence analysis of the Gremlin locus in the *ld*^{J} allele reveals a specific G to A base change at the first intron-exon 2 boundary (asterisk, Fig. 2B). This point mutation eliminates the intronic AG motif at the 3'splice site, which is essential for correct pre-mRNA splicing (Faustino and Cooper, 2003). Indeed, a single aberrantly spliced transcript with a 65 bases deletion removing the 5'part of exon 2 was identified in *ld*^{J} homozygous embryos (Fig. 2C and data not shown). This aberrant splice makes use of a downstream AG dinucleotide within exon 2 that is preceded by a pyrimidine-rich stretch required for splicing (Figure 1F, Faustino and Cooper, 2003). This deletion within the *Gremlin* transcript removes the AUG translational start codon, thereby abolishing translation of full length secreted Gremlin protein (Fig. 2C).

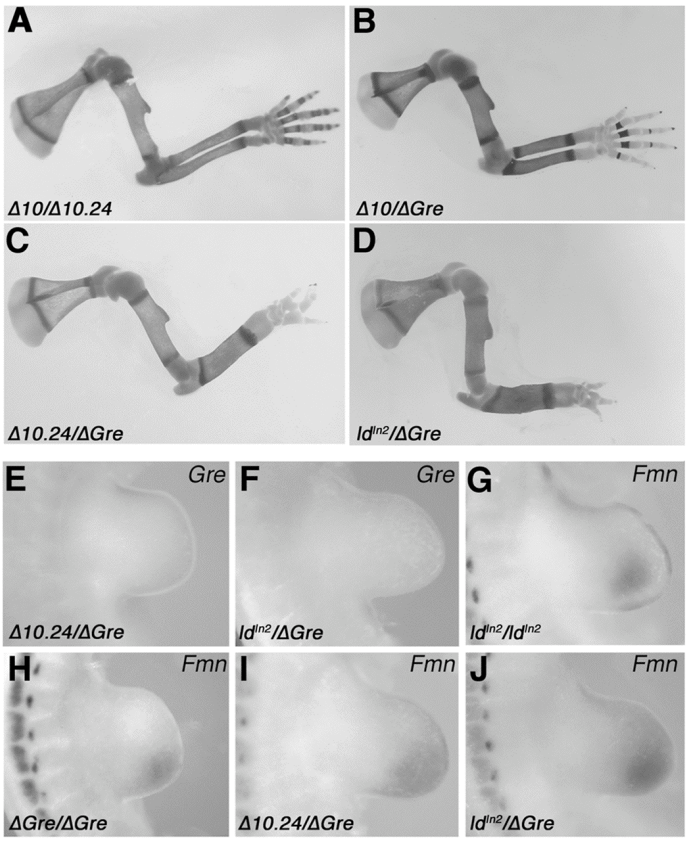

Fig.5 The *Fmn*$^{\Delta 10.24}$ and *ld*^{In2} mutations are allelic to *Gre*$^{\Delta ORF}$ by disrupting cis-regulation of *Gremlin* in the limb bud mesenchyme.
(A-D) Skeletal phenotypes of compound heterozygous mice. (E, F) *Gremlin* is no longer expressed in the limb bud mesenchyme of *Fmn*$^{\Delta 10.24/+}$; *Gre*$^{\Delta ORF/+}$ (E) and *ld*$^{In2/+}$; *Gre*$^{\Delta ORF/+}$ (F) compound heterozygous embryos. (G-J) *Fmn* remains expressed in the limb bud mesenchyme of *ld*$^{In2/In2}$ (G), *Gre*$^{\Delta ORF/\Delta ORF}$ (H), *Fmn*$^{\Delta 10.24/+}$; *Gre*$^{\Delta ORF/+}$ (I) and *ld*$^{In2/+}$; *Gre*$^{\Delta ORF/+}$ (J) compound heterozygous embryos.
Note: samples (G-J) were pre-treated prior to *in situ* hybridization for optimal detection of *Fmn* transcripts in the mesenchyme. Such pre-treatment results in loss of the AER. Genotypes are indicated as defined in the legend to Fig. 3A.

4.2. Not the disruption of the Formin FH2 domain, but deletion of the corresponding genomic region causes the *ld* limb phenotype

The fact that the ld^{OR} and ld^{J} alleles are *Gremlin* loss-of-function mutations (Fig. 1,2) reiterates the question, whether the disruption of Formin functions is indeed the primary cause of the *ld* limb phenotype. In particular, the Gremlin gene is located about 40kb downstream of Formin and transcribed in opposite orientation, extending the *ld* complementation group to around 450-500kb in size (Fig. 3A). Previous analysis showed that the other three *ld* alleles (ld^{In2}, ld^{TgBri} and ld^{TgHd}; for details see Wang et al., 1997) disrupt the genomic region encoding the C-terminal part of Formin (encoded by exons 10 to 24; Fig. 3A). In an attempt to reproduce the *ld* limb phenotype and possibly generate a null allele by reverse genetics, Formin exon 10 was deleted ($Fmn^{\Delta 10}$ allele, Fig. 3B**;** for details see Materials and methods). Exon 10 was chosen as its deletion results in a frame shift that disrupts translation of the C-terminal protein domain completely (Fig. 3E). Rather unexpectedly, $Fmn^{\Delta 10}$ homozygous mice are phenotypically wild type (Fig. 3C and data not shown), thereby establishing that deletion of exon 10 is not sufficient to reproduce the *ld* limb phenotype. Next, we deleted the complete genomic region spanning exons 10 to 24 (Fig. 3A; region 10.24), which results in the $Fmn^{\Delta 10.24}$ allele (Fig. 3B; for details see Materials and methods). Mice homozygous for the $Fmn^{\Delta 10.24}$ allele indeed display the characteristic *ld* limb phenotype (Fig. 3C). However, $Fmn^{\Delta 10.24}$ homozygous newborn mice display neither renal agenesis nor lung patterning phenotypes and survive to adult hood (data not shown). Molecular analysis of $Fmn^{\Delta 10.24}$ homozygous embryos reveals that *Gremlin* expression is lost specifically from the limb bud mesenchyme, while it is normal in $Fmn^{\Delta 10}$ homozygous embryos (Fig. 3C and data not shown). In agreement with limb bud specific loss of *Gremlin* expression, activation of *Fgf* in the posterior AER and SHH-GRE/AER feedback signaling are disrupted in $Fmn^{\Delta 10.24}$ homozygous embryos (Fig. 4), but not in $Fmn^{\Delta 10}$ homozygous embryos (data not shown). One possible explanation for the lack of an *ld* limb phenotype in $Fmn^{\Delta 10}$ homozygous embryos could be the rescue of Formin function due to aberrant splicing. However, thorough analysis of *Formin* transcripts extending 3' to exon 9 by RT-PCR provided no evidence for aberrant splicing (Fig. 3D and data not shown). Furthermore, sequence analysis of the altered *Formin* transcripts in $Fmn^{\Delta 10}$ and $Fmn^{\Delta 10.24}$ homozygous embryos establishes that the Formin ORF is truncated in both alleles at the level of the exon 9-10 boundary (Fig. 3E). These results show that the *ld* limb phenotype in the $Fmn^{\Delta 10.24}$ mutation is not caused by disruption of the C-terminal Formin protein domain as previously concluded (Zeller et al., 1999), but by the deletion of other essential elements located in the genomic region 10.24.

4.3 The genomic region 10.24 exerts cis effects on *Gremlin* expression in the limb bud mesenchyme

The phenotypic analysis indicated that all *ld* mutations belong to the same complementation group in spite of them disrupting either the Formin or Gremlin loci (Fig. 3A); therefore, allelism between the $Fmn^{\Delta 10}$, $Fmn^{\Delta 10.24}$ and $Gre^{\Delta ORF}$ mutations was assessed. Limbs of $Fmn^{\Delta 10/\Delta 10.24}$ and $Fmn^{\Delta 10}$; $Gre^{\Delta ORF}$ compound heterozygous mice are normal (Fig. 5A,B), confirming the wild type phenotypic nature of the $Fmn^{\Delta 10}$ mutation. In contrast, the $Fmn^{\Delta 10.24}$ mutation is a hypomorphic allele of the $Gre^{\Delta ORF}$ null mutation

as *Fmn*$^{\Delta 10.24}$; *Gre*$^{\Delta ORF}$ mice display a fully penetrant *ld* limb phenotype (Fig. 5C), but not the phenotypes causing neonatal lethality (data not shown). The *ld*^{In2} allele is of particular interest as an inversion between Formin and Agouti (Woychik et al., 1990) relocates the Gremlin gene about 40Mb away on mouse chromosome 2. Compound *ld*^{In2}; *Gre*$^{\Delta ORF}$ heterozygous mice also display the *ld* limb phenotype (Fig. 5D), which indicates that integrity of the genomic region encoding Formin and Gremlin (Fig. 3A) is required in cis for normal limb bud development. Therefore, the loss of *Gremlin* expression in *Fmn*$^{\Delta 10.24}$ (Fig. 3E) and *ld*^{In2} homozygous limb buds seems to be a consequence of either deleting (*Fmn*$^{\Delta 10.24}$) or disrupting (*ld*^{In2}) a distant cis-regulatory element of *Gremlin* expression in limb buds rather than disrupting Formin functions (Zuniga et al., 1999). Indeed, *Gremlin* transcription is lost from the limb bud mesenchyme of *Fmn*$^{\Delta 10.24}$; *Gre*$^{\Delta ORF}$ and *ld*^{In2}; *Gre*$^{\Delta ORF}$ compound heterozygous embryos (Fig. 5E,F). Conversely, *Formin* remains expressed in limb buds of *ld*^{In2} and *Gre*$^{\Delta ORF}$ homozygous (Fig. 5G,H) and compound heterozygous embryos (Fig. 5I,J). These results indicate that the relevant elements in question are located upstream of Formin coding exon 23. As no additional genes have been found in the genomic region 10.24 (data not shown), these results indicate that this region is required for cis-regulation of *Gremlin* expression in the limb bud mesenchyme.

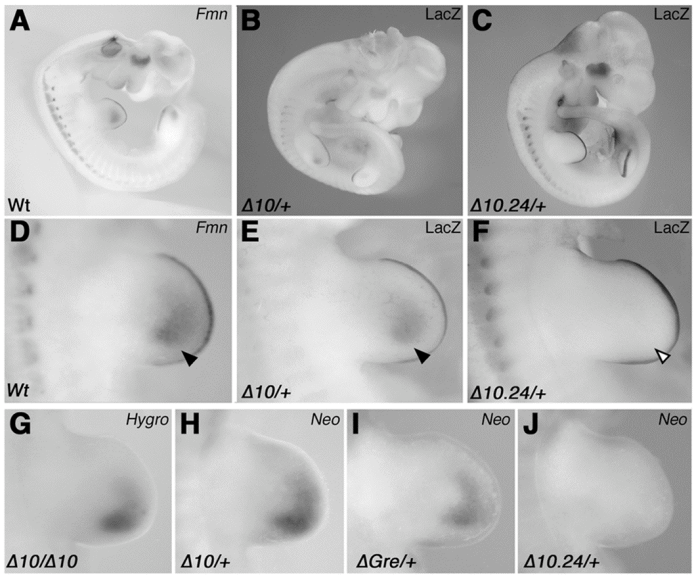

Fig.6 The Fmn genomic region 10.24 regulates expression of endogenous and exogenous transcription units inserted into the *ld* locus.
(A) *Fmn* transcript distribution in a wild type embryo around gestational day 10.5 (hemi-section). (B) *LacZ* recapitulates the *Fmn* transcript distribution in the *Fmn*$^{\Delta 10}$ allele. (C) Limb bud mesenchymal *LacZ* is specifically lost in the *Fmn*$^{\Delta 10.24}$ allele. (D-F) Fore limb buds of the embryos shown in panels A to C. Black arrowheads indicate *Fmn*/*LacZ* distribution, open arrowhead loss of *LacZ* in the *Fmn*$^{\Delta 10.24}$ allele. (G-J) Limb bud mesenchyme specific expression of the *Hygro*^{R} (G) and *Neo*^{R} (H-J) genes inserted into the *ld* locus. Genotypes are defined in the legend to Fig. 3A.

4.4. Cis-regulatory elements in region 10.24 mediate activation and SHH responsiveness in the limb bud mesenchyme

To explore the molecular mechanism for cis-regulation of *Gremlin*, we analyzed the expression of exogenous genes inserted into the *ld* locus (Fig. 3A,B). In the *Fmn*$^{\Delta 10}$ and *Fmn*$^{\Delta 10.24}$ alleles expression of the LacZ reporter gene is controlled by the

endogenous Fmn promoters (Fig. 3B). As a consequence, the *LacZ* distribution recapitulates *Formin* expression perfectly in *Fmn*$^{\Delta 10}$ heterozygous embryos (compare Fig. 6A to Fig. 6B). In *Fmn*$^{\Delta 10.24}$ heterozygous embryos, LacZ activity (Fig. 6C) is specifically lost from the limb bud mesenchyme (arrowheads, compare Fig. 6D,E to Fig. 6F). These results reveal that the genomic region 10.24 is required for limb bud mesenchymal expression of both *Gremlin* and *Formin* (Fig. 5E and Fig. 6C,F). Furthermore, insertion of PGK promoters driving expression of *Neo*^{R} and *Hygro*^{R} genes at various positions (Fig. 3B) results in these exogenous transcripts being expressed like *Formin* and *Gremlin* in the limb bud mesenchyme (Fig. 6G-I), irrespective of transgene insertion site and orientation (Fig. 3B). In contrast, expression of the *Neo*^{R} transgene is lost in limb buds heterozygous for the *Fmn*$^{\Delta 10.24}$ mutation (Fig. 6J). These results reveal the presence of cis-regulatory elements within *Fmn* genomic region 10.24 able to drive expression of exogenous genes in the limb bud mesenchyme. As both *Gremlin* and *Formin* expression are positively regulated by SHH signaling in the limb bud mesenchyme (Zuniga et al., 1999), a potential role of region 10.24 in mediating this SHH responsiveness was assessed. Indeed, anterior grafts of *Shh*-expressing cells induce ectopic *LacZ* expression in cultured limb buds of *Fmn*$^{\Delta 10}$ heterozygous embryos (compare Fig. 7A to 7B). In contrast, SHH is unable to induce *LacZ* expression in limb buds of *Fmn*$^{\Delta 10.24}$ heterozygous embryos (compare Fig. 7C to 7D), which indicates that this region participates in mediating SHH responsiveness of *Formin* and *Gremlin* in the limb bud mesenchyme. In contrast to the *Fmn*$^{\Delta 10.24}$ allele (Fig. 7D), *Formin* but not *Gremlin* (Zuniga et al., 1999) expression can be ectopically induced by SHH in *ld*^{In2} homozygous limb buds (compare Fig. 7E to 7F and data not shown). These results show that the inversion affecting the *ld*^{In2} allele separates the *Gremlin*, but not *Formin* transcription unit from the SHH response elements (see also Fig. 10A).

Analysis of *Gremlin* expression in chicken embryos suggested that its expression in the limb bud mesenchyme may depend on FGF signaling by the AER (Merino et al., 1999c). However, limb buds of *Fmn*$^{\Delta 10/\Delta 10}$ embryos cultured in the presence the FGF signaling inhibitor SU5402 (Mohammadi et al., 1997) continue to express *LacZ* and *Gremlin* (compare Fig 7G,I to 7H,J). As expected, inhibition of FGF signaling causes flattening of the AER (data not shown) and subsequent down-regulation of *Shh* and *Fgf* expression due to disrupting feedback signaling (Fig. 7K,L and data not shown). The results shown in Figure 7G-7J indicate that mesenchymal *Formin* and *Gremlin* expression does not depend significantly on FGF signaling. In agreement, genetic analysis reveals that *Gremlin*, but not *Shh*, remains expressed in mouse limb buds lacking both *Fgf8* and *4* (Sun et al., 2002).

4.5. The genomic region 19.23 is sufficient to activate gene expression in the limb bud mesenchyme

Using a BAC based strategy to generate transient transgenic mouse embryos; we have positively identified the relevant cis-regulatory region (Fig. 8). Initially, a BAC containing the mouse Fmn genomic region spanning exons 19 to 24, the intergenic region and the complete Gremlin transcription unit (tagged by LacZ in exon 2) was injected into fertilized oocytes and embryos stained for LacZ activity during gestational days 10.5 (Fig. 8A). This transgene (BAC construct A) is expressed in the posterior

limb bud mesenchyme (arrowheads, Fig. 8A, n= 5/6), which indicates that all the required cis-regulatory elements are present. In contrast, LacZ activity is specifically lost from the limb bud mesenchyme of embryos harboring BAC construct B, which lacks region 19.23 (Fig. 8B, n= 7/7). The potential autonomy of region 19.23 (Fig. 8C) was assessed by inserting it downstream of a LacZ gene under control of a minimal ß-globin promoter (Morgan et al., 1996). Indeed, BAC constructs C (Fig. 8C) and a shorter construct-containing region 20.23 (data not shown) is sufficient to drive *LacZ* expression into the posterior limb bud mesenchyme (arrowheads, Fig. 8C, n= 2/6). These results establish that region 19.23 encodes cis-regulatory elements sufficient to activate gene expression in combination with either the endogenous *Gremlin* or an exogenous minimal promoter (albeit with lower efficiency, compare Fig. 8A to 8C). Furthermore, region 19.23 is sufficient to activate *LacZ* expression in both dorsal and ventral posterior limb bud mesenchyme similar to *Formin* and *Gremlin* (Fig. 9). Reduction of this genomic region reduces expression further, indicating that the required regulatory elements are spread over a larger region (see also Fig. 10 and data not shown).

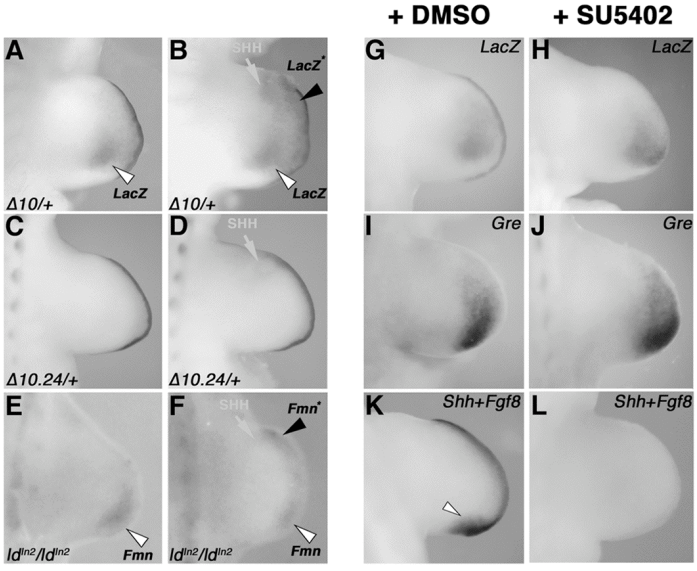

Fig.7 The limb bud regulatory region 10.24 is responsive to SHH signaling. *Shh*-expressing cells were grafted to the anterior limb bud mesenchyme (E10.25, 32-34 somites) and trunks cultured for 16-20hrs. (A) Non-grafted limb bud of an $Fmn^{\Delta 10}$ heterozygous embryo (control). (B) Ectopic *LacZ* in the contra-lateral limb bud having received an anterior graft of *Shh*-expressing cells. (C) Control $Fmn^{\Delta 10.24}$ heterozygous limb bud. (D) Failure to induce *LacZ* expression in response to *Shh*-expressing cells in an $Fmn^{\Delta 10.24}$ heterozygous limb bud. (E) Control limb bud of an ld^{In2} homozygous embryo. (F) Induction of *Fmn* expression in response to ectopic SHH signaling in an ld^{In2} homozygous embryo. A arrow in panels (A-F) indicates the position of *Shh*-expressing cells. A black arrowhead and an asterisk in panels (A-F) indicate ectopic gene expression, while an open arrowhead indicates endogenous expression. (G-L) *Gre* and *Fmn* expression are maintained in limb buds in which FGF signaling transduction has been blocked by the inhibitor SU5402. Fore limb buds of $Fmn^{\Delta 10/\Delta 10}$ embryos (E10.0, 29-32 somites) were cultured in the presence of 10mM SU5402 (+SU5402; stock dissolved in DMSO) for 14-16hrs prior to analysis. Controls were cultured in the presence of an equal concentration of DMSO (+DMSO; 0.03% final concentration in medium). (G) *LacZ* detection in an untreated limb bud. (H) *LacZ* remains in a limb bud cultured in the presence of SU5402. Note the down-regulation of *LacZ* in the AER due to flattening in absence of FGF signal transduction. (I) *Gre* expression in an untreated limb bud. (J) *Gre* remains in a limb bud cultured in the presence of SU5402. (K) Detection of *Shh* (arrowhead) and *Fgf8* transcripts (AER) in an untreated limb bud. (L) Loss of both *Shh* and *Fgf8* expression in a limb bud cultured in the presence of SU5402.

5. Discussion

We establish that the *ld* limb phenotype is caused by disrupting either the regulatory landscape controlling transcriptional activation of the BMP antagonist Gremlin in the limb bud mesenchyme or directly the *Gremlin* transcription unit. Therefore, the *ld* limb phenotype has been wrongly attributed to disruption of Formin functions. We now show that all *ld* alleles together with the $Fmn^{\Delta 10.24}$ and $Gre^{\Delta ORF}$ mutations define one allelic series of variable phenotypic strength. The ld^{OR}, ld^{J} and $Gre^{\Delta ORF}$ alleles are the strongest alleles as the Gremlin gene products are either deleted or truncated, which causes a pleiotropic loss-of-function phenotype. The complete renal agenesis and lung septation defects in ld^{OR} homozygous newborn mice result in fully penetrant neonatal lethality identical to the $Gre^{\Delta ORF}$ null allele generated by gene targeting (Michos et al., 2004). A second class of *ld* alleles is hypomorphic ($Fmn^{\Delta 10.24}$, ld^{In2}, ld^{TgBri}, ld^{TgHd}). These *ld* alleles display the characteristic and fully penetrant *ld* limb phenotype, but either lack or only show low frequencies of renal abnormalities and thereby generally survive to adult hood (see also Maas et al., 1994). A cis-regulatory region located within Formin that is required for *Gremlin* activation in the limb bud mesenchyme is either deleted or disrupted by all these hypomorphic *ld* alleles (Fig. 10A). Therefore, these mutations induce limb bud specific loss of *Gremlin* expression in cis and not in trans as a consequence of disrupting *Formin* (Zuniga et al., 1999). Despite the fact that $Fmn^{\Delta 10}$ homozygous mice (lacking the complete C-terminal Formin domain) are normal, it cannot be excluded that other Formin protein domains function during embryonic development in pathways other than the ones disrupted due to the lack of the BMP antagonist Gremlin. In particular, specific inactivation of Formin isoform IV results in low penetrance and mostly partial renal agenesis phenotypes, while limbs are phenotypically wild type (Chao et al., 1998; Wynshaw-Boris et al., 1997). The partial disruption of kidney development in these mutations and some of the hypomorphic *ld* alleles (see before) correlate well with abundant *Formin* expression during kidney morphogenesis (Zeller et al., 1999).

Our studies reveal the molecular disruption of *Gremlin* in the ld^{OR} and ld^{J} alleles and positively identify the shared limb bud cis-regulatory elements in Formin genomic region 19.23. In particular, these latter studies explain satisfactory why disruption of Gremlin functions is the primary cause of the limb phenotypes observed in *ld* homozygous mice. In the ld^{In2} allele, the inversion between Formin and Agouti (Woychik et al., 1990) relocates the Gremlin gene about 40Mb away from the genomic region 19.23 (Fig. 10A). The ld^{TgHd} allele arose by insertion of multiple copies of a MMTV-myc transgene in combination with an about 1kb deletion between Formin exons 19 and 20 (Maas et al., 1990; Woychik et al., 1985). The transgene insertion site disrupts the genomic region 19.23 and is likely to tether long range enhancing activity due to insertion of several strong exogenous promoters (Fig. 10A). Last but not least, the genomic region 19.23 is deleted in the ld^{TgBri} allele (Vogt et al., 1992). We establish that such a deletion completely abolishes *Gremlin* activation in the posterior limb bud mesenchyme (Fig. 10A).

The positively identified cis-regulatory region 19.23 (Fig. 10A) activates transcription of unrelated genes in a promoter and orientation independent manner at large distances. These features are strikingly similar to the ones of a recently identified global control region (GCR), which regulates limb bud specific expression of *5'Hoxd* and the

unrelated *Evx2* and *Lunapark* (*Lnp*) genes (Spitz et al., 2003). Such GCRs seem to consist of multiple regulatory regions and/or enhancers that form a chromosomal regulatory landscape and act at a distance to co-activate sets of neighboring genes in specific tissues. Comparison of the orthologous mouse and human genomic regions 19.23 reveals highly conserved sequences within introns (at least 100 bases with more than 75% identity) that are spread over the whole region (Fig. 10B). However, no obvious consensus binding sites for e.g. Gli transcription factors have been found within theses conserved blocks (F. S., unpublished results).

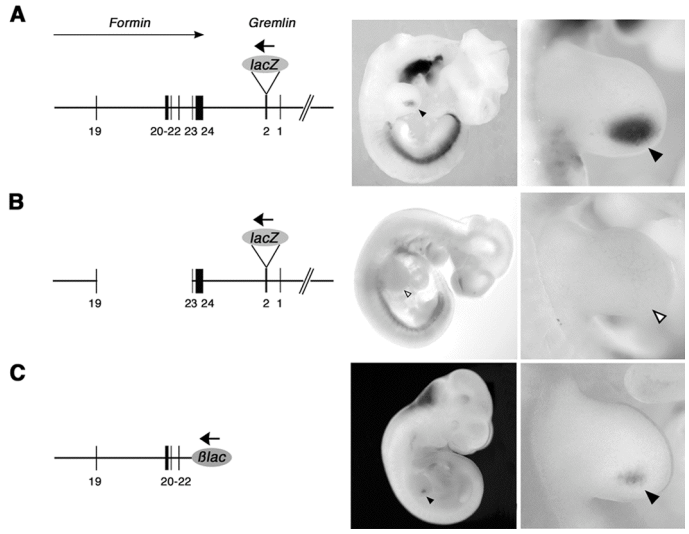

Fig.8 The Fmn locus encodes a regulatory region sufficient to activate *Gremlin* transcription in the limb bud mesenchyme. (A) Construct A was generated by in frame insertion of a LacZ gene 30 bases downstream the *Gremlin* ATG into BAC #113H17. This BAC encodes Fmn exons 19 to 24, the intergenic region, and entire Gre gene and extends about 150kb upstream of Gre exon 1. Note that Gre (bold arrow) is transcribed in reverse orientation to Fmn (arrow). (B) Construct B was generated by deleting the genomic region delimited by exons 19 to 23 from construct A. (C) Construct C was generated by replacing Fmn exon 23 and downstream sequences with the ß-lac reporter gene in BAC #113H17. Note that the ß-lac reporter gene inserted in construct C is transcribed like Gremlin; exons are numbered like in Fig. 3A. For all constructs, the *LacZ* distribution is shown in founder embryos around gestational day 10.5. Left panels show whole embryo views while right panels show fore limb buds. Note that different embryos are shown in the left and right panels. Black arrowheads point to the *LacZ* expression domains in the limb bud. Open arrowheads indicate the lack of *LacZ* expression in the limb bud of an embryo transgenic for construct B.

Interestingly, neither Lnp nor Formin are essential for limb development in spite of these loci harboring the essential GCR and being expressed during limb bud development. Cis-regulation of the further downstream 5'Hoxd and Gremlin genes by the GCR is however essential for distal limb bud morphogenesis (Khokha et al., 2003; Michos et al., 2004; Zákány and Duboule, 1996). Experimental evidence indicates that the Formin landscape region 10.24 not only contains the regulatory elements necessary for activation, but also the ones mediating response to SHH signaling (Fig. 10A). Regulation of these two genes in the limb bud mesenchyme is likely regulated by interaction of several control regions scattered over the genomic landscape (Fig. 10A,B). Our studies also reveal for the first time that such landscapes and GCRs are not a peculiar feature of regulating functionally related and clustered genes such as, for example, 5'Hoxd and globin genes (Zeller and Deschamps, 2002). Rather, they

seem to represent a novel mechanism by which tissue-specific co-expression of neighboring genes is orchestrated, even if they are structurally and functionally not related. These studies are likely to reveal the tip of the iceberg and further exploration of these regulatory landscapes will be necessary to understand if GCRs are composed of novel types of tissue-specific activator/enhancer elements or if they harbor elements enabling the known activators and enhancers to act over greater than usual distances (Fig. 10 and Spitz et al., 2003). Last but not least, *Shh* expression in the limb bud mesenchyme is itself controlled by regulatory region located about 800kb upstream within the unrelated Lmbr1 gene (Lettice et al., 2002).

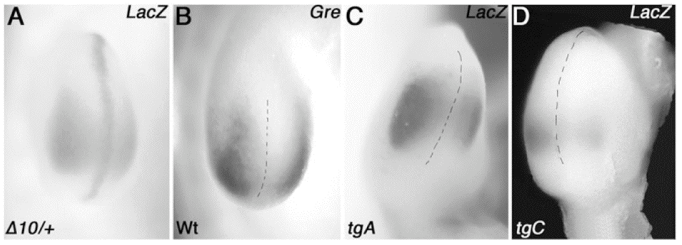

Fig.9 The regulatory region 19.23 is sufficient to activate *Gremlin* and *Formin* expression in both dorsal and ventral limb bud mesenchyme.
(A) *LacZ* distribution in an $Fmn^{\Delta 10/+}$ fore limb bud. (B) Endogenous *Gre* expression in a wild type fore limb bud. (C) *LacZ* distribution in a fore limb bud of an embryo expressing BAC construct A. (D) *LacZ* distribution in a fore limb bud of an embryo expressing BAC construct C. Note the enhanced dorsal expression in both wild type and transgenic limb buds.

It could well be that during evolution of vertebrates an initial selective constraint resulted in Formin and Gremlin being kept neighboring genes and their expression became co-regulated as part of a larger regulatory landscape. In fact, both genes are also expressed in similar, but not identical patterns during kidney organogenesis and genetic analysis has revealed essential functions for both genes during kidney development (Wynshaw-Boris et al., 1997). Initial intertwining of their regulation could have resulted in them becoming inseparably linked or trapped into this regulatory landscape, in spite of eventual diversification of their functions during vertebrate evolution. The present study establishes that Gremlin and Formin are neither part of the same pathway, nor a common synexpression group (Niehrs and Pollet, 1999), in spite of these two genes being co-expressed in various embryonic tissues. Much of the gene diversity during vertebrate evolution is thought to have arisen following gene and chromosomal duplications. Interestingly, the arrangement of Formin2 (Leader and Leder, 2000) and Gremlin2 (or Prdc; Minabe-Saegusa et al., 1998) on mouse chromosome 1 is identical to chromosome 2, as the two genes are also located next to one another and transcribed in reverse orientation (see also UGSC Genome Browser, http://genome.ucsc.edu). During organogenesis, both *Formin2* and *Gremlin2* are expressed in the developing neural tube (Leader and Leder, 2000; Minabe-Saegusa et al., 1998), suggesting that they could also be part of a common regulatory landscape.
Large-scale phenotypic screens have become a renewed and major effort to genetically analyze vertebrate model organisms such as zebrafish and mouse (Justice, 2000). Such screens provide powerful tools to identify the gene cascades controlling development, physiology and disease by scoring for the relevant phenotypes. However, the present study reveals that in specific cases, the

identification and analysis of the essential gene and/or cascades can be rather tedious. The molecular alterations in the Formin locus together with the *Formin* transcript and protein distribution established this gene as the obvious candidate, whose disruption causes the *ld* limb phenotype (Panman and Zeller, 2003; Zeller et al., 1999). Only the combination of experimental embryology with advanced reverse genetics and transgenesis has finally revealed the true nature of the *ld* limb phenotype and established Gremlin as the essential one of the two disrupted genes. As many vertebrate genes contain rather large intronic and non-coding regions, such large regulatory landscapes may be rather common and more surprises with respect to assigning phenotypes to alterations of particular genes and/or pathways may well be in store.

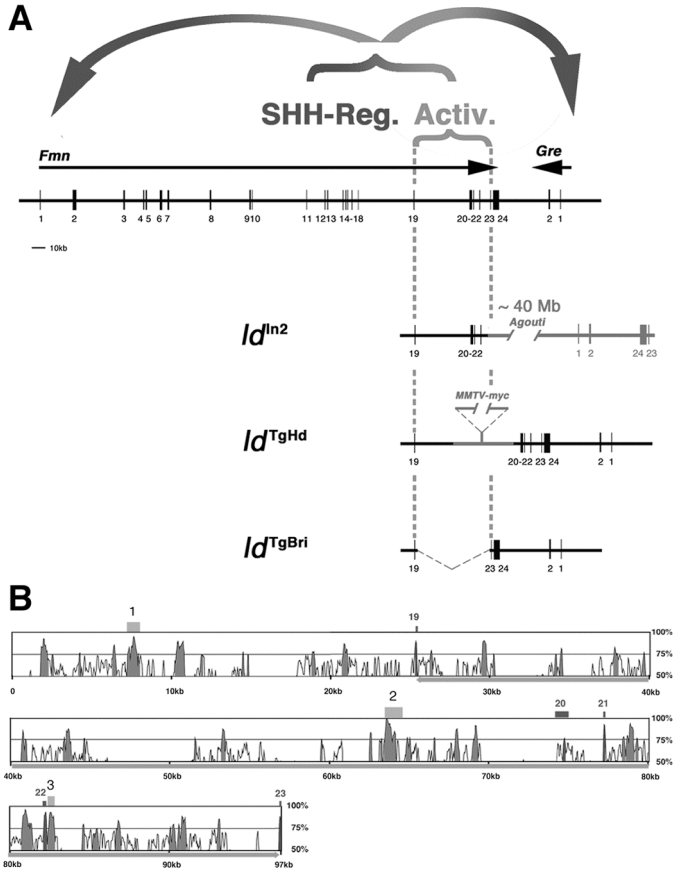

Fig.10 The large regulatory landscape required for activation of *Gremlin* expression in the limb bud mesenchyme.
(A) Region 19.23 is disrupted by all relevant *ld* alleles. Activ.: a global control region (GCR) located in the genomic region encompassing Fmn exons 19 to 23 is required in cis for activation of *Gre* and *Fmn* expression in the posterior limb bud mesenchyme. This region is disrupted in the ld^{In2}, ld^{TgHd}, *and* ld^{TgBri} alleles. *Shh*-Reg.: the region necessary for SHH-mediated regulation of *Gre* and *Fmn* (see Fig. 5A-F) is most likely located upstream of Fmn exon 19. Schemes show how the ld^{In2}, ld^{TgHd} and ld^{TgBri} mutations disrupt the activator GCR. (B) Alignment of region 19.23 from the mouse and human genome using the mVISTA program (window size: 100 bases, homology threshold: 65%; (Mayor et al. 2000). This alignment reveals multiple blocks of intronic sequences highly conserved between the 2 species. Exons 19 to 23 are indicated and the parts of intronic sequences conserved more than 75% are marked as read peaks. The chicken region 19.23 is only partially available, with some gaps in the regions containing the blocks of sequence conserved between mouse and human genome that precluded complete analysis. However, three regions, highly conserved among all three species have been identified. Region1 (upstream of e19): 77.4% identity over 243 bases, region2 (upstream of e20): 85.1% over 329 bases, region3 (just downstream of e22): 81% over 352 bases. The human, mouse and chicken genomic sequences were obtained from the ENSEMBL Genome Browser (www.ensembl.org) using genome assembly releases v19.34b, v.19.32.2 and pre-release1, respectively.

Acknowledgements

The authors are grateful to H. Goedemans, N. Lagarde, and C. Lehmann for technical assistance and mouse husbandry and to K. O'Leary for help in preparation of the manuscript. We are grateful to T. Kondo, M. Kmita, S.L. Ang and F. Guillemot for providing targeting vectors, probes and advice, and A.M van der Linden for advice in mapping and isolating the deletion breakpoints in the *Id*^{OR} mutation. We thank J. Deschamps, F. Meijlink, I. Mattaj, D. Sussman and C. Torres de los Reyes for helpful discussions and comments on the manuscript. This research was supported by the Faculty of Biology at Utrecht University, grants from the Dutch KNAW (to A.Z.) and NWO (to R.Z.), the Swiss National Science Foundation (to R.Z. and D.D.) and the two cantons of Basel (to R.Z).

CHAPTER 5
Summarizing Discussion

My studies demonstrate the requirement of Gremlin-mediated modulation of BMP signaling in the extra-cellular space during epithelial-mesenchymal feedback signaling. As expected from its embryonic expression pattern, Gremlin is not required for primary axis specification or germ layer formation. However, Gremlin is essential to enable progression of morphogenesis of particular organs such as lungs, kidneys and limbs. Antagonism of BMP activity by Gremlin is critical to initiate and maintain epithelial-mesenchymal signaling interactions in these organs during their morphogenesis, indicating that tight control of ligand availability is key to coordinated development. During limb bud and kidney development, Gremlin is required to maintain and propagate morphoregulatory signaling centers (organizers). Gremlin is also required to coordinate and propagate "distal" outgrowth and lack of *Gremlin* provokes an early arrest of development. During lung development, Gremlin is however not essential to maintain the so-called distal signaling center, but it is essential for the proper epithelial-mesenchymal signaling interactions that regulate branching and differentiation of the lung primordia. In the lung, Gremlin is required for epithelial cell differentiation similar to its critical role during limb bud AER maturation.

1. Gremlin functions in limb bud development

The maturation and maintenance of the AER as a signaling center is key to limb development as it controls proliferation of the mesenchymal cells that form the distal limb (Tickle, 2003). The studies presented here reveal an important and general role of Gremlin in the establishment of a functional AER, its maintenance and possibly also in its regression (see below). BMPs are known to regulate AER formation through activation of *Msx* expression (Pizette et al., 2001). My studies show that a functional AER fails to form in *Gremlin* deficient limb buds inspite of AER type cells being specified correctly. Previous studies provided evidence that BMP signaling is required for both dorso-ventral limb axis establishment and AER induction (Ahn et al., 2001; Pizette et al., 2001). As dorso-ventral axis is already specified prior to activation of *Gremlin* expression in the limb bud mesenchyme, the lack of *Gremlin* does not alter dorso-ventral axis specification. Distal limb bud outgrowth is controlled by a SHH/FGF feedback loop (Panman and Zeller, 2003) and Gremlin was proposed sufficient for maintenance of this feedback loop (Zuniga et al., 1999). Indeed, Khokha et al. (2003) first showed that Gremlin is the BMP antagonist required to maintain the SHH/FGF feedback loop. In contrast, my studies reveal a much earlier and general requirement for Gremlin-mediated BMP antagonism in induction of AER signaling and establishment of a functional and morphologically distinct AER.

Recently, Scherz and coworkers (2004) proposed a mechanism by which termination of the SHH/FGF feedback loop results in cessation of limb patterning. They show that *Shh*-expressing cells and their descendants are not competent to express *Gremlin*. During limb bud outgrowth, the expansion of the population of descendants of *Shh*-expressing cells creates a gap that separates polarizing region cells from *Gremlin*-expressing cells. This gap eventually disrupts maintenance of *Gremlin* expression in the distal limb bud mesenchyme. This suggests that the increasing inability of posterior mesenchymal cells to express *Gremlin* in response to SHH signaling is the primary cause by which the SHH/FGF feedback loop breaks down (Scherz et al., 2004). Another important aspect of advanced autopodal development is the elimination of the

interdigital mesenchyme by programmed cell death (PCD). Experimental evidence shows that elevated BMP signaling is directly involved in induction of interdigital PCD (Merino et al., 1999a; Rodriguez-Leon et al., 1999; Zuzarte-Luis and Hurle, 2002), that interestingly *Gremlin* is expressed by cells of the interdigital mesenchyme prior to PCD (Merino et al., 1999c; Chapter 1, Fig. 8) and misexpression of *Gremlin* in chicken limb buds inhibits PCD. In the duck leg, *Gremlin* is expressed in a broader domain by the interdigital mesenchyme, where the lack of PCD results in interdigital tissue webbing (Merino et al., 1999c). Finally, I have also shown that the lack of *Gremlin* in early limb buds results in aberrant apoptosis of the core mesenchymal cells. In conclusion, *Gremlin* functions as an essential cell survival factor both in the early and late limb bud mesenchyme.

2. Gremlin and the *ld* limb phenotype

One of the major findings presented in this thesis is the fact that the mouse *limb deformity (ld)* limb phenotype is caused by disruption of *Gremlin* activation in the limb bud mesenchyme rather than disruption of *Formin* function as previously assumed (Zeller et al., 1999). A region of cis-regulatory elements with features of a global control region (GCR; Spitz et al., 2003) is located in the 3'part of the Formin gene and controls *Gremlin* expression in the distal limb bud mesenchyme. This GCR controls activation of both *Gremlin* and *Formin* in the posterior limb bud mesenchyme and is disrupted by several of the existing *ld* alleles (Chapter 4). Future analysis is necessary to identify and study the evolutionary conserved cis-regulatory elements, which are essential to *Gremlin* transcriptional regulations in the limb bud.

3. Gremlin is part of the mechanism that induces metanephric kidney organogenesis

The analysis of *Gremlin* deficient mouse embryos has revealed an important role of Gremlin-mediated BMP antagonism during initiation of metanephric kidney development, as ureter outgrowth and branching morphogenesis are completely disrupted in *Gremlin* deficient mouse embryos. It is well established that ureteric bud formation, outgrowth and branching depend on the RET/GDNF signaling pathway (Vainio and Lin, 2002). However, genetic analysis of transcription factors in the mouse reveals that ureteric bud outgrowth can be impaired without disrupting RET/GDNF feedback signaling (Vainio and Lin, 2002). These studies imply the existence of additional signaling pathways that participate in metanephric kidney induction in response to these transcription factors (Wt1, Pax2, Six1 and Sall1; Chapter 2, Fig. 7). Interestingly, most of these transcription factors are initially expressed normally in *Gremlin* deficient kidney rudiments, indicating that Gremlin acts downstream to induce metanephric kidney organogenesis. Of particular interest is Sall1, as it is expressed in a similar way to *Gremlin*. In addition the ureteric bud fails to induce metanephric development in *Sall1* deficient mouse embryos (Nishinakamura et al., 2001). The authors speculated that Sall1 would induce an unknown mesenchymal-derived signal that triggers ureteric bud growth. My studies indicate that the BMP antagonist Gremlin could be this signal. Analysis of *Gremlin* expression in *Sall1* deficient mouse kidney rudiments should reveal if Gremlin is indeed the postulated downstream signal. Furthermore, Gremlin is most likely required throughout metanephric kidney

organogenesis to regulate spatial and temporal aspects of ureter branching morphogenesis. To study the functions of Gremlin during kidney development further, we will make use of an established kidney culture system (Lin et al., 2003; Saxén, 1987; Watanabe and Costantini, 2004). We will combine tissue recombination experiments with grafting of *Gremlin*-expressing cells to assess the potential involvement of this BMP antagonist in guidance of metanephric branching morphogenesis. Finally, we will also generate mouse embryos lacking both *Bmp4* and *Gremlin* to study the functional importance of Gremlin/BMP4 signaling interactions during metanephric kidney organogenesis.

4. Gremlin and differentiation of epithelial cell layers

An interesting and general feature of the *Gremlin* loss-of-function phenotype is the failure to form different types of functional epithelia in limb buds, kidney and lung rudiments. This defect is caused directly by disruption of Gremlin-mediated BMP antagonism and indicates that balanced BMP signaling activity is critical to establishment of epithelial cell polarity. Therefore, it will be interesting to examine if the ureteric bud epithelial cells are also as morphologically abnormal as AER and lung epithelial cells. Interestingly, Moniot et al. (2004) recently reported that Gremlin is involved in the epithelial-mesenchymal signaling interactions that specify the pyloric sphincter epithelium in chicken embryos.

5. Does alteration of Gremlin underlie human disease?

Two human genetic diseases with phenotypes similar to *Gremlin* deficient mice have been mapped to human chromosome 15q13 (Bacchelli et al., 2001; Morgan et al., 2003), which encodes both the Formin and Gremlin genes (Topol et al., 2000). These authors excluded Gremlin and Formin as candidate genes, but their analysis was limited to the ORF of both genes (Bacchelli et al., 2001; Morgan et al., 2003). Such analysis would neither have detected mutations in intronic regions causing disruption of cis-regulatory elements nor one base substitution, which alter splicing. Indeed, about 15% of all mutations affecting the human population alter splicing and thereby cause congenital malformations or diseases (Faustino and Cooper, 2003). Recently, mutations affecting a very distant cis-regulatory element controlling *Shh* expression in the limb bud mesenchyme have been identified as the molecular cause of identical congenital limb malformations in mice, chickens and humans (Lettice et al., 2003; Lettice et al., 2002; Ros et al., 2003). Therefore, it is important to re-evaluate the cis-regulatory elements controlling limb bud expression of *Formin* and *Gremlin* in the aforementioned human congenital malformations.

Additional evidence for a possible involvement of Gremlin in human disease is obtained by analysis of a rare genetic disorder, called fibrodisplasia ossificans progressiva (FOP), which causes progressive heterotopic bone formation (Ahn et al., 2003). In FOP patients, *Bmp4* is over expressed and cells derived from FOP patients fail to increase *Noggin* and *Gremlin* expression in response to BMP4 signaling (Ahn et al., 2003). Normally, excess BMP signaling increases *Gremlin* and *Noggin* expression, which limits BMP activity due to an autoregulatory feedback loop (Ahn et al., 2003; Pereira et al., 2000). Therefore, the levels of Gremlin and/or Noggin may be too low in comparison with the elevated BMP4 activity in FOP patients, which may result in

progressive ectopic bone formation (Ahn et al., 2003). These results also establish the importance of negative feedback regulation and relevance of Gremlin and other antagonists as potential therapeutic agents for such genetic disorders. Finally, there is increasing evidence supporting an involvement of Gremlin-mediated BMP antagonism in progressive renal dysfunction. Several studies have shown that *Gremlin* is induced in mesangial cell models of diabetic nephropathy in both humans and rodents (Lappin et al., 2000; McMahon et al., 2000; Wang et al., 2001). In particular, Gremlin may act as a modulator of mesangial cell proliferation and induce epithelial-mesenchymal transdifferentiation of renal cells in a high glucose (diabetic) environment (Lappin et al., 2000; 2002; McMahon et al., 2000; Murphy et al., 2002; Wang et al., 2001). Therefore, Gremlin may also serve as a therapeutic target for progressive renal diseases like diabetic nephropathy, which is a major cause of renal insufficiency (Dolan et al., 2003; Wang et al., 2001).

References

Affolter, M., Bellusci, S., Itoh, N., Shilo, B., Thiery, J.-P. and Werb, Z. (2003). Tube or not tube: remodeling epithelial tissues by branching morphogenesis. *Developmental Cell* **4**, 11-18.

Ahn, J., Serrano de la Pena, L., Shore, E. M. and Kaplan, F. S. (2003). Paresis of a bone morphogenetic protein-antagonist response in a genetic disorder of heterotopic skeletogenesis. *J Bone Joint Surg Am* **85-A**, 667-74.

Ahn, K., Mishina, Y., Hanks, M. C., Behringer, R. R. and Crenshaw, E. B., 3rd. (2001). BMPR-IA signaling is required for the formation of the apical ectodermal ridge and dorsal-ventral patterning of the limb. *Development* **128**, 4449-61.

Attisano, L. and Wrana, J. L. (2002). Signal transduction by the TGF-beta superfamily. *Science* **296**, 1646-7.

Avantaggiato, V., Dathan, N. A., Grieco, M., Fabien, N., Lazzaro, D., Fusco, A., Simeone, A. and Santoro, M. (1994). Developmental expression of the RET protooncogene. *Cell Growth Differ* **5**, 305-11.

Avsian-Kretchmer, O. and Hsueh, A. J. (2003). Comparative Genomic Analysis of the Eight-Membered-Ring Cystine-Knot-Containing Bone Morphogenetic Protein (BMP) Antagonists. *Mol Endocrinol* **18**, 1-12.

Bacchelli, C., Goodman, F. R., Scambler, P. J. and Winter, R. M. (2001). Cenani-Lenz syndrome with renal hypoplasia is not linked to FORMIN or GREMLIN. *Clin Genet* **59**, 203-5.

Bachiller, D., Klingensmith, J., Kemp, C., Belo, J. A., Anderson, R. M., May, S. R., McMahon, J. A., McMahon, A. P., Harland, R. M., Rossant, J. et al. (2000). The organizer factors Chordin and Noggin are required for mouse forebrain development. *Nature* **403**, 658-61.

Balemans, W. and Van Hul, W. (2002). Extracellular regulation of BMP signaling in vertebrates: a cocktail of modulators. *Dev Biol* **250**, 231-50.

Barrow, J. R., Thomas, K. R., Boussadia-Zahui, O., Moore, R., Kemler, R., Capecchi, M. R. and McMahon, A. P. (2003). Ectodermal Wnt3/beta-catenin signaling is required for the establishment and maintenance of the apical ectodermal ridge. *Genes Dev* **17**, 394-409.

Bellusci, S., Furuta, Y., Rush, M. G., Henderson, R., Winnier, G. and Hogan, B. L. (1997a). Involvement of Sonic hedgehog (Shh) in mouse embryonic lung growth and morphogenesis. *Development* **124**, 53-63.

Bellusci, S., Grindley, J., Emoto, H., Itoh, N. and Hogan, B. L. (1997b). Fibroblast growth factor 10 (FGF10) and branching morphogenesis in the embryonic mouse lung. *Development* **124**, 4867-78.

Bellusci, S., Henderson, R., Winnier, G., Oikawa, T. and Hogan, B. L. (1996). Evidence from normal expression and targeted misexpression that bone morphogenetic protein (Bmp-4) plays a role in mouse embryonic lung morphogenesis. *Development* **122**, 1693-702.

Bragg, A. D., Moses, H. L. and Serra, R. (2001). Signaling to the epithelium is not sufficient to mediate all of the effects of transforming growth factor beta and bone

morphogenetic protein 4 on murine embryonic lung development. *Mech Dev* **109**, 13-26.
Brunet, L., McMahon, J., McMahon, A. and Harland, R. (1998). Noggin, cartilage morphogenesis, and joint formation in the mammalian skeleton. *Science* **280**, 1455-7.
Cacalano, G., Farinas, I., Wang, L. C., Hagler, K., Forgie, A., Moore, M., Armanini, M., Phillips, H., Ryan, A. M., Reichardt, L. F. et al. (1998). GFRalpha1 is an essential receptor component for GDNF in the developing nervous system and kidney. *Neuron* **21**, 53-62.
Canalis, E., Economides, A. N. and Gazzerro, E. (2003). Bone morphogenetic proteins, their antagonists, and the skeleton. *Endocr Rev* **24**, 218-35.
Capdevila, J. and Izpisua Belmonte, J. C. (2001). Patterning mechanisms controlling vertebrate limb development. *Annu Rev Cell Dev Biol* **17**, 87-132.
Capdevila, J., Tsukui, T., Rodriquez Esteban, C., Zappavigna, V. and Izpisua Belmonte, J. C. (1999). Control of vertebrate limb outgrowth by the proximal factor Meis2 and distal antagonism of BMPs by Gremlin. *Mol Cell* **4**, 839-49.
Cardoso, W. V. (2001). Molecular regulation of lung development. *Annu Rev Physiol* **63**, 471-94.
Cebra-Thomas, J. A., Bromer, J., Gardner, R., Lam, G. K., Sheipe, H. and Gilbert, S. F. (2003). T-box gene products are required for mesenchymal induction of epithelial branching in the embryonic mouse lung. *Dev Dyn* **226**, 82-90.
Chang, H., Brown, C. W. and Matzuk, M. M. (2002). Genetic analysis of the mammalian transforming growth factor-beta superfamily. *Endocr Rev* **23**, 787-823.
Chao, C. W., Chan, D. C., Kuo, A. and Leder, P. (1998). The mouse formin (Fmn) gene: abundant circular RNA transcripts and gene-targeted deletion analysis. *Mol Med* **4**, 614-28.
Charite, J., McFadden, D. G. and Olson, E. N. (2000). The bHLH transcription factor dHAND controls Sonic hedgehog expression and establishment of the zone of polarizing activity during limb development. *Development* **127**, 2461-70.
Chen, B., Athanasiou, M., Gu, Q. and Blair, D. G. (2002). Drm/Gremlin transcriptionally activates p21(Cip1) via a novel mechanism and inhibits neoplastic transformation. *Biochem Biophys Res Commun* **295**, 1135-41.
Chen, J., Knowles, H. J., Hebert, J. L. and Hackett, B. P. (1998). Mutation of the mouse hepatocyte nuclear factor/forkhead homologue 4 gene results in an absence of cilia and random left-right asymmetry. *J Clin Invest* **102**, 1077-82.
Chen, Y., Knezevic, V., Ervin, V., Hutson, R., Ward, Y. and Mackem, S. (2004). Direct interaction with Hoxd proteins reverses Gli3-repressor function to promote digit formation downstream of Shh. *Development* **131**, 2339-47.
Chiang, C., Litingtung, Y., Harris, M. P., Simandl, B. K., Li, Y., Beachy, P. A. and Fallon, J. F. (2001). Manifestation of the Limb Prepattern: Limb Development in the Absence of Sonic Hedgehog Function. *Developmental Biology* **236**, 421-435.
Chiang, C., Litingtung, Y., Lee, E., Young, K. E., Corden, J. L., Westphal, H. and Beachy, P. A. (1996). Cyclopia and defective axial patterning in mice lacking *Sonic hedgehog* gene function. *Nature* **383**, 407-413.
Colvin, J. S., White, A. C., Pratt, S. J. and Ornitz, D. M. (2001). Lung hypoplasia and neonatal death in Fgf9-null mice identify this gene as an essential regulator of lung mesenchyme. *Development* **128**, 2095-106.

Dahn, R. D. and Fallon, J. F. (2000). Interdigital regulation of digit identity and homeotic transformation by modulated BMP signaling. *Science* **289**, 438-41.
Derynck, R., Gelbart, W. M., Harland, R. M., Heldin, C. H., Kern, S. E., Massague, J., Melton, D. A., Mlodzik, M., Padgett, R. W., Roberts, A. B. et al. (1996). Nomenclature: vertebrate mediators of TGFbeta family signals. *Cell* **87**, 173.
Derynck, R. and Zhang, Y. E. (2003). Smad-dependent and Smad-independent pathways in TGF-beta family signalling. *Nature* **425**, 577-84.
Dolan, V., Hensey, C. and Brady, H. R. (2003). Diabetic nephropathy: renal development gone awry? *Pediatr Nephrol* **18**, 75-84.
Dono, R., Texido, G., Dussel, R., Ehmke, H. and Zeller, R. (1998). Impaired cerebral cortex development and blood pressure regulation in FGF-2-deficient mice. *EMBO J.* **17**, 4213-4225.
Donovan, M. J., Natoli, T. A., Sainio, K., Amstutz, A., Jaenisch, R., Sariola, H. and Kreidberg, J. A. (1999). Initial differentiation of the metanpheric mesenchyme is independent of WT1 and the ureteric bud. *Developmental Genetics* **24**, 252-62.
Drossopoulou, G., Lewis, K. E., Sanz-Ezquerro, J. J., Nikbakht, N., McMahon, A. P., Hofmann, C. and Tickle, C. (2000). A model for anteroposterior patterning of the vertebrate limb based on sequential long- and short-range Shh signalling and Bmp signalling. *Development* **127**, 1337-48.
Dudley, A. T., Lyons, K. M. and Robertson, E. J. (1995). A requirement for bone morphogenetic protein-7 during development of the mammalian kidney and eye. *Genes Dev* **9**, 2795-807.
Dudley, A. T. and Robertson, E. J. (1997). Overlapping expression domains of bone morphogenetic protein family members potentially account for limited tissue defects in BMP7 deficient embryos. *Dev Dyn* **208**, 349-62.
Dudley, A. T., Ros, M. A. and Tabin, C. J. (2002). A re-examination of proximodistal patterning during vertebrate limb development. *Nature* **418**, 539-44.
Durbec, P., Marcos-Gutierrez, C. V., Kilkenny, C., Grigoriou, M., Wartiowaara, K., Suvanto, P., Smith, D., Ponder, B., Costantini, F., Saarma, M. et al. (1996). GDNF signalling through the Ret receptor tyrosine kinase. *Nature* **381**, 789-93.
Ehrenfels, C. W., Carmillo, P. J., Orozco, O., Cate, R. L. and Sanicola, M. (1999). Perturbation of RET signaling in the embryonic kidney. *Dev Genet* **24**, 263-72.
Evangelista, M., Zigmond, S. and Boone, C. (2003). Formins: signaling effectors for assembly and polarization of actin filaments. *J Cell Sci* **116**, 2603-11.
Faustino, N. A. and Cooper, T. A. (2003). Pre-mRNA splicing and human disease. *Genes Dev* **17**, 419-37.
Fernandez-Teran, M., Piedra, M. E., Kathiriya, I. S., Srivastava, D., Rodriguez-Rey, J. C. and Ros, M. A. (2000). Role of dHAND in the anterior-posterior polarization of the limb bud: implications for the Sonic hedgehog pathway. *Development* **127**, 2133-2142.
Fujii, T., Pichel, J. G., Taira, M., Toyama, R., Dawid, I. B. and Westphal, H. (1994). Expression patterns of the murine LIM class homeobox gene lim1 in the developing brain and excretory system. *Dev Dyn* **199**, 73-83.
Grieshammer, U., Le, M., Plump, A. S., Wang, F., Tessier-Lavigne, M. and Martin, G. R. (2004). SLIT2-mediated ROBO2 signaling restricts kidney induction to a single site. *Dev Cell* **6**, 709-17.

Gupta, I. R., Macias-Silva, M., Kim, S., Zhou, X., Piscione, T. D., Whiteside, C., Wrana, J. L. and Rosenblum, N. D. (2000). BMP-2/ALK3 and HGF signal in parallel to regulate renal collecting duct morphogenesis. *Journal of Cell Science* **113**, 269-78.
Gupta, I. R., Piscione, T. D., Grisaru, S., Phan, T., Macias-Silva, M., Zhou, X., Whiteside, C., Wrana, J. L. and Rosenblum, N. D. (1999). Protein Kinase A is a negative regulator of renal branching morphogenesis and modulates inhibitory and stimulatory morphogenetic proteins. *The Journal of Biological Chemistry* **274**, 26305-14.
Gurrieri, F., Kjaer, K. W., Sangiorgi, E. and Neri, G. (2002). Limb anomalies: Developmental and evolutionary aspects. *Am J Med Genet* **115**, 231-44.
Haramis, A. G., Brown, J. M. and Zeller, R. (1995). The limb deformity mutation disrupts the SHH/FGF-4 feedback loop and regulation of 5'HoxD genes during limb pattern formation. *Development* **121**, 4237-4245.
Heine, U. I., Munoz, E. F., Flanders, K. C., Roberts, A. B. and Sporn, M. B. (1990). Colocalization of TGF-beta 1 and collagen I and III, fibronectin and glycosaminoglycans during lung branching morphogenesis. *Development* **109**, 29-36.
Hellmich, H. L., Kos, L., Cho, E. S., Mahon, K. A. and Zimmer, A. (1996). Embryonic expression of glial cell-line derived neurotrophic factor (GDNF) suggests multiple developmental roles in neural differentiation and epithelial-mesenchymal interactions. *Mech Dev* **54**, 95-105.
Hogan, B. L. (1996). Bone morphogenetic proteins: multifunctional regulators of vertebrate development. *Genes Dev* **10**, 1580-94.
Hogan, B. L. (1999). Morphogenesis. *Cell* **96**, 225-233.
Hsu, D., Economides, A., Wang, X., Eimon, P. and Harland, R. (1998). The Xenopus dorsalizing factor Gremlin identifies a novel family of secreted proteins that antagonize BMP activities. *Mol Cell* **5**, 673-83.
Hyatt, B. A., Shangguan, X. and Shannon, J. M. (2002). BMP4 modulates fibroblast growth factor-mediated induction of proximal and distal lung differentiation in mouse embryonic tracheal epithelium in mesenchyme-free culture. *Dev Dyn* **225**, 153-65.
Jansen, G., Hazendonk, E., Thijssen, K. L. and Plasterk, R. H. (1997). Reverse genetics by chemical mutagenesis in Caenorhabditis elegans. *Nat Genet* **17**, 119-21.
Justice, M. J. (2000). Capitalizing on large-scale mouse mutagenesis screens. *Nat Rev Genet* **1**, 109-15.
Kawabata, M., Imamura, T. and Miyazono, K. (1998). Signal transduction by bone morphogenetic proteins. *Cytokine Growth Factor Rev* **9**, 49-61.
Kawakami, Y., Capdevila, J., Buscher, D., Itoh, T., Rodriguez Esteban, C. and Izpisua Belmonte, J. C. (2001). WNT signals control FGF-dependent limb initiation and AER induction in the chick embryo. *Cell* **104**, 891-900.
Khokha, M. K., Hsu, D., Brunet, L. J., Dionne, M. S. and Harland, R. M. (2003). Gremlin is the BMP antagonist required for maintenance of Shh and Fgf signals during limb patterning. *Nat Genet* **34**, 303-7.
Kimura, S., Hara, Y., Pineau, T., Fernandez-Salguero, P., Fox, C. H., Ward, J. M. and Gonzalez, F. J. (1996). The T/ebp null mouse: thyroid-specific enhancer-binding protein is essential for the organogenesis of the thyroid, lung, ventral forebrain, and pituitary. *Genes Dev* **10**, 60-9.
King, J. A., Marker, P. C., Seung, K. J. and Kingsley, D. M. (1994). BMP5 and the molecular, skeletal, and soft-tissue alterations in short ear mice. *Dev Biol* **166**, 112-22.

Kingsley, D. M. (1994). The TGF-beta superfamily: new members, new receptors, and new genetic tests of function in different organisms. *Genes Dev* **8**, 133-46.
Knittel, T., Kessel, M., Kim, M. H. and Gruss, P. (1995). A conserved enhancer of the human and murine Hoxa-7 gene specifies the anterior boundary of expression during embryonal development. *Development* **121**, 1077-88.
Kobielak, A., Pasolli, H. A. and Fuchs, E. (2004). Mammalian formin-1 participates in adherens junctions and polymerization of linear actin cables. *Nat Cell Biol* **6**, 21-30.
Kreidberg, J. A., Sariola, H., Loring, J. M., Maeda, M., Pelletier, J., Housman, D. and Jaenisch, R. (1993). WT-1 is required for early kidney development. *Cell* **74**, 679-91.
Kume, T., Deng, K. and Hogan, B. L. (2000). Murine forkhead/winged helix genes Foxc1 (Mf1) and Foxc2 (Mfh1) are required for the early organogenesis of the kidney and urinary tract. *Development* **127**, 1387-95.
Lappin, D. W., Hensey, C., McMahon, R., Godson, C. and Brady, H. R. (2000). Gremlins, glomeruli and diabetic nephropathy. *Curr Opin Nephrol Hypertens* **9**, 469-72.
Lappin, D. W., McMahon, R., Murphy, M. and Brady, H. R. (2002). Gremlin: an example of the re-emergence of developmental programmes in diabetic nephropathy. *Nephrol Dial Transplant* **17 Suppl 9**, 65-7.
Laufer, E., Nelson, C. E., Johnson, R. L., Morgan, B. A. and Tabin, C. (1994). Sonic hedgehog and Fgf-4 act through a signalling cascade and feedback loop to integrate growth and patterning of the development limb bud. *Cell* **79**, 993-1003.
Leader, B. and Leder, P. (2000). Formin-2, a novel formin homology protein of the cappuccino subfamily, is highly expressed in the developing and adult central nervous system. *Mech Dev* **93**, 221-31.
Lebeche, D., Malpel, S. and Cardoso, W. V. (1999). Fibroblast growth factor interactions in the developing lung. *Mech Dev* **86**, 125-36.
Lettice, L. A., Heaney, S. J., Purdie, L. A., Li, L., de Beer, P., Oostra, B. A., Goode, D., Elgar, G., Hill, R. E. and de Graaff, E. (2003). A long-range Shh enhancer regulates expression in the developing limb and fin and is associated with preaxial polydactyly. *Hum Mol Genet* **12**, 1725-35.
Lettice, L. A., Horikoshi, T., Heaney, S. J., Van Baren, M. J., Van Der Linde, H. C., Breedveld, G. J., Joosse, M., Akarsu, N., Oostra, B. A., Endo, N. et al. (2002). Disruption of a long-range cis-acting regulator for Shh causes preaxial polydactyly. *Proc Natl Acad Sci U S A* **99**, 7548-53.
Lewandoski, M., Sun, X. and Martin, G. R. (2000). Fgf8 signalling from the AER is essential for normal limb development. *Nat Genet* **26**, 460-3.
Li, X. and Cao, X. (2003). BMP signaling and HOX transcription factors in limb development. *Front Biosci* **8**, s805-12.
Lin, Y., Zhang, S., Tuukkanen, J., Peltoketo, H., Pihlajaniemi, T. and Vainio, S. (2003). Patterning parameters associated with the branching of the ureteric bud regulated by epithelial-mesenchymal interactions. *Int J Dev Biol* **47**, 3-13.
Litingtung, Y., Dahn, R. D., Li, Y., Fallon, J. F. and Chiang, C. (2002). Shh and Gli3 are dispensable for limb skeleton formation but regulate digit number and identity. *Nature* **418**, 979-83.
Litingtung, Y., Lei, L., Westphal, H. and Chiang, C. (1998). Sonic hedgehog is essential to foregut development. *Nat Genet* **20**, 58-61.

Loomis, C. A., Harris, E., Michaud, J., Wurst, W., Hanks, M. and Joyner, W. L. (1996). The mouse *Engrailed-1* gene and ventral limb patterning. *Nature* **382**, 360-363.
Lu, M. M., Yang, H., Zhang, L., Shu, W., Blair, D. G. and Morrisey, E. E. (2001). The bone morphogenic protein antagonist gremlin regulates proximal-distal patterning of the lung. *Dev Dyn* **222**, 667-80.
Luna, L. G. (1968). Manual of HISTOLOGIC STAINING METHODS of the Armed Forces Institute of Pathology. New York: McGRAW-HILL BOOK COMPAGNY.
Luo, G., Hofmann, C., Bronckers, A. L., Sohocki, M., Bradley, A. and Karsenty, G. (1995). BMP-7 is an inducer of nephrogenesis, and is also required for eye development and skeletal patterning. *Genes Dev* **9**, 2808-20.
Maas, R., Elfering, S., Glaser, T. and Jepeal, L. (1994). Deficient outgrowth of the ureteric bud underlies the renal agenesis phenotype in mice manifesting the limb deformity (ld) mutation. *Dev Dyn* **199**, 214-28.
Maas, R. L., Zeller, R., Woychik, R. P., Vogt, T. F. and Leder, P. (1990). Disruption of formin-encoding transcripts in two mutant limb deformity alleles. *Nature* **346**, 853-855.
Macias, D., Ganan, Y., Sampath, T. K., Piedra, M. E., Ros, M. A. and Hurle, J. M. (1997). Role of BMP-2 and OP-1 (BMP-7) in programmed cell death and skeletogenesis during chick limb development. *Development* **124**, 1109-17.
Mariani, F. V. and Martin, G. R. (2003). Deciphering skeletal patterning: clues from the limb. *Nature* **423**, 319-25.
Martin, G. R. (1998). The roles of FGFs in the early development of vertebrate limbs. *Genes Dev* **12**, 1571-1586.
Martinez, G. and Bertram, J. F. (2003). Organisation of bone morphogenetic proteins in renal development. *Nephron Exp Nephrol* **93**, e18-22.
Massague, J. (1998). TGF-beta signal transduction. *Annu Rev Biochem* **67**, 753-91.
Massague, J. and Chen, Y. G. (2000). Controlling TGF-beta signaling. *Genes Dev* **14**, 627-44.
McMahon, R., Murphy, M., Clarkson, M., Taal, M., Mackenzie, H. S., Godson, C., Martin, F. and Brady, H. R. (2000). IHG-2, a mesangial cell gene induced by high glucose, is human gremlin. Regulation by extracellular glucose concentration, cyclic mechanical strain, and transforming growth factor-beta1. *J Biol Chem* **275**, 9901-4.
Merino, R., Ganan, Y., Macias, D., Rodriguez-Leon, J. and Hurle, J. M. (1999a). Bone morphogenetic proteins regulate interdigital cell death in the avian embryo. *Ann N Y Acad Sci* **887**, 120-32.
Merino, R., Macias, D., Ganan, Y., Economides, A. N., Wang, X., Wu, Q., Stahl, N., Sampath, K. T., Varona, P. and Hurle, J. M. (1999b). Expression and function of Gdf-5 during digit skeletogenesis in the embryonic chick leg bud. *Dev Biol* **206**, 33-45.
Merino, R., Rodriguez-Leon, J., Macias, D., Ganan, Y., Economides, A. N. and Hurle, J. M. (1999c). The BMP antagonist Gremlin regulates outgrowth, chondrogenesis and programmed cell death in the developing limb. *Development* **126**, 5515-22.
Metzger, R. J. and Krasnow, M. A. (1999). Genetic control of branching morphogenesis. *Science* **284**, 1635-9.
Michos, O., Panman, L., Vintersten, K., Beier, K., Zeller, R. and Zuniga, A. (2004). Gremlin-mediated BMP antagonism induces the epithelial-mesenchymal feedback

signaling controlling metanephric kidney and limb organogenesis. *Development* **131**, 3401-10.
Min, H., Danilenko, D. M., Scully, S. A., Bonlon, B., Ring, B. D., Tarpley, J. E., DeRose, M. and Simonet, W. S. (1998). Fgf-10 is required for both limb and lung development and exhibits striking functional similarity to Drosophila branchless. *Genes & Development* **12**, 3156-3161.
Minabe-Saegusa, C., Saegusa, H., Tsukahara, M. and Noguchi, S. (1998). Sequence and expression of a novel mouse gene PRDC (protein related to DAN and cerberus) identified by a gene trap approach. *Dev Growth Differ* **40**, 343-53.
Minoo, P., Hamdan, H., Bu, D., Warburton, D., Stepanik, P. and deLemos, R. (1995). TTF-1 regulates lung epithelial morphogenesis. *Dev Biol* **172**, 694-8.
Minoo, P., Su, G., Drum, H., Bringas, P. and Kimura, S. (1999). Defects in tracheoesophageal and lung morphogenesis in Nkx2.1(-/-) mouse embryos. *Dev Biol* **209**, 60-71.
Miyamoto, N., Yoshida, M., Kuratani, S., Matsuo, I. and Aizawa, S. (1997). Defects of urogenital development in mice lacking Emx2. *Development* **124**, 1653-64.
Miyazaki, Y., Oshima, K., Fogo, A., Hogan, B. L. and Ichikawa, I. (2000). Bone morphogenetic protein 4 regulates the budding site and elongation of the mouse ureter. *J Clin Invest* **105**, 863-73.
Miyazaki, Y., Oshima, K., Fogo, A. and Ichikawa, I. (2003). Evidence that bone morphogenetic protein 4 has multiple biological functions during kidney and urinary tract development. *Kidney International* **63**, 835-44.
Mohammadi, M., McMahon, G., Sun, L., Tang, C., Hirth, P., Yeh, B. K., Hubbard, S. R. and Schlessinger, J. (1997). Structures of the tyrosine kinase domain of fibroblast growth factor receptor in complex with inhibitors. *Science* **276**, 955-60.
Moniot, B., Biau, S., Faure, S., Nielsen, C. M., Berta, P., Roberts, D. J. and De Santa Barbara, P. (2004). SOX9 specifies the pyloric sphincter epithelium through mesenchymal-epithelial signals. *Development* **131**, 3795-804.
Moon, A. M., Boulet, A. M. and Capecchi, M. R. (2000). Normal limb development in conditional mutants of Fgf4. *Development* **127**, 989-96.
Moon, A. M. and Capecchi, M. R. (2000). Fgf8 is required for outgrowth and patterning of the limbs. *Nat Genet* **26**, 455-9.
Morgan, B. A., Conlon, F. L., Manzanares, M., Millar, J. B., Kanuga, N., Sharpe, J., Krumlauf, R., Smith, J. C. and Sedgwick, S. G. (1996). Transposon tools for recombinant DNA manipulation: characterization of transcriptional regulators from yeast, Xenopus, and mouse. *Proc Natl Acad Sci U S A* **93**, 2801-6.
Morgan, N. V., Bacchelli, C., Gissen, P., Morton, J., Ferrero, G. B., Silengo, M., Labrune, P., Casteels, I., Hall, C., Cox, P. et al. (2003). A locus for asphyxiating thoracic dystrophy, ATD, maps to chromosome 15q13. *J Med Genet* **40**, 431-5.
Mountford, P., Zevnik, B., Duwel, A., Nichols, J., Li, M., Dani, C., Robertson, M., Chambers, I. and Smith, A. (1994). Dicistronic targeting constructs: reporters and modifiers of mammalian gene expression. *Proc Natl Acad Sci U S A* **91**, 4303-7.
Murphy, M., McMahon, R., Lappin, D. W. and Brady, H. R. (2002). Gremlins: is this what renal fibrogenesis has come to? *Exp Nephrol* **10**, 241-4.
Nagy, A., Gertsensten, M., Vintersten, K. and Behringer, R. (2002). Manipulating the Mouse Embryo; A Laboratory Manual. Cold Spring Harbor, New York: Cold Spring Harbour Press.

Nagy, A., Rossant, J., Nagy, R., Abramow-Newerly, W. and Roder, J. C. (1993). Viable cell culture-derived mice from early passage embryonic stem cells. *Proc. Natl. Acad. Sci. USA* **90**, 8424-8428.
Niederreither, K., Subbarayan, V., Dolle, P. and Chambon, P. (1999). Embryonic retinoic acid synthesis is essential for early mouse post- implantation development. *Nat Genet* **21**, 444-8.
Niederreither, K., Vermot, J., Schuhbaur, B., Chambon, P. and Dolle, P. (2002). Embryonic retinoic acid synthesis is required for forelimb growth and anteroposterior patterning in the mouse. *Development* **129**, 3563-3574.
Niehrs, C. and Pollet, N. (1999). Synexpression groups in eukaryotes. *Nature* **402**, 483-7.
Nishinakamura, R., Matsumoto, Y., Nakao, K., Nakamura, K., Sato, A., Copeland, N. G., Gilbert, D. J., Jenkins, N. A., Scully, S., Lacey, D. L. et al. (2001). Murine homolog of SALL1 is essential for ureteric bud invasion in kidney development. *Development* **128**, 3105-15.
Niswander, L. (2003). Pattern formation: old models out on a limb. *Nat Rev Genet* **4**, 133-43.
Niswander, L., Jeffrey, S., Martin, G. R. and Tickle, C. (1994). A positive feedback loop coordinates growth and patterning in the vertebrate limb. *Nature* **371**, 609-612.
Niswander, L. and Martin, G. R. (1993). FGF-4 regulates expression of *Evx-1* in the developing mouse limb. *Development* **119**, 287-294.
Pachnis, V., Mankoo, B. and Costantini, F. (1993). Expression of the c-ret proto-oncogene during mouse embryogenesis. *Development* **119**, 1005-17.
Panman, L. and Zeller, R. (2003). Patterning the limb before and after SHH signalling. *J Anat* **202**, 3-12.
Park, W. Y., Miranda, B., Lebeche, D., Hashimoto, G. and Cardoso, W. V. (1998). FGF-10 is a chemotactic factor for distal epithelial buds during lung development. *Dev Biol* **201**, 125-34.
Pearce, J. J., Penny, G. and Rossant, J. (1999). A mouse cerberus/Dan-related gene family. *Dev Biol* **209**, 98-110.
Pepicelli, C. V., Kispert, A., Rowitch, D. H. and McMahon, A. P. (1997). GDNF induces branching and increased cell proliferation in the ureter of the mouse. *Dev Biol* **192**, 193-8.
Pepicelli, C. V., Lewis, P. M. and McMahon, A. P. (1998). Sonic hedgehog regulates branching morphogenesis in the mammalian lung. *Curr Biol* **8**, 1083-6.
Pereira, R. C., Economides, A. N. and Canalis, E. (2000). Bone morphogenetic proteins induce gremlin, a protein that limits their activity in osteoblasts. *Endocrinology* **141**, 4558-63.
Perkins, A. S. (2002). Functional genomics in the mouse. *Funct Integr Genomics* **2**, 81-91.
Piccolo, S., Sasai, Y., Lu, B. and De Robertis, E. M. (1996). Dorsoventral patterning in Xenopus: inhibition of ventral signals by direct binding of chordin to BMP-4. *Cell* **86**, 589-98.
Pichel, J. G., Shen, L., Sheng, H. Z., Granholm, A. C., Drago, J., Grinberg, A., Lee, E. J., Huang, S. P., Saarma, M., Hoffer, B. J. et al. (1996). Defects in enteric innervation and kidney development in mice lacking GDNF. *Nature* **382**, 73-6.

Pizette, S., Abate-Shen, C. and Niswander, L. (2001). BMP controls proximodistal outgrowth, via induction of the apical ectodermal ridge, and dorsoventral patterning in the vertebrate limb. *Development* **128**, 4463-74.
Pizette, S. and Niswander, L. (1999). BMPs negatively regulate structure and function of the limb apical ectodermal ridge. *Development* **126**, 883-94.
Raatikainen-Ahokas, A., Hytonen, M., Tenhunen, A., Sainio, K. and Sariola, H. (2000). BMP-4 affects the differentiation of metanephric mesenchyme and reveals an early anterior-posterior axis of the embryonic kidney. *Dev Dyn* **217**, 146-58.
Reddi, A. H. (1997). Bone morphogenetic proteins: an unconventional approach to isolation of first mammalian morphogens. *Cytokine Growth Factor Rev* **8**, 11-20.
Reddi, A. H. (2000). Bone morphogenetic proteins and skeletal development: the kidney-bone connection. *Pediatr Nephrol* **14**, 598-601.
Riddle, R. D., Johnson, R. L., Laufer, E. and Tabin, C. (1993). *Sonic hedgehog* mediates the polarizing activity of the ZPA. *Cell* **75**, 1401-1416.
Rodriguez-Leon, J., Merino, R., Macias, D., Ganan, Y., Santesteban, E. and Hurle, J. (1999). Retinoic acid regulates programmed cell death through BMP signalling. *Nat Cell Biol.* **1**, 125-126.
Ros, M. A., Dahn, R. D., Fernandez-Teran, M., Rashka, K., Caruccio, N. C., Hasso, S. M., Bitgood, J. J., Lancman, J. J. and Fallon, J. F. (2003). The chick oligozeugodactyly (ozd) mutant lacks sonic hedgehog function in the limb. *Development* **130**, 527-37.
Sainio, K., Suvanto, P., Davies, J., Wartiovaara, J., Wartiovaara, K., Saarma, M., Arumae, U., Meng, X., Lindahl, M., Pachnis, V. et al. (1997). Glial-cell-line-derived neurotrophic factor is required for bud initiation from ureteric epithelium. *Development* **124**, 4077-87.
Sakiyama, J., Yamagishi, A. and Kuroiwa, A. (2003). Tbx4-Fgf10 system controls lung bud formation during chicken embryonic development. *Development* **130**, 1225-34.
Sanchez, M. P., Silos-Santiago, I., Frisen, J., He, B., Lira, S. A. and Barbacid, M. (1996). Renal agenesis and the absence of enteric neurons in mice lacking GDNF. *Nature* **382**, 70-3.
Sanz-Ezquerro, J. J. and Tickle, C. (2000). Autoregulation of Shh expression and Shh induction of cell death suggest a mechanism for modulating polarising activity during chick limb development. *Development* **127**, 4811-23.
Saunders, J. W. (1977). The experimental analysis of chick limb bud development. *Vertebrate limb and somite morphoogenesis (ed. D.A. Ede, J.R. Hinchliffe, and M. Balls) Cambridge University Press, Cambridge, England*, 1-24.
Saunders, J. W., Jr. and Gasseling, M. T. (1968). Ectoderm-mesenchymal interaction in the origins of wing symmetry. In *Epithelial-Mesenchymal Interactions*, (ed. R. Fleischmajer and R. E. Billingham), pp. 78-97. Baltimore: WIlliams
Wilkins.
Saunders, J. W. J. (1948). The proximo-distal sequence of origin of limb parts of the chick wing and the role of the ectoderm. *J. Exp. Zoology*, 363-404.
Saxén, L. (1987). Organogenesis of the Kidney. Cambridge: Cambridge University Press.

Scherz, P. J., Harfe, B. D., McMahon, A. P. and Tabin, C. J. (2004). The limb bud Shh-Fgf feedback loop is terminated by expansion of former ZPA cells. *Science* **305**, 396-9.
Schuchardt, A., D'Agati, V., Larsson-Blomberg, L., Costantini, F. and Pachnis, V. (1994). Defects in the kidney and enteric nervous system of mice lacking the tyrosine kinase receptor Ret. *Nature* **367**, 380-3.
Schuchardt, A., D'Agati, V., Pachnis, V. and Costantini, F. (1996). Renal agenesis and hypodysplasia in ret-k- mutant mice result from defects in ureteric bud development. *Development* **122**, 1919-29.
Schwenk, F., Baron, U. and Rajewsky, K. (1995). A cre-transgenic mouse strain for the ubiquitous deletion of loxP-flanked gene segments including deletion in germ cells. *Nucleic Acids Res* **23**, 5080-1.
Sekine, K., Ohuchi, H., Fujiwara, M., Yamasaki, M., Yoshizawa, T., Sato, T., Yagashita, N., Matsui, D., Koga, Y., Itoh, N. et al. (1999). Fgf10 is essential for limb and lung formation. *Nature Genetics* **21**, 138-141.
Serra, R. and Moses, H. L. (1995). pRb is necessary for inhibition of N-myc expression by TGF-beta 1 in embryonic lung organ cultures. *Development* **121**, 3057-66.
Shannon, J. M. and Hyatt, B. A. (2004). Epithelial-mesenchymal interactions in the developing lung. *Annu Rev Physiol* **66**, 625-45.
Shi, W., Zhao, J., Anderson, K. D. and Warburton, D. (2001). Gremlin negatively modulates BMP-4 induction of embryonic mouse lung branching morphogenesis. *Am J Physiol Lung Cell Mol Physiol* **280**, L1030-9.
Soshnikova, N., Zechner, D., Huelsken, J., Mishina, Y., Behringer, R. R., Taketo, M. M., Crenshaw, E. B., 3rd and Birchmeier, W. (2003). Genetic interaction between Wnt/beta-catenin and BMP receptor signaling during formation of the AER and the dorsal-ventral axis in the limb. *Genes Dev* **17**, 1963-8.
Spemann, H. a. M. H. (2001, reprinted). Induction of Embryonic Primordia by Implantation of Organizers from a Different Species. *International Journal of Developmental Biology* **45**, 13-38.
Spitz, F., Gonzalez, F. and Duboule, D. (2003). A global control region defines a chromosomal regulatory landscape containing the HoxD cluster. *Cell* **113**, 405-17.
Spitz, F., Gonzalez, F., Peichel, C., Vogt, T. F., Duboule, D. and Zakany, J. (2001). Large scale transgenic and cluster deletion analysis of the HoxD complex separate an ancestral regulatory module from evolutionary innovations. *Genes Dev* **15**, 2209-14.
Srinivas, S., Wu, Z., Chen, C. M., D'Agati, V. and Costantini, F. (1999). Dominant effects of RET receptor misexpression and ligand-independent RET signaling on ureteric bud development. *Development* **126**, 1375-86.
Summerbell, D. (1974). A quantitative analysis of the effect of excision of the AER from the chick limb-bud. *J Embryol Exp Morphol* **32**, 651-60.
Sun, X., Lewandoski, M., Meyers, E. N., Liu, Y. H., Maxson, R. E., Jr. and Martin, G. R. (2000). Conditional inactivation of Fgf4 reveals complexity of signalling during limb bud development. *Nat Genet* **25**, 83-6.
Sun, X., Mariani, F. V. and Martin, G. R. (2002). Functions of FGF signalling from the apical ectodermal ridge in limb development. *Nature* **418**, 501-8.

Tang, M. J., Worley, D., Sanicola, M. and Dressler, G. R. (1998). The RET-glial cell-derived neurotrophic factor (GDNF) pathway stimulates migration and chemoattraction of epithelial cells. *J Cell Biol* **142**, 1337-45.
te Welscher, P., Fernandez-Teran, M., Ros, M. A. and Zeller, R. (2002a). Mutual genetic antagonism involving GLI3 and dHAND prepatterns the vertebrate limb bud mesenchyme prior to SHH signaling. *Genes Dev* **16**, 421-6.
te Welscher, P., Zuniga, A., Kuijper, S., Drenth, T., Goedemans, H. J., Meijlink, F. and Zeller, R. (2002b). Progression of Vertebrate Limb Development through SHH-Mediated Counteraction of GLI3. *Science* **298**, 827-30.
Ten Have-Opbroek, A. A. (1991). Lung development in the mouse embryo. *Exp Lung Res* **17**, 111-30.
Tichelaar, J. W., Lim, L., Costa, R. H. and Whitsett, J. A. (1999a). HNF-3/forkhead homologue-4 influences lung morphogenesis and respiratory epithelial cell differentiation in vivo. *Dev Biol* **213**, 405-17.
Tichelaar, J. W., Wert, S. E., Costa, R. H., Kimura, S. and Whitsett, J. A. (1999b). HNF-3/forkhead homologue-4 (HFH-4) is expressed in ciliated epithelial cells in the developing mouse lung. *J Histochem Cytochem* **47**, 823-32.
Tickle, C. (2003). Patterning systems--from one end of the limb to the other. *Dev Cell* **4**, 449-58.
Tickle, C. and Munsterberg, A. (2001). Vertebrate limb development--the early stages in chick and mouse. *Curr Opin Genet Dev* **11**, 476-81.
Topol, L. Z., Marx, M., Laugier, D., Bogdanova, N. N., Boubnov, N. V., Clausen, P. A., Calothy, G. and Blair, D. G. (1997). Identification of drm, a novel gene whose expression is suppressed in transformed cells and which can inhibit growth of normal but not transformed cells in culture. *Mol Cell Biol* **17**, 4801-10.
Topol, L. Z., Modi, W. S., Koochekpour, S. and Blair, D. G. (2000). DRM/GREMLIN (CKTSF1B1) maps to human chromosome 15 and is highly expressed in adult and fetal brain. *Cytogenet Cell Genet* **89**, 79-84.
Torres, M., Gomez-Pardo, E., Dressler, G. R. and Gruss, P. (1995). Pax-2 controls multiple steps of urogenital development. *Development* **121**, 4057-65.
Towers, P. R., Woolf, A. S. and Hardman, P. (1998). Glial cell line-derived neurotrophic factor stimulates ureteric bud outgrowth and enhances survival of ureteric bud cells in vitro. *Exp Nephrol* **6**, 337-51.
Vainio, S. and Lin, Y. (2002). Coordinating early kidney development: lessons from gene targeting. *Nat Rev Genet* **3**, 533-43.
Vega, Q. C., Worby, C. A., Lechner, M. S., Dixon, J. E. and Dressler, G. R. (1996). Glial cell line-derived neurotrophic factor activates the receptor tyrosine kinase RET and promotes kidney morphogenesis. *Proc Natl Acad Sci U S A* **93**, 10657-61.
Vogel, A. and Tickle, C. (1993). FGF-4 maintains polarizing activity of posterior limb bud cells in vivo and in vitro. *Development* **119**, 199-206.
Vogt, T. F., Jackson Grusby, L., Wynshaw Boris, A. J., Chan, D. C. and Leder, P. (1992). The same genomic region is disrupted in two transgene-induced limb deformity alleles. *Mamm Genome* **3**, 431-7.
von Bubnoff, A. and Cho, K. W. (2001). Intracellular BMP signaling regulation in vertebrates: pathway or network? *Dev Biol* **239**, 1-14.

Wang, B., Fallon, J. F. and Beachy, P. A. (2000). Hedgehog-Regulated Processing of Gli3 Produces an Anterior/Posterior Repressor gradient in the Developing Vertebrate Limb. *Cell* **100**, 423-434.
Wang, C. C., Chan, D. C. and Leder, P. (1997). The mouse formin (Fmn) gene: genomic structure, novel exons, and genetic mapping. *Genomics* **39**, 303-11.
Wang, S. N., Lapage, J. and Hirschberg, R. (2001). Loss of tubular bone morphogenetic protein-7 in diabetic nephropathy. *J Am Soc Nephrol* **12**, 2392-9.
Warburton, D., Schwarz, M., Tefft, D., Flores-Delgado, G., Anderson, K. D. and Cardoso, W. V. (2000). The molecular basis of lung morphogenesis. *Mech Dev* **92**, 55-81.
Watanabe, T. and Costantini, F. (2004). Real-time analysis of ureteric bud branching morphogenesis in vitro. *Dev Biol* **271**, 98-108.
Waterston, R. H. Lindblad-Toh, K. Birney, E. Rogers, J. Abril, J. F. Agarwal, P. Agarwala, R. Ainscough, R. Alexandersson, M. An, P. et al. (2002). Initial sequencing and comparative analysis of the mouse genome. *Nature* **420**, 520-62.
Weaver, M., Batts, L. and Hogan, B. L. (2003). Tissue interactions pattern the mesenchyme of the embryonic mouse lung. *Dev Biol* **258**, 169-84.
Weaver, M., Dunn, N. R. and Hogan, B. L. (2000). Bmp4 and Fgf10 play opposing roles during lung bud morphogenesis. *Development* **127**, 2695-704.
Weaver, M., Yingling, J. M., Dunn, N. R., Bellusci, S. and Hogan, B. L. (1999). Bmp signaling regulates proximal-distal differentiation of endoderm in mouse lung development. *Development* **126**, 4005-15.
Woychik, R. P., Generoso, W. M., Russell, L. B., Cain, K. T., Cacheiro, N. L. A., Bultman, S. J., Selby, P. B., Dickinson, M. E., Hogan, B. L. M. and Rutledge, J. C. (1990). Molecular and genetic characterisation of a radiation-induced structural rearrangement in mouse chromosome 2 causing mutations at the limb deformity and agouti loci. *Proc. Natl. Acad. Sci.* **87**, 2588-2592.
Woychik, R. P., Stewart, T. A., Davis, L. G., D'Eustachio, P. and Leder, P. (1985). An inherited limb deformity created by insertional mutagenesis in a transgenic mouse. *Nature* **318**, 36-40.
Wynshaw-Boris, A., Ryan, G., Deng, C. X., Chan, D. C., Jackson-Grusby, L., Larson, D., Dunmore, J. H. and Leder, P. (1997). The role of a single formin isoform in the limb and renal phenotypes of limb deformity. *Mol Med* **3**, 372-84.
Xu, P.-X., Adams, A., Peters, H., Brown, M. C., Heaney, S. and Maas, R. (1999). Eya1-deficient mice lack ears and kidneys and show abnormal apoptosis of organ primordia. *Nature Genetics* **23**, 113-17.
Xu, P.-X., Zheng, W., Huang, L., Maire, P., Laclef, C. and Silvius, D. (2003). Six1 is required for the early organogenesis of mammalian kidney. *Development* **130**, 3085-94.
Zákány, J. and Duboule, D. (1996). Synpolydactyly in mice with a targeted deficiency in the *HoxD* complex. *Nature* **384**, 69-71.
Zakany, J., Kmita, M. and Duboule, D. (2004). A dual role for Hox genes in limb anterior-posterior asymmetry. *Science* **304**, 1669-72.
Zeller, R. and Deschamps, J. (2002). Developmental biology: first come, first served. *Nature* **420**, 138-9.
Zeller, R., Haramis, A., Zuniga, A., McGuigan, C., Dono, R., Davidson, G., Chabanis, S. and Gibson, T. (1999). *Formin* defines a large family of

morphoregulatory genes and functions in establishment of the polarising region. *Cell Tissue Res* **296**, 85-93.
Zhang, Q., Topol, L. Z., Athanasiou, M., Copeland, N. G., Gilbert, D. J., Jenkins, N. A. and Blair, D. G. (2000). Cloning of the murine Drm gene (Cktsf1b1) and characterization of its oncogene suppressible promoter. *Cytogenet Cell Genet* **89**, 242-51.
Zhao, G. Q. (2003). Consequences of knocking out BMP signaling in the mouse. *Genesis* **35**, 43-56.
Zhao, J., Bu, D., Lee, M., Slavkin, H. C., Hall, F. L. and Warburton, D. (1996). Abrogation of transforming growth factor-beta type II receptor stimulates embryonic mouse lung branching morphogenesis in culture. *Dev Biol* **180**, 242-57.
Zhu, N. L., Li, C., Xiao, J. and Minoo, P. (2004). NKX2.1 regulates transcription of the gene for human bone morphogenetic protein-4 in lung epithelial cells. *Gene* **327**, 25-36.
Zimmerman, L., De Jesus-Escobar, J. and Harland, R. (1996). The Spemann organizer signal noggin binds and inactivates bone morphogenetic protein 4. *Cell* **86**, 599-606.
Zuniga, A., Haramis, A. P., McMahon, A. P. and Zeller, R. (1999). Signal relay by BMP antagonism controls the SHH/FGF4 feedback loop in vertebrate limb buds. *Nature* **401**, 598-602.
Zuniga, A., Michos, O., Spitz, F., Haramis, A. P., Panman, L., Galli, A., Vintersten, K., Klasen, C., Mansfield, W., Kuc, S. et al. (2004). Mouse limb deformity mutations disrupt a global control region within the large regulatory landscape required for Gremlin expression. *Genes Dev* **18**, 1553-64.
Zuniga, A. and Zeller, R. (1999). Gli3 (Xt) and formin (ld) participate in the positioning of the polarising region and control of posterior limb-bud identity. *Development* **126**, 13-21.
Zuzarte-Luis, V. and Hurle, J. M. (2002). Programmed cell death in the developing limb. *Int J Dev Biol* **46**, 871-6.

Summary

Epithelial-mesenchymal signaling interactions are critical events that regulate organogenesis. The research presented in this thesis establishes that the extracellular BMP antagonist Gremlin is essential to initiate, maintain and propagate such epithelial-mesenchymal feedback signaling during limb and metanephric kidney organogenesis. Furthermore, modulating BMP activity by Gremlin-mediated antagonism appears to be critical to epithelial morphogenesis. In particular, Gremlin-mediated BMP antagonism is essential for proper differentiation of AER epithelial cells, a key event in initiation of distal limb bud outgrowth. Moreover, Gremlin is also involved in the differentiation of lung epithelial cells that play a major role in supporting gas exchange. Finally, genetic studies establish that the *Gremlin* loss-of-function allele generated by gene targeting is allelic to the mouse *limb deformity* (*ld*) mutation. These studies show that Gremlin, not Formin, is the gene whose disruption causes the *ld* limb phenotype. The *ld* limb phenotype is caused either by disruption of the *Gremlin* transcription unit or by disruption of distant cis-regulatory elements with features of a global control region (GCR) that regulates activation of both *Gremlin* and *Formin* expression in the posterior limb bud mesenchyme.

Samenvatting

Signaal overdracht tussen het epithelium en het mesenchyme speelt een belangrijke rol tijdens organogenese. Het onderzoek dat in dit proefschrift wordt beschreven, bevestigd dat de extracellulaire BMP antagonist Gremlin essentieel is voor de initiatie en handhaving van dergelijke feedback signalering tussen het epithilium en mesenchyme tijdens de organogenese van de nieren en ledematen. Ook voor de morfogenese van het epithelium is het van belang dat de activiteit van BMP door Gremlin wordt tegengewerkt. De antagonistische werking van Gremlin op de BMP activiteit is essentieel voor de differentiatie van AER epithelium cellen, wat belangrijk is voor de initiatie van de distale uitgroei van de zich ontwikkelende ledematen. Voorts is Gremlin ook betrokken bij de differentiatie van het epithelium van de longen wat belangrijk is voor de gasuitwisseling. Genetische studies laten tenslotte zien dat een door homologe recombinatie geïnactiveerd gremlin allel de limb deformity mutatie niet completeert. Deze studies laten zien dat de mutatie van Gremlin en niet van Formin de ld ledemaat fenotype veroorzaakt. De ld ledemaat fenotype kan worden veroorzaakt door zowel een mutatie in het Gremlin gen zelf als door een mutatie in een cis-regulerend element dat zich op een afstand bevindt en eigenschappen vertoont van een global control region (GCR) dat de activatie van zowel Gremlin als Formin expressie in het posteriore gedeelte van de ledematen reguleert.

(Bedankt Tony and Lia)

Acknowledgements

Iedereen Bedankt Thanks Everybody Merci Villmool
Vielen Dank An Alle Dzienkuje Bardzo Grazie A Tutti
Muchos Gracias Salamat Sa Inyong Lahat Obrigado Muito
Efcharisto Se Olous Shoukran Merci A Tous

I finally would like to thank my bosses Rolf and Aimée.
Rolf merci de m'avoir accepté dans ton laboratoire il y a quatre ans, et de m'avoir fait confiance…. Thanks for everything, to be always there when I needed and finally thanks for teaching me what excellent science is about….
Ma cheffe que dire!!! Tout simplement merci. Ce fut un réel plaisir et un honneur d'etre ton premier étudiant et j'espere avoir été a la hauteur… Mon séjour avec vous fut aussi passionant et intéressant qu'un Carnaval au pays des Zuni (mais pas les gaga)!!!

And of course I would like to thank my two favorites Italian Doctresses Antonella and Rosanna. Rosanna thanks a lot for all the good that I have had in Utrecht both in and outside the lab… I hope to see you in Marseille one day… Anto, thanks for being there since 4 years….

Et Vive la Grece Championne d'europe 2004!!!!!!….

Curriculum vitae

Odyssé Michos was born on the 20th of August 1977, in Cherbourg, France. He studied Biology in the University of Caen. He obtained his master degree in Biology, neurosciences in 2000 from the University of Paris 6 "Pierre et Marie Curie", doing his experimental thesis in "the laboratoire des signaux intercellulaires, Institut des Neuroscinces, Paris, France". Since the first of November 2000 he works in the Department of Developmental Biology, at the University of Utrecht investigating the role of Gremlin during mouse embryogenesis. In September 2003 he moved in the Institute of Anatomy of the University of Basel, Switzerland to finish his research. The research described in this thesis was carried out under the supervision of Dr. Aimée Zuniga. From November 2004 he will start to work as a postdoctoral fellow in the Developmental Genetics group of Prof. Dr. Rolf Zeller at the Department of Clinical Biological Sciences, University of Basel Medical School, Switzerland.

Publications

Michos O, Panman L, Vintersten K, Beier K, Zeller R, Zuniga A. Gremlin-mediated BMP antagonism induces the epithelial-mesenchymal feedback signaling controlling metanephric kidney and limb organogenesis. Development. 2004 Jul;131(14):3401-10. Epub 2004 Jun 16.

Zuniga A, **Michos O**, Spitz F, Haramis AP, Panman L, Galli A, Vintersten K, Klasen C, Mansfield W, Kuc S, Duboule D, Dono R, Zeller R. Mouse limb deformity mutations disrupt a global control region within the large regulatory landscape required for Gremlin expression. Genes Dev. 2004 Jul 1;18(13):1553-64. Epub 2004 Jun 15.